Aus dem Walther-Straub-Institut für Pharmakologie und Toxikologie
Institut der Ludwig-Maximilians-Universität München
Vorstand: Dr. med. Thomas Gudermann

Pharmakologische Beeinflussbarkeit der TRPM7 Kanalkinase

Dissertation
zum Erwerb des Doktorgrades der Medizin
an der Medizinischen Fakultät der
Ludwig-Maximilians-Universität zu München

vorgelegt von

Sebastian Schäfer

aus

München

2019

Mit Genehmigung der Medizinischen Fakultät
der Universität München

Berichterstatter:	Prof. Dr. Thomas Gudermann
Mitberichterstatter:	Prof. Dr. Antje Gorsche Prof. Dr. Dejana Mokranjac Prof. Dr. Axel Steiger
Mitbetreuung durch den promovierten Mitarbeit:	Dr. Vladimir Chubanov
Dekan:	Prof. Dr. med. dent. Reinhard Hickel
Tag der mündlichen Prüfung:	21.02.2019

Einleitende Zusammenfassung der schriftlichen, kumulativen Promotion

gemäß § 4a der Promotionsordnung der LMU vom 1. Juni 1983 in der Fassung der zehnten Änderungssatzung vom 6. Juli 2012

Inhaltsverzeichnis

Abkürzungsverzeichnis

2-APB	2-Aminoethyldiphenylborinat
AchR	Acetylcholin-Rezeptor
AGS	humane Magen-Adenokarzinomazellen
ALS	Amyotrophe Laterale Sklerose
ATP	Adenosintriphosphat
CA1	Cornu Ammonis 1
EC_{50}	mittlere effektive Konzentration
GPCR	G-Protein-gekoppelter Rezeptor
HEK293	humane embryonale Nierenzellen 293
IC_{50}	mittlere inhibitorische Konzentration
MBP	Myelin-basisches Protein
MCF-7	Michigan Cancer Foundation 7-Zellen
MP	Morbus Parkinson
NGF	Nervenwachstumsfaktor
PIP_2	Phophatidylinositol-4,5-bisphosphat
PLC	Phospholipase C
rat RBL	ratten basophile Leukämie-Zellen
Ser	Serin
SHR	Spontan hypertensive Ratten
SK-Kanal	Small conductance calcium-activated potassium channels
SOCE	Speicher abhängiger Ca^{2+}-Einstrom
Thr	Threonin
TRPM	Protein kodiert durch *TRPM* Gene
Trpm6	Maus Gene
TRPM6	Humane Gene
TRPM7	Protein kodiert durch *TRPM7* Gen
Trpm7	Maus Gene
TRPM7	Humane Gene
VSMC	vaskuläre glatte Muskelzellen
WKY	Wistar-Kyoto-Ratten

α-Kinase	Atypische Kinase
qRT-PCR	quantitative Echtzeit-PCR

Publikationsliste

Mibefradil represents a new class of benzimidazole TRPM7 channel agonists.

Schäfer, S.; Ferioli, S.; Hofmann, T.; Sierler, S.; Gudermann, T.; Chubanov, V.

Pflugers Arch. 2016, 468, 623–634.

Eigenanteil:

- Durchführung aller gezeigten Versuche

Activation of TRPM7 channels by small molecules under physiological conditions.

Hofmann, T.; Schäfer, S.; Linseisen, M.; Sytik, L.; Gudermann, T.; Chubanov, V.

Pflugers Arch. 2014, 466, 2177–2189.

Eigenanteil:

- Durchführung des Primärscreens von TRPM7-Aktivatoren (zusammenfassend aufgeführt in Abbildung 1B)

Natural and synthetic modulators of SK (Kca2) potassium channels inhibit magnesium-dependent activity of the kinase-coupled cation channel TRPM7.

Chubanov, V.; Schnitzler, M.M.; Meißner, M.; Schäfer, S.; Abstiens, K.; Hofmann, T.; Gudermann, T.

Br. J. Pharmacol. 2012, 166, 1357–1376.

Eigenanteil:

- Durchführung des Primärscreens zur Identifizierung von TRPM7-Blockern
- Darstellung des NS8593 Effektes an TRPM7 im Barium-Assay (aufgeführt in Abbildung 2E und 2F
- Spezifitätstestung des NS8593 auf verwandte TRP Proteine (aufgeführt in suppl. Figure 4, 5 und 6)

Einleitung

Struktur der TRPM7 Kanalkinase

Das Gen *human transient receptor potential cation channel, subfamily M, member 7* (*TRPM7*) ist auf dem Chromosom 15q21.2 lokalisiert. Es besteht aus 39 Exons und kodiert ein Protein von 1865 Aminosäuren (Schmitz et al., 2005). Strukturell findet sich in dem TRPM7-Protein eine N-terminal gelegene, Ionenkanal bildende Domäne, fusioniert mit einer C-terminal gelegenen Kinasendomäne. Diese Proteinstruktur ermöglicht eine Bifunktionalität, welche lediglich bei einem weiteren Säugetiergen, dem zur gleichen Genfamilie gehörenden Gen und *TRPM6* bekannt ist (Fleig and Chubanov, 2014; Perraud et al., 2001; Schlingmann et al., 2002; Walder et al., 2002). TRPM2 zeigt eine ähnliche Struktur, weist jedoch im Gegensatz zu TRPM7 und TRPM6 eine Nudix-Enzym Region anstatt einer Kinasendomäne auf (Kuhn and Luckhoff, 2004).

TRPM7 strukturiert sich von N- nach C-terminal beginnend mit vier Melastin-Untereinheiten (M1-M4), an die sich sechs putative transmembranäre Helixsegmente (S1-S6) anschließen (Fleig and Chubanov, 2014; Nadler et al., 2001). Die Porenregion wird zwischen S5 und S6 vermutet. Die TRP-Box findet sich im Anschluss an S6. Diese TRP-Box ist als hochkonservierte Sequenz Bestandteil der meisten TRP-Proteine (Fleig and Chubanov, 2014; Venkatachalam and Montell, 2007). C-terminal findet sich eine coiled coil (CC) Domäne. Sie übernimmt mutmaßlich Funktionen bei der Steuerung der Kanalzusammensetzung und dem Proteintransport. Es schließt sich eine Substratbindedomäne (SD) an, welche an eine atypische Serin/Threonin α-Kinasedomäne grenzt (Fleig and Chubanov, 2014; Fujiwara and Minor, 2008) (Abb. 1).

Es wird angenommen, dass sich zur Ausbildung einer funktionalen Quartärstruktur jeweils vier TRPM7-Proteine zu einem tetrameren Proteinkomplex anlagern (Fleig and Chubanov, 2014). Diese Komplexierung wird bei allen TRP-Proteinen vermutet und scheint strukturelle Ähnlichkeiten zu spannungsabhängigen K^+-Kanälen aufzuweisen (Chubanov et al., 2007; Jiang et al., 2003; Mederos y Schnitzler et al., 2008; Paravicini et al., 2012).

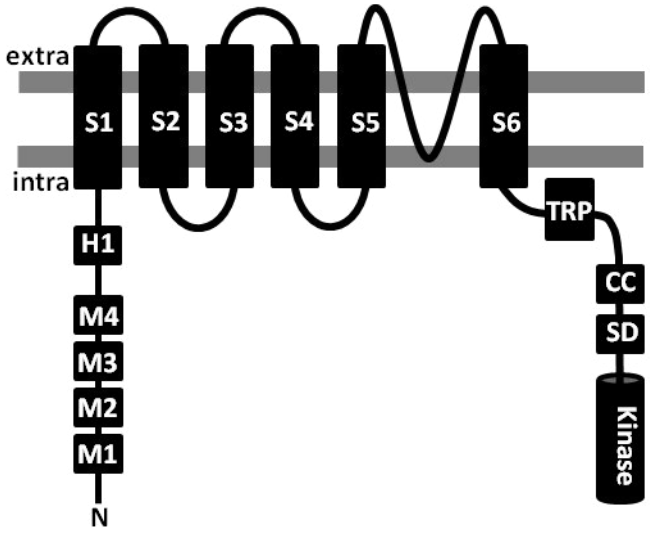

Abb. 1: Schematischer Aufbau des TRPM7-Proteins an der Zellmembran mit extrazellulärem (extra) und intrazellulärem (intra) Bereich, Melastin-Untereinheiten 1-4 (M), hydrophober Region (H), transmembranären Segmenten 1-6 (S), TRP-Domäne (TRP), coiled coil-Domäne (CC), Substratbindedomäne (SD) und α-Kinase (Kinase)

Biophysikalische Charakteristika des TRPM7 Kanals

TRPM7 zeigt ein komplexes biophysikalisches Verhalten, welches der Kanalkinase seine außergewöhnliche Bifunktionalität ermöglicht. Die Kanalfunktion zeichnet sich unter hyperpolarisierten Potentialen durch ihre Selektivität für divalente Kationen aus (Monteilh-Zoller et al., 2003; Nadler et al., 2001). Die Strom-Spannungs-Kurve wird durch ein Umkehrpotential bei 0 mV und einer Rektifizierung der Auswärtsströme bei depolarisierten Potentialen charakterisiert (Abb. 2). Diese Eigenschaft wird durch eine spannungsabhängige Permeabilitätsblockade durch extrazelluläre divalente Kationen, hauptsächlich Ca^{2+} und Mg^{2+}, bedingt (Kerschbaum et al., 2003; Nadler et al., 2001). In Divalent-freien Konditionen findet sich dementsprechend eine über das Umkehrpotential fortgeleitete, lineare IV-Relation (Fleig and Chubanov, 2014).

TRPM7 ist unter negativen Potentialen selektiv für divalente Kationen durchlässig. Erst bei deutlich positiven Potentialen zeigt der Kanal eine Leitfähigkeit für monovalente Auswärtsströme (Nadler et al., 2001). Die Permeabilität des Kanals unterscheidet sich hierbei für die verschiedenen Ionen und stellt sich wie folgt dar: Zn ≈ Ni > Ba > Co > Mg > Mn > Sr > Cd > Ca (Fleig and Chubanov, 2014; Li et al., 2006; Monteilh-Zoller et al., 2003).

Die Permeabilität für Ca^{2+} und Mg^{2+} wird durch mehrere Aminosäuren der Proteinsequenz beeinflusst. Der Austausch der sauren Glutaminsäure an Position 1047 reduziert die

Permeabilität für divalente Kationen um bis zu 100 % (Li et al., 2007). Ein Austausch der Glutaminsäure 1047 zu Glutamin und Tyrosin 1049 zu Prolin führt hingegen zu linearisierten Strömen und dem Verlust der Ca^{2+}-Leitfähigkeit (Mederos y Schnitzler et al., 2008). Des Weiteren wurde nachgewiesen, dass Asparaginsäure 1054 und 1059 Einfluss auf den Permeabilitätsblock der divalenten Kationen nehmen (Numata and Okada, 2008).

Freies, intrazelluläres Mg^{2+} ist der wichtigste regulatorische Faktor der Kanalaktivität (Fleig and Chubanov, 2014; Nadler et al., 2001). Ausführliche biophysikalische Experimente konnten zeigen, dass TRPM7 zwischen zwei Leitfähigkeitszuständen alterniert. Die Hauptkonfiguration ist hierbei umschrieben mit einer Leitfähigkeit von 39 pS neben einer weiteren bei 186 pS (Chokshi et al., 2012b). Beide Stadien sind durch Mg^{2+} reversibel blockierbar. Die Blockade wird hierbei über die Reduktion der Summe der aktiven Kanäle ausgeübt, anstatt über eine Senkung der Leitfähigkeit einzelner Kanäle (Chokshi et al., 2012a).

Bislang gibt es Hinweise auf zwei Mg^{2+}-Bindestellen. Eine befindet sich in der Kinasedomäne, eine weitere in der Porendomäne (Schmitz et al., 2003). Die Bindungsaffinität des Proteins für Mg^{2+} und somit seine Sensitivität für eine Mg^{2+}-Blockade wird durch unterschiedliche Faktoren beeinflusst, welche im Folgenden diskutiert werden (Fleig and Chubanov, 2014).

Das Nukleotid Adenosintriphosphat (ATP) bildet einen intrazellulären Regulations-Mechanismus der TRPM7-Kanalaktivität. Während Na-ATP einen aktivierenden Effekt auf den Kanal besitzt, inhibiert das natürlich vorkommende Mg-ATP seine Aktivität (Fleig and Chubanov, 2014; Nadler et al., 2001; Runnels et al., 2001). Es wird davon ausgegangen, dass ungebundenes ATP als Puffer fungiert und freie Mg^{2+}-Ionen bindet, wodurch die durch Mg^{2+} vermittelte Blockade aufgehoben wird. TRPM7 besitzt in der Kinasedomäne eine separate Nukleotidbindestelle (K1648), an der Mg-ATP bindet und, unabhängig von freiem Mg^{2+}, die Kanalaktivität inhibieren kann (Schmitz et al., 2003). Eine plausible Erklärung hierfür bietet das Vorhandensein eines zellulären Schutzmechanismus für die Regulation der TRPM7-Aktivität bei variierenden zellulären Energiezuständen (Demeuse et al., 2006; Fleig and Chubanov, 2014).

TRPM7 wird ebenfalls über einen Proteinkinase C(PLC)-abhängigen Signalweg reguliert (Park et al., 2014). So zeigten Versuche in HEK293-Zellen, in denen membranäres PIP_2 über die Aktivierung von PLC verbraucht wurde, eine Inhibierung TRPM7-vermittelter Ionenströme

(Runnels et al., 2002).

In einer sauren Umgebung mit pH-Werten unter 6 wird TRPM7 aktiviert (Monteilh-Zoller et al., 2003). Es wird davon ausgegangen, dass freie Protonen Mg^{2+}-Bindestellen besetzen und somit der Mg^{2+}-Block aufgehoben wird (Jiang et al., 2005). Unter pathophysiologischen Gesichtspunkten gewinnt dieser Vorgang eine besondere Bedeutung, da er eine Aktivierung der Kanalaktivität unter sauren Bedingungen, wie sie beispielsweise in minderperfundiertem Geweben vorzufinden sind, induziert (Fleig and Chubanov, 2014).

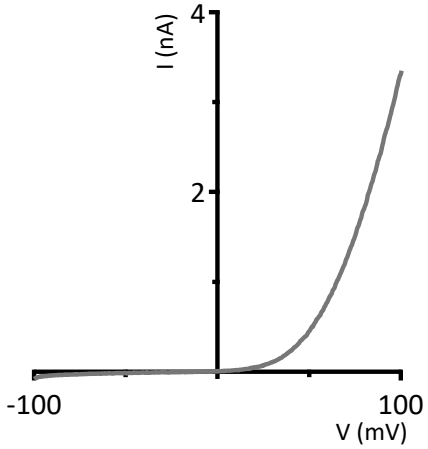

Abb. 2: Exemplarische Strom(I)-Spannungs(V)-Kurve des TRPM7-Proteins in PatchClamp-Versuchen. Die Versuche wurden in Ganzzellkonfiguration durchgeführt.

Physiologische und pathophysiologische Funktion des TRPM7

TRPM7 wird ubiquitär in nahezu allen Geweben exprimiert (Fleig and Chubanov, 2014). Die Funktionen des Proteins sind nicht vollständig geklärt und Gegenstand aktueller Forschung. Eine wichtige Funktion zeigt sich in der Regulation der Ca^{2+}- und Mg^{2+}-Homöostase. *Knockout*-Versuche in Hühner-B-Lymphozyten (DT40) sowie in Maus-embryonalen Stammzellen (MES) führten in beiden Zelllinien zu einem Arrest der Zellproliferation. Dieses Defizit konnte in beiden Fällen überwunden werden, indem die Zellen höheren Magnesiumkonzentrationen ausgesetzt wurden (Fleig and Chubanov, 2014; Ryazanova et al., 2010; Schmitz et al., 2003). Eine Erklärung hierfür wird in der Hochregulation alternativer Mg^{2+}-Transporter als Ersatz für das nicht funktionale TRPM7 gesehen (Deason-Towne et al., 2011; Kolisek et al., 2008; Sahni et al., 2007). Auch in der Regulation der systemischen Mg^{2+}-Homöostase spielt der Kanal eine wichtige Rolle. Eine heterozygote Mutation in der TRPM7-Kinasedomäne in Mäusen führt zu einer systemischen Hypomagnesiämie. Es wird somit eine

Beteiligung des Kanals an der intestinalen Resorption von Mg^{2+}-Ionen angenommen (Ryazanova et al., 2010).

TRPM7 ist ein selektiver Kationenkanal für divalente Ionen. Die Eigenschaft, transmembranäre Calciumströme zu leiten, wird aktuell in einem pathophysiologischem Kontext gesehen. Einen Überblick gibt hierbei der Artikel „The pathophysiological role of TRPM7“ von Park et al. (Park et al., 2014). So wurde eine Aktivierung des Kanals mit neuronalem Zelltod im Verlauf von ischämischen Schlaganfällen (Aarts et al., 2003) und mit der Entstehung von kardialem Vorhofflimmern (Du et al., 2010) in Verbindung gebracht.

TRPM7 ist in der Funktion zytoskelletaler Zellbestandteile involviert. Eine Überexpression des Proteins in HEK293-Zellen führt zu einer Abrundung der Zellen und zum Verlust der Zelladhäsion (Nadler et al., 2001). Eine durch die TRPM7-Kinase eingeleitete Steigerung der intrazellulären Calziumkonzentration beeinflusst zudem die Actomyosin-Kontraktilität und Zelladhäsion (Clark et al., 2006; Park et al., 2014).

Des Weiteren konnte ein Zusammenhang zwischen der Kanalakivität und der Migrationsgeschwindigkeit von T-Lymphozyten nachgewiesen werden (Kuras et al., 2012).

In Nervenzellen übernimmt TRPM7 verschiedene Funktionen. Es wurde ein Zusammenhang zwischen der Proteinfunktion und der Transmitterausschüttung in cholinergen Synapsen festgestellt. In sympathischen Neuronen wurde TRPM7 in synaptischen Vesikeln nachgewiesen, in denen es Komplexe mit Synapsin I und Synaptotagmin I bildet und als solche mit vesikulärem Snapin interagiert (Krapivinsky et al., 2006).

Eine weitere Funktion des Proteins findet sich bei der embryonalen Herzentwicklung. TRPM7 ist essenziell für die Proliferation des Myokards in frühen Entwicklungsstadien. Am reifen Herzen wurde eine indirekte Einflussnahme des Proteins auf die diastolische Membrandepolarisation und die Autonomie des Sinusknoten nachgewiesen (Sah et al., 2013).

Im Intestinaltrackt sind Cajal-Zellen die Vermittler zwischen Informationen des autonomen Nervensystem und der glatten Muskulatur des Intestinums. TRPM7 ist Bestandteil des Membrankomplexes der Cajal-Zellen und als solches beteiligt an der Vermittlung dieser Informationen (Kim et al., 2005).

Als Regulator der zellulären Differenzierung und Proliferation nimmt TRPM7 Einfluss auf die Entstehung und Ausprägung verschiedener Krebserkrankungen und ist somit mögliches Ziel therapeutischer Interventionen (Sahni et al., 2010). Es konnte durch eine Reduktion der

TRPM7-Expression die Proliferation in Zellen von Kopf-Hals-Karzinomen (Jiang et al., 2007) und Adenokarzinomen des Magendarmtraktes (Kim et al., 2008) unterdrückt werden. Zusätzlich konnte durch vergleichbare Interventionen in Zellen von Brustkrebs (Meng et al., 2013), Lungenkrebs (Gao et al., 2011), Nasopharyngealkarzinomen (Chen et al., 2010b) und Pankreaskarzinomen (Rybarczyk et al., 2012) Einfluss auf die Malignität der Tumorzellen im Bezug auf Zellmigrations- und Invasionsverhalten genommen werden(Park et al., 2014).

Erst kürzlich konnte eine Beteiligung des Proteins an der Thrombopoese nachgewiesen werden. Eine Punktmutation in TRPM7 führt in Menschen zur Ausbildung einer Makrothrombozytopenie. Es wird vermutet, dass eine Beteiligung des Proteins an der Ausbildung dieses Krankheitsbildes auf eine Einflussname auf die zytoskellettale Struktur der Thrombozyten zurückzuführen ist (Stritt et al., 2016).

Während eines ischämischen Schlaganfalls kommt es zu neuronalem Zelltod. Unter anderem führt eine erhöhte intrazelluläre Ca^{2+}-Konzentration zu einem Absterben der Zellen. In diesem Zusammenhang konnte TRPM7 als einer der Kanäle identifiziert werden, die den hierfür verantwortlichen transmembranären Ca^{2+}-Einstrom leiten. Durch die Inhibierung der TRPM7-Expression mittels siRNA konnte ein Zellsterben unter ischämischen Konditionen reduziert werden (Aarts et al., 2003). Diese Beobachtungen zeigen, dass TRPM7 am neuronalen Zelltod im Verlauf eines ischämischen Schlaganfalls beteiligt ist. Eine intermittierende Blockade der Kanalfunktion stellt sich als mögliche Therapieoption zur Minimierung neuronaler Verluste dar (Park et al., 2014).

Aufgrund der neurotoxischen Funktion des TRPM7-Proteinkanals wurden epidemiologische Studien im Rahmen von Genexpressionsvergleichsanalysen in Mäusen durchgeführt. Es sollte eine mögliche Korrelation zwischen Proteinexpression und neurodegenerativen Erkrankungen, wie der Multiple Sklerose und der Alzheimererkrankung, geklärt werden (Tseveleki et al., 2010). TRPM7 gehört zwar zu den 18 häufigsten Genen, die in betroffenen Mausmodellen dysreguliert sind, jedoch konnte keine Variation des Gens mit einem erhöhten Risiko die jeweilige Krankheit zu entwickeln assoziiert werden (Fleig and Chubanov, 2014; Romero et al., 2009).

Die familiäre Amyotrophe Laterale Sklerose (ALS) sowie der Morbus Parkinson (MP) sind mit verminderten Umgebungskonzentrationen für Ca^{2+} und Mg^{2+} assoziiert. Aufgrund dieses Umstandes wurde eine Beteiligung des TRPM7-Proteins in der Entstehung der Erkrankungen untersucht. Sowohl bei ALS als auch bei MP konnte eine TRPM7 Mutation nachgewiesen

werden, wobei die Beteiligung des Proteins kontrovers diskutiert wird, da sowohl Belege für (Hermosura et al., 2005) als auch gegen (Hara et al., 2010) eine solche beobachtet wurden. Es ist davon auszugehen, dass nicht ein einzelnes Gen für das Ausbrechen der Erkrankungen verantwortlich ist. Vielmehr handelt es sich um eine Komposition mehrerer Gene, von denen *TRPM7* einen Vertreter darstellt (Fleig and Chubanov, 2014).

Das TRPM7-Protein spielt eine Rolle in einer Vielzahl kardiovaskulärer Erkrankungen. TRPM7-assoziierte Ionenströme konnten in verschiedenen Tiermodellen (Gwanyanya et al., 2004) und in humane Kardiomyozyten (Macianskiene et al., 2012; Zhang et al., 2012) nachgewiesen werden. Die Funktion der Kanalkinase in diesen Zellen bleibt weitestgehend unbekannt. Ebenfalls wurde eine Expression des Gens in Kardiofibroblasten identifiziert. Bei Patienten mit Vorhofflimmern konnte ein verstärkter TRPM7-vermittelter zellulärer Ca^{2+}-Influx mit der Folge einer ausgeprägten Myofibroblastendifferenzierung und Fibrosierung nachgewiesen werden (Du et al., 2010).

Arterielle Hypertonie wird als eine der häufigsten chronischen Krankheiten und Hauptrisikofaktor für kardiovaskulärer-assoziierte Morbidität und Mortalität angesehen. TRPM7 ist an der Regulation des Blutdrucks beteiligt (Fleig and Chubanov, 2014; Touyz et al., 2006). Vaskuläre glatte Muskelzellen werden durch Mg^{2+}-Influx reguliert, eine erhöhte intrazelluläre Magnesiumkonzentration führt wiederum zu einer Vasodillatation sowie einer abgeschwächten Stimmulierbarkeit der Zellen durch Vasokonstriktoren (He et al., 2005). Analog hierzu führen niedrige intrazelluläre Magnesiumkonzentration zu einer Hyperkontraktibilität und mangelnden Stimulierbarkeit durch Vasodillatatoren (Rubin, 2007; Yoshimura et al., 1997). TRPM7 wird in spontan hypertensiven Ratten, im Vergleich zu normotensiven Wistar Kyoto Tieren, vermindert exprimiert. Gleichzeitig wurden in vaskulären glatten Muskelzellen dezimierte intrazelluläre Magnesiumkonzentrationen nachgewiesen. Dieser Effekt ist Angiotensin II-abhängig. Die Stimulation durch Angiotensin regt wiederum TRPM7-vermittelten Mg^{2+}-Influx an (He et al., 2005). Ergänzend wurde gezeigt, dass bei vaskulären glatten Muskelzellen, isoliert aus Maus-Aortagewebe, eine Expression von TRPM7 durch Angiotensin II induzierbar ist und zu Zellproliferation führt (Zhang 2012b). Nach Penetration der Zellen durch strömungsinduzierte Scheerkräfte werden in vaskulären glatten Muskelzellen doppelt so viele TRPM7-Kanäle in der Plasmamembran nachgewiesen als vor einer solchen (Sun et al., 2009). Die Ergebnisse deuten darauf hin, dass TRPM7 in der Sensorik für mechanische Reize in vaskulären glatten Muskelzellen und der

Regulation des Blutdrucks beteiligt ist (Park et al., 2014).

Zusammenfassend ist TRPM7 in einer Vielzahl basaler zellulärer Mechanismen involviert, zu denen unter anderem der Zellzyklus, die Ausbildung zytoskelletaler Strukturen mit Einfluss auf Zellform und Migration, sowie die Ca^{2+} und Mg^{2+} Homöostase und neuronale Kommunikation zählen. Analog hierzu zeigt sich ein Einfluss der Kanalfunktion unter anderem auf pathologische Prozesse wie Tumorzellentstehung und -malignität, neuronale Dysfunktionen sowie die Entstehung von Bluthochdruck und Herzrhythmusstörungen. Konsequenterweise wurde TRPM7 mehrfach als vielversprechende pharmakologische Zielstruktur genannt.

Molekulare Pharmakologie des TRPM7

Durch den zunehmenden Nachweis der wichtigen pathophysiologischen Funktionen des TRPM7-Kanalproteins rückt die Notwendigkeit eines besseren Verständnisses seiner Eigenschaften und seines Wirkungsmechanismus in den Vordergrund. Die Identifizierung von Antagonisten bzw. Agonisten ist eine Grundvoraussetzung für die Erforschung der Proteineigenschaften *in vitro* wie *in vivo*.

Zu Beginn dieses Projektes waren lediglich wenige TRPM7-Kanalblocker, wie beispielsweise 2-APB oder Polyamine, als unspezifische Modulatoren verschiedener Ionenkanäle bekannt. Weiterhin lagen keine Erkenntnisse zu TRPM7-Aktivatoren vor. Davon ausgehend führten wir, sowie weitere Forschungsgruppen, einen Wirkstoff-Screen auf TRPM7-Modulatoren durch. Unsere Arbeit resultierte in der Entdeckung mehrerer Moleküle, welche die Eigenschaft aufwiesen, die TRPM7-Kanalaktivität unter physiologischen Bedingungen zu beeinflussen.

Seit längerem ist bekannt, dass verschiedene bereits bekannte Kanalblocker in der Lage sind, die TRPM7-Funktion zu inhibieren. Beim Einsatz dieser Moleküle zeigte es sich als problematisch, dass diese eine zu geringe Spezifität und/oder Potenz aufwiesen, was ihre Einsatzmöglichkeiten stark einschränkte. Erst in den letzten Jahren sind verschiedene Antagonisten und Agonisten mit einem verbesserten Wirkprofil identifiziert worden.

Eine Zusammenfassung der derzeit bekannten Modulatoren wird in dem Artikel „Natural and Synthetic Modulators of the TRPM7 Channel“ gegeben (Chubanov et al., 2014). Die derzeit bekannten Blocker lassen sich nach ihren Eigenschaften in verschiedene Gruppen einteilen (Tab. 1). Zu den unspezifischen Kanalblockern gehören das Spermin, SKF-96365 und 2-Aminoethyldiphenylborinat (2-APB). Die Blocker Waixenicin A, Quinin und Sphingosin bilden

eine heterogene Gruppe natürlich vorkommender Metaboliten. Ergänzend wurden mehrere kleine Moleküle mit bekannten pharmakologischen Eigenschaften identifiziert, die ebenfalls in der Lage sind, TRPM7 zu antagonisieren.

Spermin inhibiert TRPM7 reversibel und in Abhängigkeit seiner Spannung mit einer IC_{50} von 2,3 µM (Kozak et al., 2002). Der Blocker 2-APB inhibiert die Kanalaktivität indirekt durch eine Verringerung des intrazellulären pH-Wertes mit einer mittleren inhibitorischen Konzentration von 174 µM (Li et al., 2006; Prakriya and Lewis, 2002). Die Applikation von 20 µM SKF-96365 führt ebenfalls zu einer kompletten Inaktivierung der TRM7-Aktivität in RBL-Zellen (Kozak et al., 2002). Das Molekül *Nafamostat mesylate* ist als Antikoagulanz und Serin-Proteaseinhibitor bekannt. Zudem blockiert es TRPM7 mit einer IC_{50} von 27 µM (Chen et al., 2010c). Mit einer weitaus geringeren Potenz und einem Wirkspektrum im hohen Mikromolbereich blockieren der Wirkstoff Carvacrol und eine Gruppe bekannter 5-Lipoxygenase Inhibitoren, zu denen NDGA, AA81 und MK886 gehören. Das Terpenoid Waixenicin A ist in der Lage, TRPM7 bei gutem Wirkprofil mit einer IC_{50}-Konzentration von 7 µM spezifisch und irreversibel zu inhibieren (Zierler et al., 2011). Unter Verwendung des Antagonisten konnte eine Beteiligung des TRPM7-Proteins bei der Ausübung der Schrittmacherfunktion interstitieller Zellen nachgewiesen werden (Kim et al., 2013). Des Weiteren konnte wurde eine Beteiligung des TRPM7-Proteins in der Regulation der Actomyosinkontraktilität und der Invadosomenformierung in N1E-115 Neuroblastomazellen nachgewiesen werden (Visser et al., 2013). Waixenicin A ist zudem in der Lage, TRPM7-vermittelte Zellproliferation humaner Magen-Tumorzellen (AGS) und Brustkrebszellen (MCF-7) zu inhibieren. Diese Erkenntnis ist hervorzuheben, da sie ein neues Feld potentieller Anwendungsgebiete der TRPM7-Antagonisten in der onkologischen Pharmakologie eröffnet. TRPM7 zeichnet sich somit als mögliches therapeutisches Ziel in Krebstherapien aus (Fleig and Chubanov, 2014; Kim et al., 2013).

Sphingosin und das Strukturanalogon Fingolimod blockieren die TRPM7-Kanalfunktion mit einer hohen Potenz bei IC_{50}-Werten von 600 nM und 720 nM. Der zugrunde liegende Inhibierungsmechanismus liegt in einer Dysbalancierung der alternierenden Konfigurationszustände des Proteins. Dies mindert die Wahrscheinlichkeit, dass sich der Kanal in seiner geöffneten Konfiguration befindet (Qin et al., 2013).

Unter Verwendung eines Biolumineszenz-basierten Hochdurchsatz-Screens konnten wir

verschiedene kalziumabhängige Kaliumkanal-Blocker als Inhibitoren des TRPM7-Proteins identifizieren (Chubanov et al., 2012). Zu den identifizierten Molekülen zählen Chinin, CyPPA, Dequalinium, NS8593, SKA31 und UCL1684. NS8593 zeigt unter diesen Stoffen die größte Potenz mit einer IC_{50} Konzentration von 1,6 µM. Bei diesem Molekül handelt es sich um einen direkten TRPM7-Blocker, der, so die Annahme, den inhibitorischen Effekt von Mg^{2+} auf den Kanal verstärkt. In *in vitro* Versuchen an HEK293-Zellen führte die Applikation von NS8593 zu einer Unterbindung der TRPM7-induzierten Zellmobilität (Chubanov et al., 2012).
Verschiedene Arbeitsgruppen verwendeten NS8593 bereits erfolgreich für weiterführende Studien. So konnte Sisquella et al. nachweisen, dass eine NS8593 vermittelte Inhibierung der TRPM7 Funktion Einfluss auf eine zytoskelletal induzierte Verformung von Erythrozyten nimmt und hierdurch die Invasion des Malariaerreger *plasmodium falciparum* verhindert. Eine Beobachtung die TRPM7 als potentielles pharmakologisches Ziel in der Bekämpfung der Malaria auszeichnet (Sisquella et al., 2017).
Wie Bernhardt et al. zeigen, inhibiert NS8593 einen spontanen Ca^{2+}-Influx in Maus-Oozyten. Weiterhin wurden durch Befruchtung induzierte Ca^{2+}-Oscillationen blockiert. Diese Beobachtungen legen nahe, dass nicht wie vormals angenommen, speicherabhängiger Ca^{2+}-Einstrom (SOCE), sondern viel mehr TRPM7 eine führende Rolle in Ca^{2+} vermittelten Signalwegen in Maus-Oozyten übernimmt (Bernhardt et al., 2017). Carvacho et al. verwendeten NS8593, um eine Verzögerung der frühembryonalen Entwicklung von Maus-Oozyten zu Blastozysten durch die Blockade von TRPM7 nachzuweisen (Carvacho et al., 2016). Faouizi et al. postulieren einen Synergismus der TRPM7 Funktion und SOCE zur Regulierung der intrazellulären Ca^{2+}-Homöostase in Hühner DT40B Lymphozyten. Hierbei handelt es sich um Erkenntnisse, die unter Verwendung einer NS8593 vermittelten TRPM7 Blockade erworben wurden (Faouzi et al., 2017). Schilling et al. zeigen unter Verwendung von NS8593, dass TRPM7-induzierte transmembranäre Ströme eine hervorgehobene Rolle in der Mobilität von Mikroglia spielen. Ins Besondere an Prozessen der Migration und Invasion einer entzündungshemmenden Zellantwort ist das Protein beteiligt (Schilling et al., 2014).
Nörenberg et al. zeigten mittels einer durch NS8593 ausgelösten Blockade, dass endogenen ATP-induzierte Ströme in Gliom-Zellen durch TRPM7 vermittelt werden und nicht, wie vormals angenommen, durch P2X7-Kanäle (Norenberg et al., 2016). Tashiro et al. konnten eine tragende Rolle der TRPM7-Kanäle in dem physiologischen Mg^{2+}-Einfluss in Ratten ventrikulären Myozyten unter Anderem mittels NS8593 nachweisen (Tashiro et al., 2014). In

Brustkrebszellen reguliert die TRPM7-Kanalfunktion einen Wachstumsfaktor gesteuerten zellulären Signalweg, der zu einer gesteigerten Malignität der Tumorzellen beiträgt, wie Davis et al. nachweisen konnten (Davis et al., 2014). Tian et al. konnten unter Verwendung von NS8593 zeigen, dass Prostaglandin E2 an einer TRPM7 induzierten Migration und Proliferation von humanen Glioblastom-Zellen beteiligt ist (Tian et al., 2018). Bernhardt et al. verwendeten sowohl NS8593 als auch die Agonisten Naltriben und Mibefradil, um einen funktionellen Verlust der TRPM7-Kanalaktivität in *Trmp7* Knockout Oocyten nachzuweisen (Bernhardt et al., 2018).

Wirkstoff	**IC_{50}(µM)**	**Inhibierungstyp**	**Referenz**
2-APB	174	Reversibel	(Li et al., 2006; Prakriya and Lewis, 2002)
Spermine	2.3	Reversibel, spannungsabhängig	(Kozak et al., 2002)
SKF-96365	n.b.	Getestet bei 20 µM	(Kozak et al., 2002)
Nafamostat	617	Reversibel, spannungsabhängig	(Chen et al., 2010c)
Carvacrol	306	Reversibel	(Parnas et al., 2009)
NDGA	n.b.	Getestet bei 10 und 20 µM	(Chen et al., 2010a)
AA861	n.b.	Getestet bei 10 und 40 µM	(Chen et al., 2010a)
MK886	n.b.	Getestet bei 10 µM	(Chen et al., 2010a)
Waixenicin A	7.0	Irreversibel, $[Mg^{2+}]_i$ abhängig	(Zierler et al., 2011)
NS8593	1.6	Reversibel, $[Mg^{2+}]_i$ abhängig	(Chubanov et al., 2012)
Quinine	n.b.	Reversibel, getestet bei 30 µM	(Chubanov et al., 2012)
CyPPA	n.b.	Getestet bei 30 µM	(Chubanov et al., 2012)
Dequalinium	n.b.	Getestet bei 30 µM	(Chubanov et al., 2012)
SKA31	n.b.	Getestet bei 30 µM	(Chubanov et al., 2012)
UCL 1684	n.b.	Getestet bei 30 µM	(Chubanov et al., 2012)
Sphingosine	0.6	Reversibel	(Qin et al., 2013)
FTY720	0.7	Reversibel	(Qin et al., 2013)

Tabelle 1: Zusammenfassung der bekannten Inhibitoren des TRPM7-Proteins (Chubanov et al., 2014). n.b. = nicht bestimmt

Im Vergleich zu der umfassenderen Liste an Antagonisten ist über Moleküle, die zu einer Aktivierung der TRPM7-Kanalfunktion führen, wenig bekannt. In dieser Arbeit ist es uns gelungen 20, positive Gate-Modulatoren für TRPM7 zu identifizieren (Hofmann et al., 2014) (Tab. 2). Es handelt sich um eine heterogene Gruppe von Molekülen, unter denen Naltriben und Mibefradil detaillierter untersucht wurden. Naltriben ist als δ-Opioid-Rezeptorblocker bekannt. Wir konnten zeigen, dass es zudem in der Lage ist, TRPM7 reversibel

und unabhängig von der zytoplasmatischen Magnesiumkonzentration mit einer mittleren effektiven Konzentration von 20 µM zu aktivieren. Die Effekte von NS8593 und Naltriben auf TRPM7 sind kompetitiv und heben sich gegenseitig auf. Naltriben hat im direkten Vergleich keinen Effekt auf die nah verwandten Proteine TRPM2, TRPM8 und TRPV1 und zeigt somit eine relative Spezifität für TRPM7 (Hofmann et al., 2014).

Mibefradil ist ein T- und L-Typ-Kalziumkanalblocker, der aufgrund seiner gefäßerweiternden und blutdrucksenkenden Wirkung im klinischen Einsatz war. Wir konnten zeigen, dass das Molekül ebenfalls ein positiver Gating-Modulator von TRPM7 ist. Mibefradil moduliert die TRPM7-Funktion reversibel und, im Gegensatz zu Naltriben, stark abhängig von der intrazellulären Magnesiumkonzentration mit einer EC_{50}-Konzentration von 53 µM (Schäfer et al., 2015). Das Molekül zeigt Strukturhomologien zu dem Blocker NS8593 (Abb. 3), hat jedoch einen konträren Effekt am TRPM7-Kanal. Wir schließen daraus, dass beide Moleküle an einer gemeinsamen Ligandenbindestelle agieren könnten. Es lässt sich mutmaßen, dass diese Sequenz eine hervorgehobene Bedeutung in der Steuerung der Kanalfunktion besitzen könnte.

Naltriben hat sich bereits mehrfach in weiterführenden Versuchen als wertvolles Werkzeug zur Erforschung der TRPM7-Funktionen bewiesen. So konnten Wong et al. eine Aktivierung des TRPM7-Kanals durch Naltriben mit einer Migration und Invasion von Glioblastomazellen in Verbindung bringen (Wong et al., 2017). Huguet et al. zeigten, dass eine Hochregulierung der TRPM7-Kanalfunktion durch Naltriben mit konsekutivem Anstieg des intrazellulären Magnesiumlevels zu einer gesteigerten Funktion eines, in der Pathophysiologie der Zystischen Fibrose beteiligten, mutierten Chloridkanals führt (Huguet et al., 2016). Toshiro et al. erforschten die Beteiligung der TRPM7-Funktion am Magnesiummetabolismus in Ratten ventrikulären Myozyten unter Verwendung von Naltriben (Tashiro et al., 2014).

Zusammenfassend wurden in der jüngeren Vergangenheit mehrere Antagonisten der TRPM7-Kanalfunktion identifiziert. Zu diesen Inhibitoren zählt NS8593. Das Molekül konnte bereits in mehreren Arbeitsgruppen erfolgreich zur Erforschung der TRPM7-Funktion eingesetzt werden. Weiterhin ist es erstmals gelungen, TRM7 Agonisten zu identifizieren. Hierdurch konnte nachgewiesen werden, dass die TRPM7-Funktion positiv moduliert werden kann. Naltriben zeigte sich als Wirkstoff mit günstigem Wirkungsprofil und wurde aufgrund dieser Eigenschaften bereits in verschiedenen wissenschaftlichen Arbeiten zur Stimulation der TRPM7-Kanalfunktion erfolgreich verwendet.

Wirkstoff	EC_{50} (µM)	Aktivierungstyp
Naltriben	20,7	Reversibel,$[Mg^{2+}]_i$ unabhängig
Clozapine	n.b.	Getestet bei 30–50 µM
Proadifen	n.b.	Getestet bei 30–50 µM
Doxepin	n.b.	Getestet bei 30–50 µM
A3 hydrochloride	n.b.	Getestet bei 30–50 µM
Mibefradil	53	Reversibel, $[Mg^{2+}]_i$ abhängig
U-73343	n.b.	Getestet bei 30–50 µM
CGP-74514A	n.b.	Getestet bei 30–50 µM
Metergoline	n.b.	Getestet bei 30–50 µM
L-733,060	n.b.	Getestet bei 30–50 µM
A-77636	n.b.	Getestet bei 30–50 µM
ST-148	n.b.	Getestet bei 30–50 µM
Clemastine	n.b.	Getestet bei 30–50 µM
Desipramine	n.b.	Getestet bei 30–50 µM
Sertraline	n.b.	Getestet bei 30–50 µM
Methiothepin	n.b.	Getestet bei 30–50 µM
NNC 55–0396	n.b.	Getestet bei 30–50 µM
Prochlorperazine	n.b.	Getestet bei 30–50 µM
Nortriptyline	n.b.	Getestet bei 30–50 µM
Loperamide	n.b.	Getestet bei 30–50 µM

Tabelle 2: Zusammenfassung der bekannten Aktivatoren des TRPM7-Proteins (Hofmann et al., 2014). n.b. = nicht bestimmt

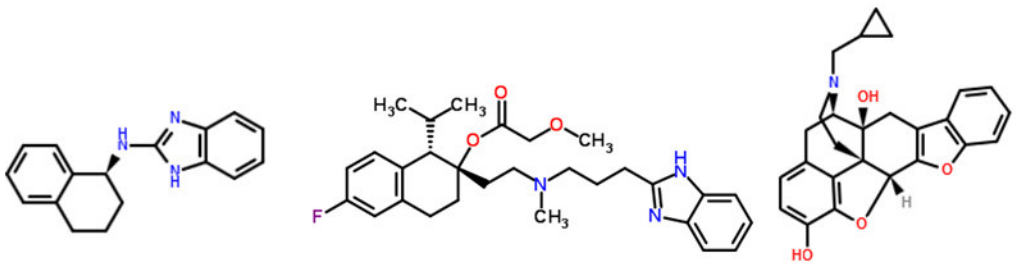

Abb. 3: Chemische Strukturen der Moleküle NS8593, Naltriben und Mibefradil. Erstellung der Molekülstrukturen unter Chemspider (www.chemspider.com).

Zielsetzung der Arbeit

Die zentrale Hypothese der Arbeit fußt auf der Annahme, dass die pharmakologische Modulation der TRPM7-Kanalfunktion angewandt werden kann, um pathologische Prozesse wie Tumorwachstum, Zellmigration und Metastasierung zu beeinflussen.
Zu Beginn des Projektes lagen bereits Daten zu verschiedenen nichtselektiven pharmakologischen Wirkstoffen zur Inhibierung des TRPM7-Kanalfunktion vor. Über die Möglichkeit einer positiven Modulation der Kanalfunktion unter physiologischen Konditionen durch als Wirkstoff agierende Moleküle lagen hingegen keine Erkenntnisse vor. Auf dieser Grundlage setzten wir uns für die vorliegende Arbeit folgende Ziele.

1. Die Entwicklung einer Ca^{2+}-Imaging basierten Methode zur Durchführung eines Hochdurchsatzscreens zur Identifizierung potentieller TRPM7-Kanal Agonisten und Antagonisten.

2. Die Verwendung der Patch-Clamp-Methode sowie zellbiologischer Methoden zur weiterführenden Charaktersierung der vielversprechendsten Wirkstoffe.

3. Die Erforschung des Effektes der neuen Modulatoren an TRPM7 abhängigen zellulären Prozessen.

Zusammenfassung

TRPM7 ist ein bifunktionales Protein, dass eine TRP-Ionenkanal Domäne, gekoppelt an eine α-Kinasedomäne, aufweist. TRPM7 ist essentiell für Zellproliferation und -wachstum. Die Hochregulierung der TRPM7-Funktion ist beteiligt an anoxischem neuronalem Zelltod, kardialer Fibrose und Tumorzellproliferation/-invasion. Zum Zeitpunkt des Projektbeginns sind wenige nichtselektive Inhibitoren der Proteinfunktion und keine Positivmodulatoren bekannt. Das Hauptziel dieser Arbeit bestand in der Identifizierung weiterer Antagonisten sowie der ersten Agonisten der TRPM7-Kanalfunktion. Identifizierte Wirkstoffe wurden zudem im Zellmodell auf ihre Eigenschaft untersucht, Einfluss auf TRPM7-abhängige Prozesse zu nehmen.

Wir führten einen bioluminiszenzbasierten Hochdurchsatzscreen zur Identifizierung von TRPM7-Modulatoren durch. In einem Primärscreen konnten 20 potentielle Aktivatoren und sechs Inhibitoren identifiziert werden. Der TRPM7-Blocker NS8593 sowie die Aktivatoren Naltriben und Mibefradil wurden für weiterführende Versuche selektiert.

Wir verwendeten Ca^{2+}-Imaging-Versuche sowie die PatchClamp-Technik, um den funktionellen Einfluss der Modulatoren auf TRPM7-vermittelte Ionenströme zu untersuchen.

Es wurde gezeigt, dass NS8593 ein potenter Blocker TRPM7-vermittelter Ströme ist. Die Blockade der Kanalfunktion ist schnell und reversibel. Weitere TRP-Proteine werden nicht durch NS8593 beeinflusst. In zellbiologischen Versuchen wurde die Zellmotilität von HEK293 Zellen durch NS8593 inhibiert. Dieser Effekt gleicht der zuvor beschriebenen Auswirkung eines TRPM7 know-downs im Zellmodell.

Naltriben ist ein potenter positiver Modulator der TRPM7-Kanalfunktion. Die Aktivierung erfolgt unabhängig von der intrazellulären Magnesiumkonzentration, ist reversibel und, im Vergleich zu weiteren TRP-Proteinen, spezifisch für TRPM7. Mibefradil übt ebenfalls einen stimulierenden Effekt auf die TRPM7-Funktion aus. Im Gegensatz zu Naltriben ist dieser Effekt stark abhängig von der zytoplasmatischen Magnesiumkonzentration.

Es ist uns gelungen, strukturell unabhängige Leitwirkstoffe zu identifizieren, die als Modulatoren der TRPM7-Kanalfunktion fungieren. Die Verbindungen erwiesen sich als sehr geeignet zur Untersuchung der funktionalen Charakeristika der TRPM7-Ströme sowie durch TRPM7 regulierter zellulärer Prozesse. Unsere Ergebnisse bieten ein neues pharmakologisches Werkzeug zur Untersuchung der TRPM7-Funktion in

physiologischen und pathophysiologischen Prozessen. Weiterhin wird ein Weg zur Erforschung neuer, hoch-spezifischer TRPM7-Modulatoren aufgezeigt.

Summary

TRPM7 is a bifunctional Protein comprising a TRP ion channel domain, fused to a α-kinase domain. TRPM7 is essential for cell proliferation and cell growth. The up-regulation of TRPM7 function is involved in anoxic neuronal cell death, cardiac fibrosis and tumor cell proliferation as well as cell invasion. At the time when this project was initiated, only a few highly nonselective inhibitors of the TRPM7 channel have been described, and no positive modulators of TRPM7 have been reported. The main aim of this work was to identify new drug-like inhibitors and first activators of the TRPM7 channel. In addition, we studied whether these molecules enable to regulate TRPM7-dependent processes in cultured cells.

Using a bioluminescence-based Ca^{2+} imaging, we performed a screen for new modulators of the TRPM7 channel. We isolated 20 activators and 6 inhibitors of the TRPM7 channel. The channel blocker, NS8593, as well as two activators, naltriben and mibefradil, were selected for a follow-up characterization. We used Ca^{2+} imaging and the patch-clamp techniques to investigate the functional impact of these molecules on TRPM7 currents. We found that NS8593 is a potent blocker of TRPM7 currents. The inhibitory effect of NS8593 on TRPM7 was fast and reversible. NS8593 did not affect activity of several other TRP channels examined. Application of NS8593 resulted in suppressed motility of HEK293 cells resembling the well-described effect of genetic knock-down of TRPM7. Naltriben was found to be a potent positive modulator of the TRPM7 channel. Naltriben-induced activation of TRPM7 currents was rapid, independent of cytosolic Mg^{2+} levels, reversible and, compared to related TRP-channels, specific for TRPM7. Mibefradil elicited stimulatory effect on the TRPM7 channel. However, compared to naltriben, the stimulatory action of mibefradil was highly dependent on cytoplasmic Mg^{2+} levels.

Taken together, we identified several structurally-unrelated lead compounds acting as inhibitors and activators of the TRPM7 channel. The identified compounds were found to be well-suited to study functional characteristics of TRPM7 currents and cellular processes regulated by TRPM7. Hence, our results provide new pharmacological tools to study a role of TRPM7 in physiological and pathophysiological processes and suggest a path to the discovery of new highly selective TRPM7 modulators.

Veröffentlichungen

Mibefradil represents a new class of benzimidazole TRPM7 channel agonists

Pflugers Arch - Eur J Physiol
DOI 10.1007/s00424-015-1772-7

ION CHANNELS, RECEPTORS AND TRANSPORTERS

Mibefradil represents a new class of benzimidazole TRPM7 channel agonists

Sebastian Schäfer[1] · Silvia Ferioli[1] · Thomas Hofmann[1] · Susanna Zierler[1] · Thomas Gudermann[1,2,3] · Vladimir Chubanov[1]

Received: 25 November 2015 / Revised: 2 December 2015 / Accepted: 4 December 2015

Abstract Transient receptor potential cation channel, subfamily M, member 7 (TRPM7) is a bi-functional protein comprising an ion channel moiety covalently linked to a protein kinase domain. Currently, the prevailing view is that a decrease in the cytosolic Mg^{2+} concentration leads to activation of divalent cation-selective TRPM7 currents. TRPM7 plays a role in immune responses, hypotension, tissue fibrosis, and tumor progression and, therefore, represents a new promising therapeutic target. Because of the dearth of pharmacological tools, our mechanistic understanding of the role of TRPM7 in physiology and pathophysiology still lags behind. Therefore, we have recently carried out a high throughput screen for small-molecule activators of TRPM7. We have characterized the phenanthrene naltriben as a first stimulatory agonist of the TRPM7 channel. Surprisingly, the effect of naltriben on TRPM7 was found to be unaffected by the physiological levels of cytosolic Mg^{2+}. Here, we demonstrate that mibefradil and NNC 50–0396, two benzimidazole relatives of the TRPM7 inhibitor NS8593, are positive modulators of TRPM7. Using Ca^{2+} imaging and the patch-clamp technique, we show that mibefradil activates TRPM7-mediated Ca^{2+} entry and whole-cell currents. The response to mibefradil was fast, reversible, and reproducible. In contrast to naltriben, mibefradil efficiently activates TRPM7 currents only at physiological intracellular Mg^{2+} concentrations, and its stimulatory effect was fully abrogated by high internal Mg^{2+} levels. Consequently, a TRPM7 variant harboring a gain-of-function mutation was insensitive to further mibefradil activation. Finally, we observed that the effect of mibefradil was selective for TRPM7 when various TRP channels were tested. Taken together, mibefradil acts as a Mg^{2+}-regulated agonist of the TRPM7 channel and, hence, uncovers a new class of TRPM7 agonists.

Keywords TRPM7 · TRP channels · Voltage-dependent calcium channels · Magnesium · Mibefradil · NNC 55–0396 · Naltriben · NS8593

Abbreviations

TRPM7	Melastatin-related TRP cation channel 7
AITC	Allyl isothiocyanate
PS	Pregnenolone sulfate

Introduction

Transient receptor potential cation channel, subfamily M, member 7 (TRPM7) is a ubiquitously expressed protein that contains a transmembrane ion channel segment linked to a cytosolic α-type serine/threonine protein kinase domain (reviewed in [24]). Studies with mouse strains carrying loss-of-function mutations in the *Trpm7* gene revealed that TRPM7 is required for early embryonic development, morphogenesis of internal organs, cardiac automaticity, and systemic Mg^{2+} homeostasis [22, 32, 33, 56, 57, 59, 60]. The genetic ablation of TRPM7 in cells showed that this bifunctional protein regulates the homeostasis of divalent cations such as Ca^{2+}, Mg^{2+}, and Zn^{2+} [14, 37, 56, 57, 61, 63]; cell

✉ Vladimir Chubanov
vladimir.chubanov@lrz.uni-muenchen.de

[1] Walther-Straub-Institute of Pharmacology and Toxicology, University of Munich, Goethestrasse 33, 80336 Munich, Germany

[2] Comprehensive Pneumology Center Munich (CPC-M), German Center for Lung Research, Munich, Germany

[3] DZHK (German Centre for Cardiovascular Research), Munich Heart Alliance, Munich, Germany

Published online: 16 December 2015

motility [9, 15, 38, 41, 65, 68, 69, 78]; proliferation [10, 19, 46, 61, 63, 83]; differentiation [2, 82]; mechanosensitivity [48, 49, 78]; and exocytosis [5]. TRPM7 may play a role in anoxic neuronal death [1], immune responses [32, 38, 62], hypertension [45, 72], neurodegenerative disorders [28, 73], tissue fibrosis [21, 23, 66], and tumor growth [8, 25–27, 31, 35, 39, 42, 43, 58, 64, 70, 76, 80, 81]. Therefore, TRPM7 represents a prime target for pharmacological modulation.

Because of the dearth of specific and effective pharmacological tools, our mechanistic understanding of the role of TRPM7 in physiology and pathophysiology still lags behind. Annexin A1, myosin II isoforms, eEF2-k, and PLCγ2 were suggested as potential physiological substrates of the TRPM7 kinase [15–17, 20, 51]. The ion channel domain of TRPM7 is selective for divalent cations [44, 46, 54]. Our current understanding of TRPM7 channel gating mainly rests on the rather artificial maneuver of cell perfusion with a Mg^{2+}-free internal solution to induce TRPM7 currents, assuming that intracellular Mg^{2+} (either free Mg^{2+} or Mg-ATP) is a physiological negative regulator of the TRPM7 channel [18, 46]. In addition, the plasma membrane phospholipid phosphatidylinositol-4,5-bisphosphate (PIP_2) appears to be required for TRPM7 channel activity, because PIP_2 depletion leads to inactivation of TRPM7 currents [55]. In this context, it has been proposed [36] that Mg^{2+} directly interacts with negatively charged PIP_2 to interfere with the gating process of TRPM7.

For many TRP channels, the discovery of small molecules acting as channel agonists greatly advanced the field. For instance, capsaicin [6, 7], 4α-phorbol 12,13-didecanoate (4alpha-PDD) [77], allyl isothiocyanate (AITC) [34], pregnenolone sulfate (PS) [75], and menthol [50] have successfully been employed to study the physiological relevance and the therapeutic potentials of TRPV1, TRPV4, TRPA1, TRPM3, and TRPM8 channels. Such molecular tools may also be instrumental in probing TRPM7 function, for instance, to acutely differentiate between TRPM7 channel and kinase activity. Furthermore, our current thinking about the physiological role of TRPM7 predominantly relies on ablation of its function, and it still remains unknown as how acute stimulation of the TRPM7 channel affects cellular processes.

Recently, our group has identified an efficient inhibitor of TRPM7, the benzimidazole NS8593, and has performed a comprehensive screen for small molecules serving as TRPM7 channel agonists [30]. In particular, we found 20 drug-like compounds with different structural backbones that stimulate TRPM7-mediated Ca^{2+} influx and TRPM7 currents [30]. Among the latter compounds, naltriben was studied in greater detail [30]. We showed that naltriben reversibly activates recombinant and native TRPM7 channels (half maximal effective concentration (EC_{50})~20 μM) without prior depletion of intracellular Mg^{2+}. More recently, Tashiro et al. employed naltriben to demonstrate that TRPM7 controls Mg^{2+} uptake in primary ventricular myocytes [71]. Thus, naltriben represents a unique molecular tool allowing for the manipulation of TRPM7 channel activity in the presence of physiological levels of intracellular Mg^{2+}.

In the present work, we set out to expand our armamentarium of TRPM7 activators and focused on the benzimidazole compound mibefradil, a broadly used inhibitor of T-type voltage-dependent calcium channels [4, 74] as well as Ca^{2+}- and volume-activated Cl^- channels [47]. We show that mibefradil acts as a stimulatory agonist of the TRPM7 channel. In contrast to naltriben, the effect of mibefradil occurs at physiological intracellular Mg^{2+} concentrations, and its stimulatory action was abolished by high intracellular Mg^{2+} concentrations. Hence, mibefradil may represent a founding member of a new class of TRPM7 agonists enabling to probe TRPM7 function under physiological conditions.

Methods

Chemicals

Mibefradil dihydrochloride, NNC 55–0396 dihydrochloride, NS8593, naltriben methanesulfonate, and PS were purchased from Tocris.

Molecular biology and cell cultures

Wild-type (WT), $TRPM7^{E1047Q}$, and $TRPM7^{S1107E}$ mutant mouse TRPM7 complementary DNA (cDNA) variants in the pIRES-eGFP vector (Clontech Laboratories) were generated as described previously [14, 40]. For transient expression of TRPM7, human embryonic kidney (HEK) 293 cells were maintained at 37 °C and 5 % CO_2 in Eagle's minimal essential medium (MEM; Invitrogen) supplemented with 10 % fetal calf serum, 100 μg/ml streptomycin, and 100 U/ml penicillin (Invitrogen). Cells were transiently transfected using the Lipofectamine 2000 reagent (Invitrogen) according to the manufacturer's instructions.

Aequorin-based $[Ca^{2+}]_i$ measurements

To monitor effects of drugs on TRPM7-mediated Ca^{2+} influx, we used aequorin-based $[Ca^{2+}]_i$ assay as described previously [30]. Briefly, HEK 293 cells cultured in 3.5-mm dishes were transfected with 2 μg/dish of TRPM7 plasmid DNA and 0.1 μg/dish pG5A construct encoding enhanced green fluorescent protein fused in-frame to *Aequorea victoria* apoaequorin [3]. Twenty-four hours after transfection, cells were washed twice with phosphate-buffered saline (PBS) and incubated with 0.05 % trypsin and 1 mM EDTA in PBS for 1 min at room temperature. Cell suspensions were centrifuged twice at 600 g for 3 min and resuspended in Mg^{2+}-free 4-(2-

hydroxyethyl)-1-piperazineethanesulfonic acid (HEPES)-buffered saline (Mg^{2+}-free HBS 140 mM NaCl, 6 mM KCl, 1 mM $CaCl_2$, 10 mM HEPES, 5 mM glucose, and 0.1 % BSA, pH 7.4). For reconstitution of aequorin, cell suspensions were incubated with 5 μM coelenterazin (Biaffin GmbH) in Mg^{2+}-free HBS for 30 min at room temperature. Cells were washed twice by centrifugation at 600 rpm for 3 min, followed by resuspension of the pellet in Mg^{2+}-free HBS, and placed in 96-well plates (1×10^5 cells per well). Luminescence was detected using a FLUOstar OPTIMA microplate reader at 37 °C (BMG LABTECH GmbH). To monitor a drug-induced TRPM7 channel activity, naltriben, mibefradil, or NNC 55–0396 were applied externally by injection of the drugs diluted in Mg^{2+}-free HBS. Experiments were terminated by lysing cells with 0.1 % (*v*/*v*) Triton X-100 in HBS to record total bioluminescence. Bioluminescence rates (c/s) were analyzed at 1-s intervals and calibrated as $[Ca^{2+}]_i$ values using the following equation:

$$p\left[Ca^{2+}\right]_i = 0.332588\,(-\log(k)) + 5.5593$$

k represents the rate of aequorin consumption, i.e., c/s divided by total number of counts.

Effects of drugs on TRPM3-, TRPV1-, and TRPA1-transfected cells were measured and analyzed analogously to TRPM7.

Electrophysiological techniques

HEK 293 cells grown in 35-mm dishes to about 70 % confluency were transfected with WT or mutant mouse TRPM7-pIRES-eGFP expression constructs (2 μg/dish) 20–30 h before analysis. Patch-clamp experiments were performed as reported previously [11, 13, 14, 30, 40] with few modifications. Whole-cell currents were measured using an EPC10 patch-clamp amplifier and PatchMaster software (Harvard Bioscience). Voltages were corrected for a liquid junction potential of 10 mV. Currents were elicited by a ramp protocol from −100 to +100 mV over 50 ms acquired at 0.5 Hz and a holding potential of 0 mV. Inward and outward current amplitudes were extracted at −80 and +80 mV and were normalized to cell size as pA/pF. Capacitance was measured using the automated capacitance cancellation function of EPC10. Patch pipettes were made of borosilicate glass (Science Products) and had resistances 2–3.5 MΩ. Unless stated otherwise, the extracellular solution contained (in mM) 140 NaCl, 2.8 KCl, 1 $CaCl_2$, 2 $MgCl_2$, 10 HEPES, and 11 glucose (all from Sigma-Aldrich). Solutions were adjusted to pH 7.3 using a FE20 pH meter (Mettler Toledo) and to 290 mOsm using a Vapro 5520 osmometer (Wescor Inc.). For determination of $[Mg^{2+}]_i$ dose responses, the intracellular pipette solution contained (in mM) 120 Cs-glutamate, 20 NaCl, 10 HEPES, 2 EGTA, and various amount of $MgCl_2$ and was adjusted to pH 7.3 and 290 mOsm. Concentrations of free Mg^{2+} were calculated using WebMaxC (maxchelator.stanford.edu).

Statistical analysis

Data are presented as means ± standard error of the mean (SEM). Unless stated otherwise, data were compared by an unpaired Student's *t* test. Significance was accepted at $P \leq 0.05$.

Results

Mibefradil stimulates TRPM7-mediated Ca^{2+} entry

In our primary screen [30], we had identified 20 compounds acting as activators of the TRPM7 channel including naltriben and the two related compounds, mibefradil and NNC 55–0396 (Fig. 1a). We noted that mibefradil and NNC 55–0396 display structural homology to NS8593 (Fig. 1a), a potent inhibitor of the TRPM7 channel [11]. Specifically, all three compounds contain a benzimidazole group linked to tetrahydronaphthalenyl moiety (Fig. 1a), supporting the notion [11] that benzimidazole-derived compounds may harbor essential pharmacophore features allowing for the pharmacological targeting of TRPM7. Therefore, we studied in detail how mibefradil and NNC 55–0396 affect the TRPM7 channel.

In our previous studies, we established a bioluminescence-based assay to monitor Ca^{2+} influx in HEK 293 cells transiently transfected with mouse TRPM7 cDNA [11, 40]. Figure 1b illustrates the Ca^{2+} response of TRPM7 expressing cells to the external application of 50 μM mibefradil. In the absence of external Mg^{2+}, both benzimidazole compounds, mibefradil and NNC 55–0396, evoked a fast and sustained elevation of $[Ca^{2+}]_i$ resembling the stimulatory effect of 50 μM naltriben, although NNC 55–0396 was somewhat weaker than naltriben and mibefradil. Consequently, we now focused on mibefradil.

First, we asked whether the effect of mibefradil on $[Ca^{2+}]_i$ levels was due to increased TRPM7 channel activity. It is well documented that external Mg^{2+} competes with Ca^{2+} for the TRPM7 channel pore and reduces inward currents, whereas NS8593 negatively affects the gating of TRPM7 [11, 46]. Therefore, we tested whether administration of Mg^{2+} or NS8593 to TRPM7 expressing cells would interfere with the mibefradil-induced $[Ca^{2+}]_i$ rise (Fig. 1c). We found that the effect of 50 μM mibefradil was abolished in the presence of either 20 μM NS8593 or 10 mM extracellular Mg^{2+}, indicating that the mibefradil-induced increase in $[Ca^{2+}]_i$ was exclusively mediated by the TRPM7 channel.

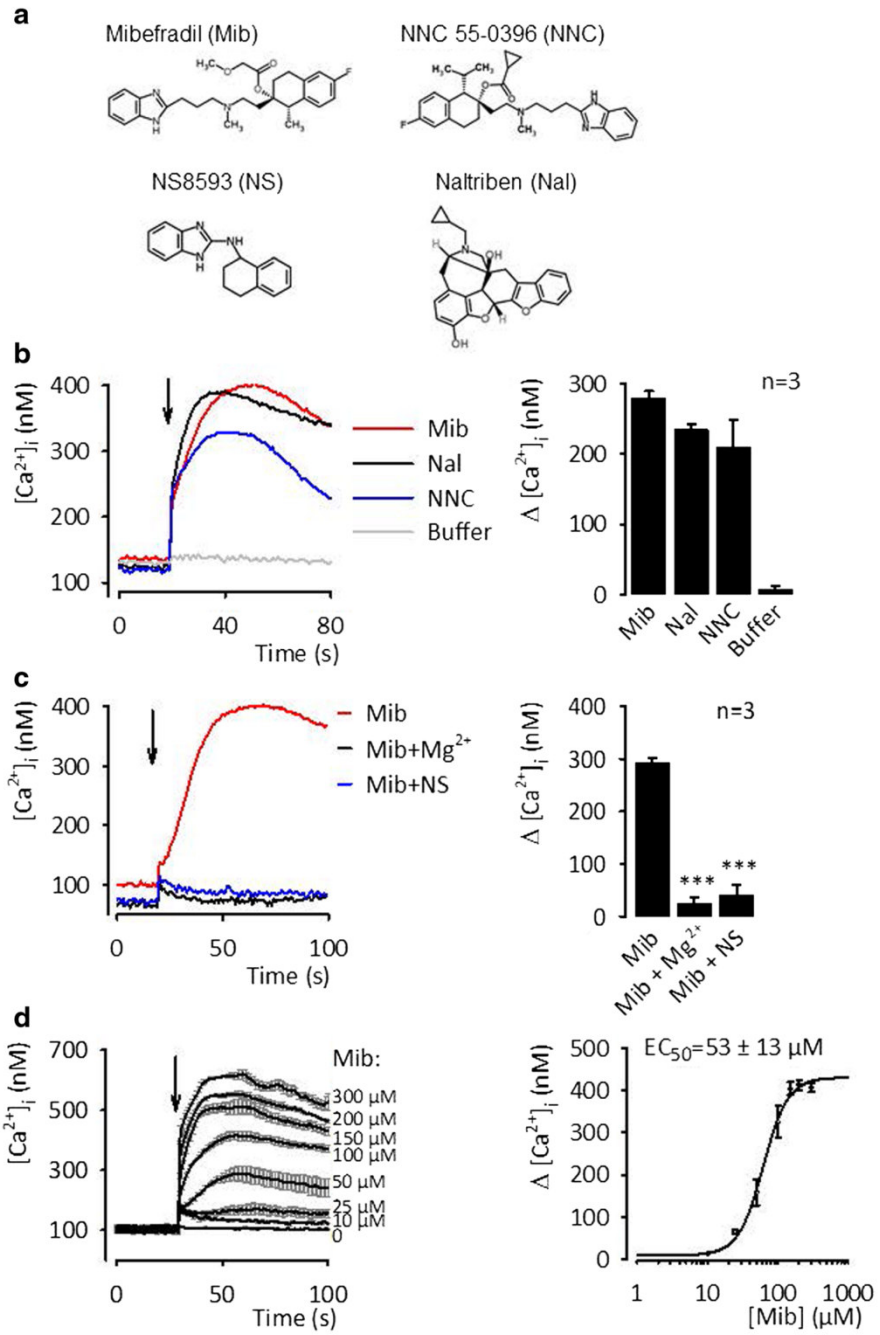

Fig. 1 Effects of mibefradil, NNC 55–0396, and naltriben on TRPM7-mediated Ca^{2+} entry in HEK 293 cells. **a** Chemical structures of the compounds used in the current study. **b** *left panel* Representative traces of $[Ca^{2+}]_i$ in HEK 293 cells (1×10^5 cells per assay) overexpressing TRPM7 are shown. Fifty-micrometer mibefradil (*Mib*), 50 μM NNC 55–0396 (*NNC*), and 50 μM naltriben (*Nal*) were applied at the time indicated by the *vertical arrow*. *right panel* Ca^{2+} rises ($\Delta[Ca^{2+}]_i$) induced by the application of drugs were calculated by subtraction of the resting $[Ca^{2+}]_i$ from the maximal $[Ca^{2+}]_i$ before and after drug application. Mean ± SEM were obtained from three independent transfections ($n = 3$). **c** Measurements were performed as shown in **b** except that 20 μM NS8593 (*NS*) or 10 mM Mg^{2+} (Mg^{2+}) were added to the cells prior to the luminescence recordings. **d** Concentration-response relationship of mibefradil and TRPM7 mediated $\Delta[Ca^{2+}]_i$. Experiments were performed similar to the ones shown in **b**

Next, we determined the concentration-response relationship of mibefradil by measuring maximum $[Ca^{2+}]_i$ levels induced in TRPM7 expressing cells (Fig. 1d). The mibefradil-induced TRPM7-mediated Ca^{2+} entry was found to be concentration-dependent with an EC_{50} value of 53 ± 13 μM ($n = 3$).

Mibefradil induces induced TRPM7 currents in a Mg^{2+}-dependent mode

We next investigated the ability of mibefradil to induce TRPM7 whole-cell currents. Previously, we have shown that naltriben counteracts the inhibitory effect of internal Mg^{2+} on

TRPM7 channel activity [30]. To initially assess the effect of mibefradil on TRPM7, we measured whole-cell TRPM7 currents in the presence of physiological levels of $[Mg^{2+}]_i$ (0.9 mM) (Fig. 2). When TRPM7 currents were developed, we applied mibefradil externally (Fig. 2a). Under these conditions, mibefradil elicited a sustained increase in TRPM7 currents (Fig. 2a). Notably, the effect of mibefradil was substantially faster and transient (Fig. 2a) when compared to the action of naltriben (Fig. 2b). Further analysis revealed that the action of mibefradil on TRPM7 was reversible. In addition, mibefradil was able to repeatedly stimulate TRPM7 currents (Fig. 2c). This finding suggests that the drug does not irreversibly modify TRPM7 protein. Furthermore, the characteristic shape of the current–voltage (I/V) relationship of TRPM7 was not altered in response to mibefradil (Fig. 2c), suggesting that ion permeation and voltage dependency of TRPM7 remained unaffected by the drug.

Next, we examined the influence of $[Mg^{2+}]_i$ on the stimulatory effect of mibefradil on TRPM7 currents. We induced whole-cell TRPM7 currents by perfusing cells with a Mg^{2+}-free intracellular solution (0 mM $[Mg^{2+}]_i$; Fig. 3a). When TRPM7 currents were fully developed, mibefradil was applied. We could only detect a moderate additional increase in TRPM7 activity, suggesting that under these conditions, nearly all TRPM7 channels were already open and, consequently, mibefradil could only modestly affect whole-cell currents. However, when cells were perfused with a more physiological concentration of 0.9 mM free $[Mg^{2+}]_i$ (Fig. 3a), the increase in current amplitude attributable to mibefradil was substantially more pronounced. In contrast, 1.8 mM free $[Mg^{2+}]_i$ was sufficient to fully suppress any TRPM7 activity as well as the response to mibefradil (Fig. 3a). Further experiments showed (Fig. 3b) that a gradual suppression by $[Mg^{2+}]_i$ was achieved in the range of 1.2–1.8 mM. Thus, mibefradil acts on TRPM7 at physiological concentrations of free $[Mg^{2+}]_i$, ranging between 0.5 and 1 mM in most mammalian cells [53]). However, in contrast to naltriben [30], mibefradil was not able to overcome the inhibitory effect of high levels of internal Mg^{2+} on TRPM7, suggesting that this drug preferentially affects TRPM7 at physiological or low intracellular Mg^{2+}.

Extracellular divalent cations such as Mg^{2+} and Ca^{2+} are known to exert a permeation block on the TRPM7 channel pore [46], resulting in very small divalent cation-selective inward currents at physiological membrane potentials. To test whether mibefradil would increase TRPM7 currents by altering the ion permeation profile of the channel, we investigated the effect of mibefradil on the $TRPM7^{E1047Q}$ mutant. Previously, we showed [40] that $TRPM7^{E1047Q}$ is essentially impermeable to divalent cations; i.e., it functions as a monovalent selective ion channel, resembling the TRPM5 channel

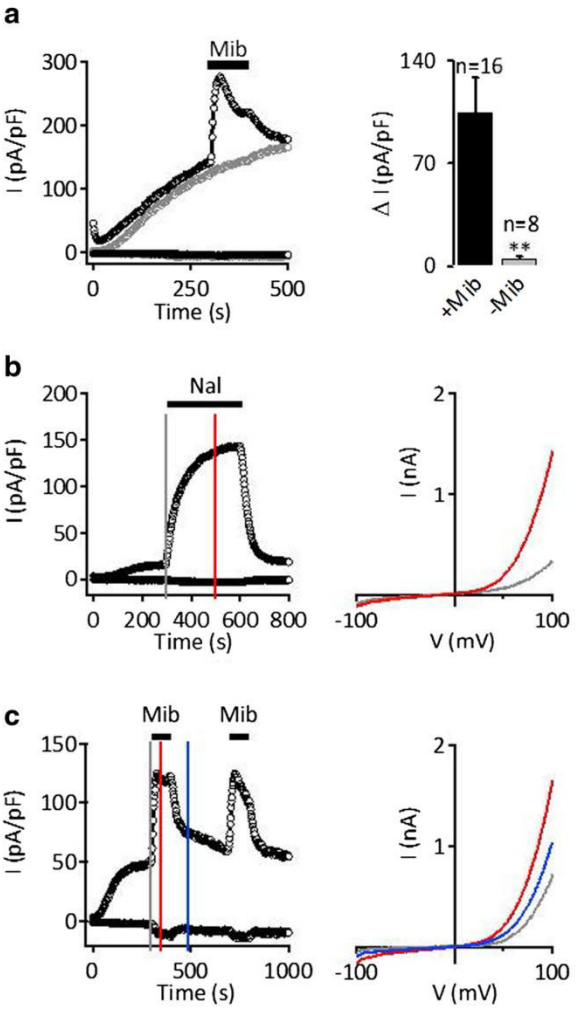

Fig. 2 Effects of naltriben and mibefradil on TRPM7 currents. **a** *left panel* Representative traces of whole-cell TRPM7 currents induced by external application of 50 μM naltriben (*Nal*) to TRPM7 expressing HEK 293 cells perfused with intracellular solution containing 0.9 mM free Mg^{2+}. Whole-cell currents at −80 and +80 mV from voltage ramps applied at 2-s intervals. *right panel* Current-voltage (I-V) relationship of TRPM7 currents obtained before (*gray line*) and after (*red line*) application of naltriben at the time points indicated by the corresponding *vertical bars* in the *left panel*. *Numbers above bars* indicate the number of cells measured. $^{**}P \leq 0.01$ (*t* test). **b** *left panel* Measurements were performed analogous to **a** except that cells were superfused with 100 μM mibefradil (*black traces*) or with standard external solution (*gray traces*). Note the fast induction and decay of the current amplitude in the presence of mibefradil. *right panel Bar graphs* of the mibefradil-induced current densities (ΔpA/pF) were calculated by subtraction of the current density measured at +80 mV before drug application from of the maximal current densities during application. **c** *left panel* Measurements were performed analogous to **b** except that the cells were perfused repeatedly with 100 μM mibefradil (*Mib*). *right panel* Current-voltage (I-V) relationship of TRPM7 currents obtained before (*gray line*), during (*red line*), and after (*blue line*) the application of mibefradil at the time points indicated by the corresponding *vertical bars* in the *left panel*

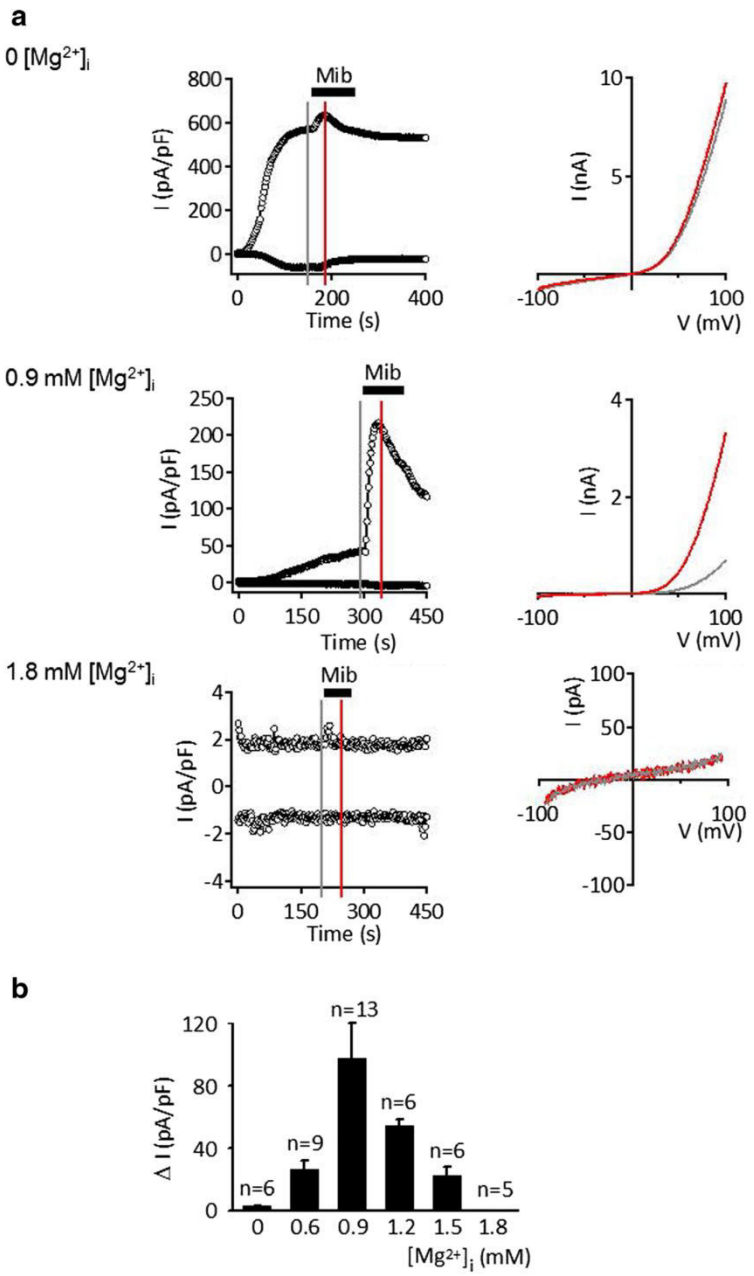

Fig. 3 Effects of internal Mg^{2+} on mibefradil-induced TRPM7 currents. **a** Representative recordings of whole-cell TRPM7 current densities in HEK 293 cells perfused with either Mg^{2+}-free intracellular solution or containing 0.9 and 1.8 mM free Mg^{2+}. Currents were measured at −80 and +80 mV. Current-voltage (I-V) relationship of TRPM7 currents were obtained before (*gray line*) and after (*red line*) application of 100 μM mibefradil at the time points indicated by the corresponding *vertical bars*. **b** Mibefradil-induced TRPM7 current densities as determined in the presence of varying free internal Mg^{2+} levels. Increase in current density amplitudes (ΔpA/pF) was calculated by subtraction of the current densities measured at +80 mV before and after mibefradil (100 μM) application as shown in **a**. *Numbers above bars* indicate the number of cells measured

[29]. As illustrated in Fig. 4a, including 0.9 mM free Mg^{2+} in the internal solution elicited $TRPM7^{E1047Q}$ channel activity characterized by substantially increased inward currents as compared to the WT channel variant (Fig. 3a). We also observed that the application of mibefradil stimulated inward as well as outward monovalent currents mediated by $TRPM7^{E1047Q}$ (Fig. 4a).

Recently, we reported that the exchange of serine at position 1107 to glutamate S1107E ($TRPM7^{S1107E}$) located in TRP domain of TRPM7 results in a constitutively active channel that becomes insensitive both to activation by naltriben and inhibition by $[Mg^{2+}]_i$ [30]. When we assessed the effect of mibefradil on this mutant, we found that the $TRPM7^{S1107E}$ variant showed no response to mibefradil (Fig. 4b), further supporting the notion that mibefradil exerts its activating effect through a modulation of channel gating rather than permeation characteristics of TRPM7.

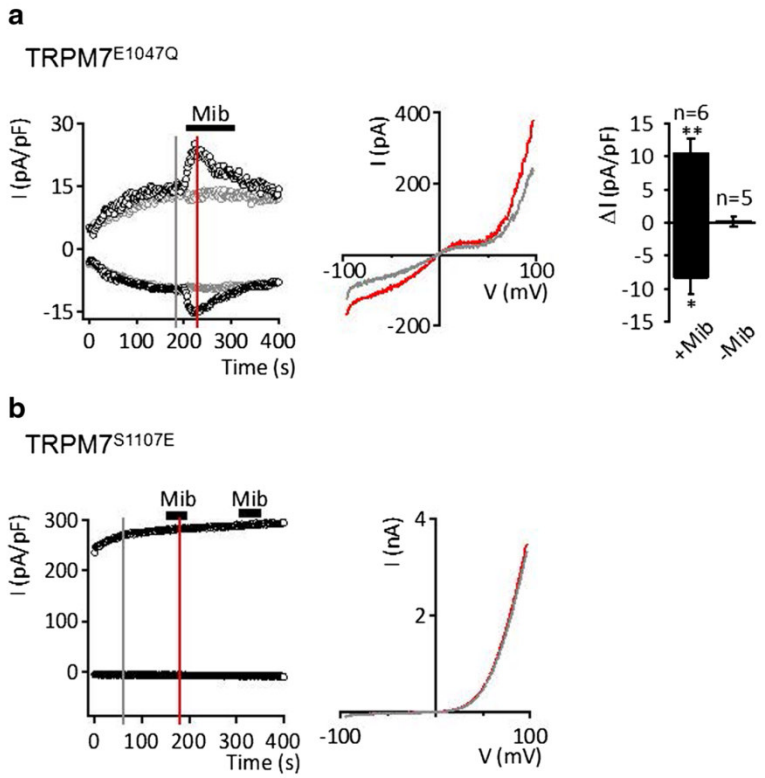

Fig. 4 Probing of mibefradil on TRPM7^{E1047Q} and TRPM7^{S1107E} mutants. **a** Representative recordings of whole-cell currents in HEK 293 cells transiently transfected with a monovalent cation-selective TRPM7^{E1047Q} channel variant. *left panel* Cells were perfused with an intracellular solution containing 0.9 mM Mg^{2+}. Either 100 μM mibefradil (*Mib*) (*black traces*) or the standard external buffer (*grey traces*) were applied in the external solution. *middle panel* Current-voltage (I-V) relationship of TRPM7 currents obtained before (*gray line*) and after (*red line*) application of mibefradil. *right panel Bar graphs* of the mibefradil-induced current densities (ΔpA/pF) were calculated by subtraction of the current density measured at −80 and + 80 mV before drug application from of the maximal current density as indicated by the *grey and red lines* on the *left panel. Numbers above bars* indicate the number of cells measured. $^{**}P \leq 0.01$ (*t* test). **b** Representative recordings of whole-cell currents in HEK 293 cells transiently transfected with a constitutively active TRPM7^{S1107E} channel variant. Measurements were performed in analogy to **a**

TRPM3, TRPV1, and TRPA1 channels are insensitive to mibefradil

In order to assess whether the action of mibefradil on TRPM7 is specific, we tested the drug's impact on a subset of TRP channels, TRPM3, (Fig. 5a) as a close relative of TRPM7 within the TRP superfamily, and TRPA1 and TRPV1, two TRP analogues both sensitive to a variety of small molecules (Fig. 5b, c). Calcium increases were quantified using aequorin in HEK 293 cells expressing the respective channel cDNAs. As positive controls, each of these three channels was challenged with a known specific activator, pregnenolone sulfate in the case of TRPM3, AITC for TRPA1, and capsaicin for TRPV1. Whereas all the positive controls showed substantial calcium rises, mibefradil did not elicit any Ca^{2+} elevations in either case.

To summarize, our findings indicate that mibefradil acts as a specific agonist of the TRPM7 channel. Furthermore, we propose that mibefradil affects TRPM7 channel gating in a Mg^{2+}-dependent mode. To this end, mibefradil and naltriben represent two distinct classes of pharmacological agents acting as TRPM7 agonists.

Discussion and conclusions

Because of the critical role of TRPM7 in physiology, there is a pressing need for pharmacological compounds allowing us to manipulate its function in situ. In addition, such drugs may be instrumental in probing the therapeutic potential of TRPM7 in a growing number of pathophysiological conditions associated with altered TRPM7 function [24]. In our recent studies, we identified a subset of activators of the TRPM7 channel [11, 12, 30]. The TRPM7 modulators identified are drug-like small organic molecules, offering a broad array of scaffold

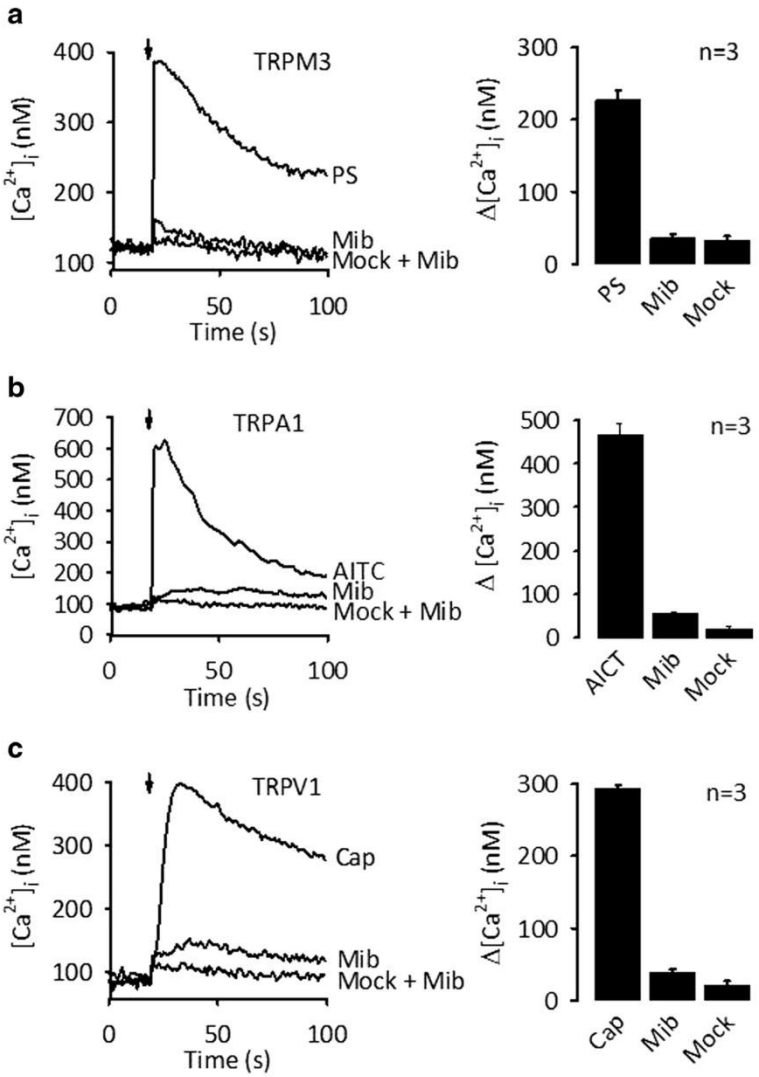

Fig. 5 Testing of mibefradil on TRPM3, TRPV1, and TRPA1 channels. HEK 293 cells were transiently transfected by expression constructs encoding TRPM3, TRPV1, and TRPA1 and were assessed using an aequorin-based approach. **a** *left panel* Representative traces obtained with mock (*Mock*) or TRPM3-transfected cells stimulated with 10 μM pregnenolone sulfate (PS) or 100 μM mibefradil (*Mib*). *right panel* Mean ± SEM of Ca^{2+} increase ($\Delta[Ca^{2+}]_i$) obtained from three independent transfections ($n = 3$, 1×10^5 cells per independent assay). **b** *left panel* Representative traces obtained with mock (*Mock*) or TRPA1-transfected cells stimulated with 10 μM allyl isothiocyanate (*AITC*) or 100 μM mibefradil (*Mib*). *right panel* Mean ± SEM of Ca^{2+} increase ($\Delta[Ca^{2+}]_i$) obtained from three independent transfections ($n = 3$, 1×10^5 cells per independent assay). **c** *left panel* Representative traces obtained with mock (*Mock*) or TRPV1-transfected cells stimulated with 1 μM capsaicin (*Cap*) or 100 μM mibefradil (Mib). *right panel* Mean ± SEM of Ca^{2+} increase ($\Delta[Ca^{2+}]_i$) obtained from three independent transfections ($n = 3$, 1×10^5 cells per independent assay)

structures that can be further exploited to increase the functional diversity and potency of TRPM7 agonists [12].

In the present study, we selected mibefradil from the list of identified activators of the TRPM7 channel [30] for further characterization. Mibefradil and its homolog NNC 55–0396 display structural similarity to NS8593, a potent negative gating modulator of the TRPM7 channel [11], compatible with the notion that all three compounds interact with a common ligand-binding site in TRPM7 with distinct functional consequences for channel function. Our experiments revealed that mibefradil is able to stimulate TRPM7-mediated Ca^{2+} entry as well as TRPM7 currents. The effect of mibefradil on TRPM7 currents was fast, partially transient, and fully reversible. Furthermore, mibefradil affected the TRPM7 channel in both divalent and monovalent cation conduction modes. The action of mibefradil was highly dependent on $[Mg^{2+}]_i$ and was not observed in the constitutively active $TRPM7^{S1107E}$ channel variant lacking any impact of $[Mg^{2+}]_i$ on gating. Taken together, these findings indicate that mibefradil is a stimulatory agonist of the TRPM7 channel.

Mibefradil was originally proposed as a specific inhibitor of T- and L-type voltage-dependent Ca^{2+} channels, with some selectivity for T-type Ca^{2+} channels [4, 74]. In addition, it was shown that mibefradil is a potent inhibitor of Ca^{2+}- and volume-activated Cl^- channels [47]. Mibefradil was used as a drug for the treatment of angina and high blood pressure. The drug also elicits poorly understood side effects such as headache, dizziness, nausea, and other complications [52]. Mibefradil was withdrawn from clinical use mainly due to pharmacokinetic interactions with a variety of commonly used drugs possibly due to its inhibitory effect on cytochrome P450 enzymes [67]. However, the compound is still broadly used as

an experimental drug to probe voltage-dependent Ca^{2+} channels in vitro and in vivo. As shown in here, mibefradil exhibits a moderate potency for TRPM7 activation when compared to voltage-gated Ca^{2+} channels. The EC_{50} value determined for TRPM7 was 53 μM, as compared to 2.7 μM described for voltage-dependent T-type Ca^{2+} channels [4] and 18.6 μM for voltage-dependent L-type Ca^{2+} channels [4]. Nevertheless, our data suggest that the ubiquitously expressed TRPM7 may contribute to the pharmacological action of mibefradil. Specifically, mibefradil-induced TRPM7 influx of divalent cations such Ca^{2+}, Zn^{2+}, and Mg^{2+} may alter cellular processes, which were thought to be affected by a block of voltage-dependent Ca^{2+} channels.

Recently, we have identified naltriben as the first drug-like activator of the TRPM7 channel [30]. In contrast to mibefradil, naltriben activates TRPM7 currents even in the presence of high levels of intracellular Mg^{2+}. Accordingly, we postulate that at least two types of TRPM7 agonists do exist, in here referred to as types 1 and 2. Naltriben is the prototype of type 1 activators allowing to induce TRPM7 activity independently of $[Mg^{2+}]_i$. Mibefradil epitomizes type 2 agonists acting on TRPM7 in a $[Mg^{2+}]_i$-dependent mode.

Mg^{2+} is the second most abundant cellular cation. Total cellular Mg^{2+} content was estimated to be in the range of 15 to 18 mM [53]. The majority of intracellular Mg^{2+} is complexed by phosphometabolites such as ATP, phospholipids, proteins, and nucleic acids [53]. Physiological levels of free $[Mg^{2+}]_i$ are in the range of 0.5–1 mM in most mammalian cells [53]. Under certain conditions, for instance in dividing cells or during extensive cell growth, free $[Mg^{2+}]_i$ can be reduced due to high Mg^{2+} consumption by the synthesis of new phosphometabolites. Therefore, it has been suggested that Mg^{2+} may serve as "the common denominator" of basic needs of cancer cells, because tumor growth/progression relies on a sustained increase in energy consumption and biosynthesis of macromolecules [79]. Our findings suggest that the type 1 and type 2 TRPM7 activators allow for a differential targeting of cellular metabolism. Naltriben (type 1) will stimulate TRPM7 irrespective of $[Mg^{2+}]_i$, whereas mibefradil (type 2) will act preferentially on cells with reduced $[Mg^{2+}]_i$. In the future, it will be enlightening to explore whether putative endogenous TRPM7 ligands act in a similar manner.

Acknowledgements S.S. was supported by the Förderprogramm für Forschung und Lehre Fellowship (FöFoLe) of the LMU, Munich. V.C., S.Z., and T.G. were supported by the Deutsche Forschungsgemeinschaft, TRR 152. S.Z. was supported by Marie-Curie Fellowship (REA) FP7-PEOPLE-2012-CIG. We thank Joanna Zaißerer and Anna Erbacher for their excellent technical assistance.

Conflicts of interest None

References

1. Aarts M, Iihara K, Wei WL, Xiong ZG, Arundine M, Cerwinski W, MacDonald JF, Tymianski M (2003) A key role for TRPM7 channels in anoxic neuronal death. Cell 115(7):863–877
2. Abed E, Martineau C, Moreau R (2011) Role of melastatin transient receptor potential 7 channels in the osteoblastic differentiation of murine MC3T3 cells. Calcif Tissue Int 88(3):246–253. doi:10.1007/s00223-010-9455-z
3. Baubet V, Le Mouellic H, Campbell AK, Lucas-Meunier E, Fossier P, Brulet P (2000) Chimeric green fluorescent protein-aequorin as bioluminescent Ca2+ reporters at the single-cell level. Proc Natl Acad Sci U S A 97(13):7260–7265
4. Bezprozvanny I, Tsien RW (1995) Voltage-dependent blockade of diverse types of voltage-gated Ca2+ channels expressed in Xenopus oocytes by the Ca2+ channel antagonist mibefradil (Ro 40–5967). Mol Pharmacol 48(3):540–549
5. Brauchi S, Krapivinsky G, Krapivinsky L, Clapham DE (2008) TRPM7 facilitates cholinergic vesicle fusion with the plasma membrane. Proc Natl Acad Sci U S A 105(24):8304–8308. doi:10.1073/pnas.0800881105
6. Cao E, Liao M, Cheng Y, Julius D (2013) TRPV1 structures in distinct conformations reveal activation mechanisms. Nature 504(7478):113–118. doi:10.1038/nature12823
7. Caterina MJ, Schumacher MA, Tominaga M, Rosen TA, Levine JD, Julius D (1997) The capsaicin receptor: a heat-activated ion channel in the pain pathway. Nature 389(6653):816–824. doi:10.1038/39807
8. Chen YF, Chen YT, Chiu WT, Shen MR (2013) Remodeling of calcium signaling in tumor progression. J Biomed Sci 20:23. doi:10.1186/1423-0127-20-23
9. Chen JP, Luan Y, You CX, Chen XH, Luo RC, Li R (2010) TRPM7 regulates the migration of human nasopharyngeal carcinoma cell by mediating Ca(2+) influx. Cell Calcium 47(5):425–432. doi:10.1016/j.ceca.2010.03.003
10. Chen KH, Xu XH, Liu Y, Hu Y, Jin MW, Li GR (2013) TRPM7 channels regulate proliferation and adipogenesis in 3T3-L1 preadipocytes. J Cell Physiol 229(1):60–67. doi:10.1002/jcp.24417
11. Chubanov V, Mederos y Schnitzler M, Meissner M, Schafer S, Abstiens K, Hofmann T, Gudermann T (2012) Natural and synthetic modulators of SK (K(ca)2) potassium channels inhibit magnesium-dependent activity of the kinase-coupled cation channel TRPM7. Br J Pharmacol 166(4):1357–1376. doi:10.1111/j.1476-5381.2012.01855.x
12. Chubanov V, Schafer S, Ferioli S, Gudermann T (2014) Natural and synthetic modulators of the TRPM7 channel. Cell 3(4):1089–1101. doi:10.3390/cells3041089
13. Chubanov V, Schlingmann KP, Waring J, Heinzinger J, Kaske S, Waldegger S, Mederos y Schnitzler M, Gudermann T (2007) Hypomagnesemia with secondary hypocalcemia due to a missense mutation in the putative pore-forming region of TRPM6. J Biol Chem 282(10):7656–7667. doi:10.1074/jbc.M611117200
14. Chubanov V, Waldegger S, Mederos y Schnitzler M, Vitzthum H, Sassen MC, Seyberth HW, Konrad M, Gudermann T (2004) Disruption of TRPM6/TRPM7 complex formation by a mutation in the TRPM6 gene causes hypomagnesemia with secondary hypocalcemia. Proc Natl Acad Sci U S A 101(9):2894–2899. doi:10.1073/pnas.0305252101
15. Clark K, Langeslag M, van Leeuwen B, Ran L, Ryazanov AG, Figdor CG, Moolenaar WH, Jalink K, van Leeuwen FN (2006) TRPM7, a novel regulator of actomyosin contractility and cell adhesion. EMBO J 25(2):290–301. doi:10.1038/sj.emboj.7600931
16. Clark K, Middelbeek J, Morrice NA, Figdor CG, Lasonder E, van Leeuwen FN (2008) Massive autophosphorylation of the Ser/Thr-

rich domain controls protein kinase activity of TRPM6 and TRPM7. PLoS One 3(3):e1876. doi:10.1371/journal.pone.0001876

17. Deason-Towne F, Perraud AL, Schmitz C (2012) Identification of Ser/Thr phosphorylation sites in the C2-domain of phospholipase C gamma2 (PLCgamma2) using TRPM7-kinase. Cell Signal 24(11): 2070–2075. doi:10.1016/j.cellsig.2012.06.015
18. Demeuse P, Penner R, Fleig A (2006) TRPM7 channel is regulated by magnesium nucleotides via its kinase domain. J Gen Physiol 127(4):421–434. doi:10.1085/jgp.200509410
19. Desai BN, Krapivinsky G, Navarro B, Krapivinsky L, Carter BC, Febvay S, Delling M, Penumaka A, Ramsey IS, Manasian Y, Clapham DE (2012) Cleavage of TRPM7 releases the kinase domain from the ion channel and regulates its participation in Fas-induced apoptosis. Dev Cell 22(6):1149–1162. doi:10.1016/j.devcel.2012.04.006
20. Dorovkov MV, Kostyukova AS, Ryazanov AG (2011) Phosphorylation of annexin A1 by TRPM7 kinase: a switch regulating the induction of an alpha-helix. Biochemistry 50(12):2187–2193. doi:10.1021/bi101963h
21. Du J, Xie J, Zhang Z, Tsujikawa H, Fusco D, Silverman D, Liang B, Yue L (2010) TRPM7-mediated Ca2+ signals confer fibrogenesis in human atrial fibrillation. Circ Res 106(5):992–1003. doi:10.1161/CIRCRESAHA.109.206771
22. Elizondo MR, Arduini BL, Paulsen J, MacDonald EL, Sabel JL, Henion PD, Cornell RA, Parichy DM (2005) Defective skeletogenesis with kidney stone formation in dwarf zebrafish mutant for trpm7. Curr Biol 15(7):667–671. doi:10.1016/j.cub.2005.02.050
23. Fang L, Huang C, Meng X, Wu B, Ma T, Liu X, Zhu Q, Zhan S, Li J (2014) TGF-beta1-elevated TRPM7 channel regulates collagen expression in hepatic stellate cells via TGF-beta1/Smad pathway. Toxicol Appl Pharmacol 280(2):335–344. doi:10.1016/j.taap.2014.08.006
24. Fleig A, Chubanov V (2014) Trpm7. Handb Exp Pharmacol 222: 521–546. doi:10.1007/978-3-642-54215-2_21
25. Gao H, Chen X, Du X, Guan B, Liu Y, Zhang H (2011) EGF enhances the migration of cancer cells by up-regulation of TRPM7. Cell Calcium 50(6):559–568. doi:10.1016/j.ceca.2011.09.003
26. Guilbert A, Gautier M, Dhennin-Duthille I, Haren N, Sevestre H, Ouadid-Ahidouch H (2009) Evidence that TRPM7 is required for breast cancer cell proliferation. Am J Physiol Cell Physiol 297(3): C493–C502. doi:10.1152/ajpcell.00624.2008
27. Hanano T, Hara Y, Shi J, Morita H, Umebayashi C, Mori E, Sumimoto H, Ito Y, Mori Y, Inoue R (2004) Involvement of TRPM7 in cell growth as a spontaneously activated Ca2+ entry pathway in human retinoblastoma cells. J Pharmacol Sci 95(4): 403–419
28. Hermosura MC, Nayakanti H, Dorovkov MV, Calderon FR, Ryazanov AG, Haymer DS, Garruto RM (2005) A TRPM7 variant shows altered sensitivity to magnesium that may contribute to the pathogenesis of two Guamanian neurodegenerative disorders. Proc Natl Acad Sci U S A 102(32):11510–11515. doi:10.1073/pnas.0505149102
29. Hofmann T, Chubanov V, Gudermann T, Montell C (2003) TRPM5 is a voltage-modulated and Ca(2+)-activated monovalent selective cation channel. Curr Biol 13(13):1153–1158
30. Hofmann T, Schafer S, Linseisen M, Sytik L, Gudermann T, Chubanov V (2014) Activation of TRPM7 channels by small molecules under physiological conditions. Pflugers Arch 466(12): 2177–2189. doi:10.1007/s00424-014-1488-0
31. Jiang J, Li MH, Inoue K, Chu XP, Seeds J, Xiong ZG (2007) Transient receptor potential melastatin 7-like current in human head and neck carcinoma cells: role in cell proliferation. Cancer Res 67(22):10929–10938. doi:10.1158/0008-5472.CAN-07-1121
32. Jin J, Desai BN, Navarro B, Donovan A, Andrews NC, Clapham DE (2008) Deletion of Trpm7 disrupts embryonic development and thymopoiesis without altering Mg2+ homeostasis. Science 322(5902):756–760. doi:10.1126/science.1163493
33. Jin J, Wu LJ, Jun J, Cheng X, Xu H, Andrews NC, Clapham DE (2011) The channel kinase, TRPM7, is required for early embryonic development. Proc Natl Acad Sci U S A 109(5):E225–E233. doi:10.1073/pnas.1120033109
34. Jordt SE, Bautista DM, Chuang HH, McKemy DD, Zygmunt PM, Hogestatt ED, Meng ID, Julius D (2004) Mustard oils and cannabinoids excite sensory nerve fibres through the TRP channel ANKTM1. Nature 427(6971):260–265. doi:10.1038/nature02282
35. Kim BJ, Park EJ, Lee JH, Jeon JH, Kim SJ, So I (2008) Suppression of transient receptor potential melastatin 7 channel induces cell death in gastric cancer. Cancer Sci 99(12):2502–2509. doi:10.1111/j.1349-7006.2008.00982.x
36. Kozak JA, Matsushita M, Nairn AC, Cahalan MD (2005) Charge screening by internal pH and polyvalent cations as a mechanism for activation, inhibition, and rundown of TRPM7/MIC channels. J Gen Physiol 126(5):499–514. doi:10.1085/jgp.200509324
37. Krapivinsky G, Krapivinsky L, Manasian Y, Clapham DE (2014) The TRPM7 chanzyme is cleaved to release a chromatin-modifying kinase. Cell 157(5):1061–1072. doi:10.1016/j.cell.2014.03.046
38. Kuras Z, Yun YH, Chimote AA, Neumeier L, Conforti L (2012) KCa3.1 and TRPM7 channels at the uropod regulate migration of activated human T cells. PLoS One 7(8):e43859. doi:10.1371/journal.pone.0043859
39. Leng TD, Li MH, Shen JF, Liu ML, Li XB, Sun HW, Branigan D, Zeng Z, Si HF, Li J, Chen J, Xiong ZG (2015) Suppression of TRPM7 inhibits proliferation, migration, and invasion of malignant human glioma cells. CNS Neurosci Ther 21(3):252–261. doi:10.1111/cns.12354
40. Mederos y Schnitzler M, Waring J, Gudermann T, Chubanov V (2008) Evolutionary determinants of divergent calcium selectivity of TRPM channels. FASEB J 22(5):1540–1551. doi:10.1096/fj.07-9694com
41. Meng X, Cai C, Wu J, Cai S, Ye C, Chen H, Yang Z, Zeng H, Shen Q, Zou F (2013) TRPM7 mediates breast cancer cell migration and invasion through the MAPK pathway. Cancer Lett 333(1):96–102. doi:10.1016/j.canlet.2013.01.031
42. Middelbeek J, Kuipers AJ, Henneman L, Visser D, Eidhof I, van Horssen R, Wieringa B, Canisius SV, Zwart W, Wessels LF, Sweep FC, Bult P, Span PN, van Leeuwen FN, Jalink K (2012) TRPM7 is required for breast tumor cell metastasis. Cancer Res 72(16):4250–4261. doi:10.1158/0008-5472.CAN-11-3863
43. Middelbeek J, Visser D, Henneman L, Kamermans A, Kuipers AJ, Hoogerbrugge PM, Jalink K, van Leeuwen FN (2015) TRPM7 maintains progenitor-like features of neuroblastoma cells: implications for metastasis formation. Oncotarget 6(11):8760–8776
44. Monteilh-Zoller MK, Hermosura MC, Nadler MJ, Scharenberg AM, Penner R, Fleig A (2003) TRPM7 provides an ion channel mechanism for cellular entry of trace metal ions. J Gen Physiol 121(1):49–60
45. Montezano AC, Zimmerman D, Yusuf H, Burger D, Chignalia AZ, Wadhera V, van Leeuwen FN, Touyz RM (2010) Vascular smooth muscle cell differentiation to an osteogenic phenotype involves TRPM7 modulation by magnesium. Hypertension 56(3):453–462. doi:10.1161/HYPERTENSIONAHA.110.152058
46. Nadler MJ, Hermosura MC, Inabe K, Perraud AL, Zhu Q, Stokes AJ, Kurosaki T, Kinet JP, Penner R, Scharenberg AM, Fleig A (2001) LTRPC7 is a Mg.ATP-regulated divalent cation channel required for cell viability. Nature 411(6837):590–595. doi:10.1038/35079092
47. Nilius B, Prenen J, Kamouchi M, Viana F, Voets T, Droogmans G (1997) Inhibition by mibefradil, a novel calcium channel antagonist, of Ca(2+)- and volume-activated Cl^- channels in

macrovascular endothelial cells. Br J Pharmacol 121(3):547–555. doi:10.1038/sj.bjp.0701140
48. Numata T, Shimizu T, Okada Y (2007) Direct mechano-stress sensitivity of TRPM7 channel. Cell Physiol Biochem 19(1–4):1–8. doi:10.1159/000099187
49. Oancea E, Wolfe JT, Clapham DE (2006) Functional TRPM7 channels accumulate at the plasma membrane in response to fluid flow. Circ Res 98(2):245–253. doi:10.1161/01.RES.0000200179.29375.cc
50. Peier AM, Moqrich A, Hergarden AC, Reeve AJ, Andersson DA, Story GM, Earley TJ, Dragoni I, McIntyre P, Bevan S, Patapoutian A (2002) A TRP channel that senses cold stimuli and menthol. Cell 108(5):705–715
51. Perraud AL, Zhao X, Ryazanov AG, Schmitz C (2010) The channel-kinase TRPM7 regulates phosphorylation of the translational factor eEF2 via eEF2-k. Cell Signal 23(3):586–593. doi:10.1016/j.cellsig.2010.11.011
52. Riley J, Wilton LV, Shakir SA (2002) A post-marketing observational study to assess the safety of mibefradil in the community in England. Int J Clin Pharmacol Ther 40(6):241–248
53. Romani AM (2011) Cellular magnesium homeostasis. Arch Biochem Biophys 512(1):1–23. doi:10.1016/j.abb.2011.05.010
54. Runnels LW, Yue L, Clapham DE (2001) TRP-PLIK, a bifunctional protein with kinase and ion channel activities. Science 291(5506):1043–1047. doi:10.1126/science.1058519
55. Runnels LW, Yue L, Clapham DE (2002) The TRPM7 channel is inactivated by PIP(2) hydrolysis. Nat Cell Biol 4(5):329–336. doi:10.1038/ncb781
56. Ryazanova LV, Hu Z, Suzuki S, Chubanov V, Fleig A, Ryazanov AG (2014) Elucidating the role of the TRPM7 alpha-kinase: TRPM7 kinase inactivation leads to magnesium deprivation resistance phenotype in mice. Sci Rep 4:7599. doi:10.1038/srep07599
57. Ryazanova LV, Rondon LJ, Zierler S, Hu Z, Galli J, Yamaguchi TP, Mazur A, Fleig A, Ryazanov AG (2010) TRPM7 is essential for Mg(2+) homeostasis in mammals. Nat Commun 1:109. doi:10.1038/ncomms1108
58. Rybarczyk P, Gautier M, Hague F, Dhennin-Duthille I, Chatelain D, Kerr-Conte J, Pattou F, Regimbeau JM, Sevestre H, Ouadid-Ahidouch H (2012) Transient receptor potential melastatin-related 7 channel is overexpressed in human pancreatic ductal adenocarcinomas and regulates human pancreatic cancer cell migration. Int J Cancer 131(6):E851–E861. doi:10.1002/ijc.27487
59. Sah R, Mesirca P, Mason X, Gibson W, Bates-Withers C, Van den Boogert M, Chaudhuri D, Pu WT, Mangoni ME, Clapham DE (2013) Timing of myocardial trpm7 deletion during cardiogenesis variably disrupts adult ventricular function, conduction, and repolarization. Circulation 128(2):101–114. doi:10.1161/CIRCULATIONAHA.112.000768
60. Sah R, Mesirca P, Van den Boogert M, Rosen J, Mably J, Mangoni ME, Clapham DE (2013) Ion channel-kinase TRPM7 is required for maintaining cardiac automaticity. Proc Natl Acad Sci U S A 110(32):E3037–E3046. doi:10.1073/pnas.1311865110
61. Sahni J, Scharenberg AM (2008) TRPM7 ion channels are required for sustained phosphoinositide 3-kinase signaling in lymphocytes. Cell Metab 8(1):84–93. doi:10.1016/j.cmet.2008.06.002
62. Schmitz C, Brandao K, Perraud AL (2014) The channel-kinase TRPM7, revealing the untold story of Mg(2+) in cellular signaling. Magnesium Res 27(1):9–15. doi:10.1684/mrh.2014.0357
63. Schmitz C, Perraud AL, Johnson CO, Inabe K, Smith MK, Penner R, Kurosaki T, Fleig A, Scharenberg AM (2003) Regulation of vertebrate cellular Mg2+ homeostasis by TRPM7. Cell 114(2):191–200
64. Shen B, Sun L, Zheng H, Yang D, Zhang J, Zhang Q (2014) The association between single-nucleotide polymorphisms of TRPM7 gene and breast cancer in Han Population of Northeast China. Med Oncol 31(7):51. doi:10.1007/s12032-014-0051-3
65. Siddiqui TA, Lively S, Vincent C, Schlichter LC (2012) Regulation of podosome formation, microglial migration and invasion by Ca(2+)-signaling molecules expressed in podosomes. J Neuroinflammation 9:250. doi:10.1186/1742-2094-9-250
66. Sontia B, Montezano AC, Paravicini T, Tabet F, Touyz RM (2008) Downregulation of renal TRPM7 and increased inflammation and fibrosis in aldosterone-infused mice: effects of magnesium. Hypertension 51(4):915–921. doi:10.1161/HYPERTENSIONAHA.107.100339
67. SoRelle R (1998) Withdrawal of Posicor from market. Circulation 98(9):831–832
68. Su LT, Agapito MA, Li M, Simonson WT, Huttenlocher A, Habas R, Yue L, Runnels LW (2006) TRPM7 regulates cell adhesion by controlling the calcium-dependent protease calpain. J Biol Chem 281(16):11260–11270. doi:10.1074/jbc.M512885200
69. Su LT, Liu W, Chen HC, Gonzalez-Pagan O, Habas R, Runnels LW (2011) TRPM7 regulates polarized cell movements. Biochem J 434(3):513–521. doi:10.1042/BJ20101678
70. Sun Y, Sukumaran P, Varma A, Derry S, Sahmoun AE, Singh BB (2014) Cholesterol-induced activation of TRPM7 regulates cell proliferation, migration, and viability of human prostate cells. Biochim Biophys Acta 1843(9):1839–1850. doi:10.1016/j.bbamcr.2014.04.019
71. Tashiro M, Inoue H, Konishi M (2014) Physiological pathway of magnesium influx in rat ventricular myocytes. Biophys J 107(9):2049–2058. doi:10.1016/j.bpj.2014.09.015
72. Touyz RM (2008) Transient receptor potential melastatin 6 and 7 channels, magnesium transport, and vascular biology: implications in hypertension. Am J Physiol Heart Circ Physiol 294(3):H1103–H1118. doi:10.1152/ajpheart.00903.2007
73. Tseveleki V, Rubio R, Vamvakas SS, White J, Taoufik E, Petit E, Quackenbush J, Probert L (2010) Comparative gene expression analysis in mouse models for multiple sclerosis, Alzheimer's disease and stroke for identifying commonly regulated and disease-specific gene changes. Genomics 96(2):82–91. doi:10.1016/j.ygeno.2010.04.004
74. Viana F, Van den Bosch L, Missiaen L, Vandenberghe W, Droogmans G, Nilius B, Robberecht W (1997) Mibefradil (Ro 40–5967) blocks multiple types of voltage-gated calcium channels in cultured rat spinal motoneurones. Cell Calcium 22(4):299–311
75. Wagner TF, Loch S, Lambert S, Straub I, Mannebach S, Mathar I, Dufer M, Lis A, Flockerzi V, Philipp SE, Oberwinkler J (2008) Transient receptor potential M3 channels are ionotropic steroid receptors in pancreatic beta cells. Nat Cell Biol 10(12):1421–1430. doi:10.1038/ncb1801
76. Wang J, Xiao L, Luo CH, Zhou H, Hu J, Tang YX, Fang KN, Zhang Y (2014) Overexpression of TRPM7 is associated with poor prognosis in human ovarian carcinoma. Asian Pac J Cancer Prev 15(9):3955–3958
77. Watanabe H, Davis JB, Smart D, Jerman JC, Smith GD, Hayes P, Vriens J, Cairns W, Wissenbach U, Prenen J, Flockerzi V, Droogmans G, Benham CD, Nilius B (2002) Activation of TRPV4 channels (hVRL-2/mTRP12) by phorbol derivatives. J Biol Chem 277(16):13569–13577. doi:10.1074/jbc.M200062200
78. Wei C, Wang X, Chen M, Ouyang K, Song LS, Cheng H (2009) Calcium flickers steer cell migration. Nature 457(7231):901–905. doi:10.1038/nature07577
79. Wolf FI, Trapani V (2012) Magnesium and its transporters in cancer: a novel paradigm in tumour development. Clin Sci 123(7):417–427. doi:10.1042/CS20120086
80. Yee NS, Kazi AA, Li Q, Yang Z, Berg A, Yee RK (2015) Aberrant over-expression of TRPM7 ion channels in pancreatic cancer: required for cancer cell invasion and implicated in tumor growth and metastasis. Biol Open 4(4):507–514. doi:10.1242/bio.20137088
81. Zhang Z, Faouzi M, Huang J, Geerts D, Yu H, Fleig A, Penner R (2014) N-Myc-induced up-regulation of TRPM6/TRPM7 channels promotes neuroblastoma cell proliferation. Oncotarget 5(17):7625–7634

82. Zhang Z, Wang M, Fan XH, Chen JH, Guan YY, Tang YB (2012) Upregulation of TRPM7 channels by angiotensin II triggers phenotypic switching of vascular smooth muscle cells of ascending aorta. Circ Res 111(9):1137–1146. doi:10.1161/CIRCRESAHA.112.273755

83. Zierler S, Yao G, Zhang Z, Kuo WC, Porzgen P, Penner R, Horgen FD, Fleig A (2011) Waixenicin A inhibits cell proliferation through magnesium-dependent block of transient receptor potential melastatin 7 (TRPM7) channels. J Biol Chem 286(45):39328–39335. doi:10.1074/jbc.M111.264341

Activation of TRPM7 channels by small molecules under physiological conditions

Pflugers Arch - Eur J Physiol (2014) 466:2177–2189
DOI 10.1007/s00424-014-1488-0

ION CHANNELS, RECEPTORS AND TRANSPORTERS

Activation of TRPM7 channels by small molecules under physiological conditions

T. Hofmann · S. Schäfer · M. Linseisen · L. Sytik · T. Gudermann · V. Chubanov

Received: 23 January 2014 / Revised: 17 February 2014 / Accepted: 18 February 2014 / Published online: 15 March 2014

Abstract Transient receptor potential cation channel, subfamily M, member 7 (TRPM7) is a cation channel covalently linked to a protein kinase domain. TRPM7 is ubiquitously expressed and regulates key cellular processes such as Mg^{2+} homeostasis, motility, and proliferation. TRPM7 is involved in anoxic neuronal death, cardiac fibrosis, and tumor growth. The goal of this work was to identify small molecule activators of the TRPM7 channel and investigate their mechanism of action. We used an aequorin bioluminescence-based assay to screen for activators of the TRPM7 channel. Valid candidates were further characterized using patch clamp electrophysiology. We identified 20 drug-like compounds with various structural backbones that can activate the TRPM7 channel. Among them, the δ opioid antagonist naltriben was studied in greater detail. Naltriben's action was selective among the TRP channels tested. Naltriben activates TRPM7 currents without prior depletion of intracellular Mg^{2+} even under conditions of low PIP_2. Moreover, naltriben interfered with the effect of the TRPM7 inhibitor NS8593. Finally, our experiments with TRPM7 variants carrying mutations in the pore, TRP, and kinase domains indicate that the site of TRPM7 activation by this small-molecule ligand is most likely located in or near the TRP domain. In conclusion, we identified the first organic small-molecule activators of TRPM7 channels, thus providing new experimental tools to study TRPM7 function in native cellular environments.

Keywords TRPM7 · Magnesium · Calcium · Phosphatidylinositol 4,5-bisphosphate · Naltriben · δ opioids

Abbreviations

TRPM7	Melastatin-related TRP cation channel 7
PIP_2	Phosphatidylinositol 4,5-bisphosphate
PLC	Phospholipid lipase C
GPCRs	G-protein-coupled receptors

Introduction

Transient receptor potential cation channel, subfamily M, member 7 (TRPM7) is a plasma membrane protein that contains a transmembrane ion channel segment linked to a cytosolic α-type serine/threonine protein kinase domain [45, 56, 58, 80]. TRPM7 is expressed in all mammalian cells examined so far [3, 49, 52, 55]. Experiments with TRPM7-deficient animals revealed that TRPM7 is required for early embryonic development, thymopoiesis, morphogenesis of the kidney, cardiac automaticity, and systemic Mg^{2+} homeostasis [23, 31, 32, 59, 61, 62]. Studies with cultured cells suggest that TRPM7 regulates many key cellular processes such as Mg^{2+} homeostasis [13, 59, 63, 64], cell motility [9, 14, 38, 41, 65, 67, 68, 78], proliferation/cell death [10, 19, 45, 63, 64, 82], differentiation [2, 81], mechanosensitivity [47, 48, 78], and exocytosis [5]. Furthermore, TRPM7 may play a causative role in anoxic neuronal death [1], hypertension [71], neurodegenerative disorders [28, 73], cardiac fibrosis [22], and tumor growth [8, 24–26, 29, 35, 42, 60].

Despite the emerging physiological and pathophysiological importance of TRPM7, a mechanistic understanding of its

T. Hofmann and S. Schäfer contributed equally to this work.

T. Hofmann (✉)
Philipps-Universität Marburg, Klinik für Innere Medizin/Nephrologie, Baldingerstraße 1, 35043 Marburg, Germany
e-mail: hofmannt@med.uni-marburg.de

S. Schäfer · M. Linseisen · L. Sytik · T. Gudermann · V. Chubanov (✉)
Walther-Straub-Institute of Pharmacology and Toxicology, University of Munich, Goethestrasse 33, 80336 Munich, Germany
e-mail: vladimir.chubanov@lrz.uni-muenchen.de

cellular action is still in its infancy and subject to considerable controversy [31, 37, 45, 56, 59]. For instance, the role of the TRPM7 kinase domain is poorly defined; yet annexin A1, myosin II isoforms, eEF2-k, and PLCγ2 as well as TRPM7 residues in a "substrate" domain have been shown to be potential physiological targets [14, 15, 17, 21, 54]. The channel segment of TRPM7 forms a constitutively active ion channel that is permeable to a broad range of divalent cations including Zn^{2+}, Ca^{2+}, and Mg^{2+} [43, 45, 56]. It has been hypothesized that permeation of all these ions may be relevant for the physiological role of TRPM7 [43, 45, 56]. Our understanding of the channel gating mechanisms is still incomplete, with the current view mainly resting on two findings: First, perfusion of cells with a Mg^{2+}-free internal solution readily induces TRPM7 currents implying that intracellular Mg^{2+} (either free Mg^{2+} or Mg^{2+}-ATP) is a physiological negative regulator of the TRPM7 channel [18, 45]. Second, the plasma membrane phospholipid phosphatidylinositol-4,5-bisphophate (PIP_2) appears to be required for TRPM7 channel activity [57]. Stimulation of phospholipase C (PLC)-coupled G-protein-coupled receptors (GPCRs) leads to PIP_2 depletion and resultant inactivation of TRPM7 currents even in the absence of Mg^{2+} [57]. Furthermore, some authors hypothesized that intracellular Mg^{2+} interacts directly with negatively charged PIP_2 to interfere with the TRPM7 gating process [37]. It should be noted that Mg^{2+} and PIP_2 are well-known modulators of many channel species, including other TRP channels. In those cases, Mg^{2+} and PIP_2 frequently modulate channel responses to endogenous ligands, changes in voltage, temperature, or mechanical force [44, 69]. Thus, it is reasonable to hypothesize that TRPM7 channel function is not solely controlled by variations of Mg^{2+} and PIP_2 levels but is subject to regulation by as yet unknown stimuli.

For many TRP channels, endogenous agonists or activation pathways have still remained unknown. Nevertheless, identification of exogenous compounds acting as channel agonists greatly advanced the field by allowing for a functional characterization of TRP channels. For instance, capsaicin [6, 7], 4α-phorbol 12,13-didecanoate (4alpha-PDD) [77], allyl isothiocyanate [33], and menthol [51] have been successfully employed to uncover activation mechanisms and therapeutic potential of TRPV1, TRPV4, TRPA1, and TRPM8, respectively (reviewed in [34, 46, 50]). However, such molecular tools are not yet available for TRPM7 despite the pressing need for pharmacological compounds allowing to acutely probe TRPM7 channel *versus* kinase activities, because genetic targeting of TRPM7 abrogates both functions.

Here, we report the first identification of small-molecule TRPM7 channel agonists. Furthermore, we take advantage of one such substance, naltriben, as a new experimental tool to assess TRPM7 channel activity by Ca^{2+} imaging and patch-clamp analysis. In contrast to current thinking, we show that TRPM7 currents can be induced under conditions of high intracellular Mg^{2+} or low PIP_2, suggesting that the as yet unknown stimuli may offset the negative regulation of the channel by Mg^{2+} or PIP_2 depletion. Thus, these new TRPM7 channel activators will be instrumental in deciphering key aspects of TRPM7 function in native environments.

Methods

Chemicals

Histamine hydrochloride, naltriben methanesulfonate, naltrindole hydrochloride, naltrexone hydrochloride, morphine sulfate, NS8593, and pregnenolone sulfate (PS) were purchased from Sigma-Aldrich.

Molecular biology and cell cultures

Wild-type (wt), $TRPM7^{K1646R}$, and $TRPM7^{Y1049P}$ mutant mouse TRPM7 complementary DNA (cDNA) variants in the pIRES-eGFP vector (Clontech Laboratories) were generated as described previously [13, 40]. Mouse TRPM3 expression constructs have been described before [13, 40]. The mouse $TRPM7^{S1107E}$ mutant was produced by site-directed mutagenesis. A mouse TRPM7 variant lacking the C terminus ($TRPM7^{\Delta C}$) was generated by replacing the entire C terminus downstream of the coiled-coil domain (L1249) by a Flag tag sequence. All TRPM7 cDNA mutations generated were confirmed by sequencing.

For transient expression of TRPM channels, human embryonic kidney (HEK) 293 cells were maintained at 37 °C and 5 % CO_2 in Eagle's minimal essential medium (MEM, Invitrogen) supplemented with 10 % fetal calf serum, 100 μg/ml streptomycin, and 100 U/ml penicillin (Invitrogen). Cells were transiently transfected using the Lipofectamine 2000 reagent (Invitrogen) according to the manufacturer's instructions. RBL-1 cells were cultured in RPMI medium supplemented with 10 % fetal calf serum, 100 μg/ml streptomycin, and 100 U/ml penicillin (Invitrogen) under culturing conditions identical with those of HEK 293 cells.

Screen for modulators of TRPM7

Primary screen In a primary screening step, we used a Library of Pharmacologically Active Compounds ($LOPAC^{1280}$, Sigma-Aldrich) comprising 1,280 pharmacologically active synthetic and natural compounds. To detect stimulatory effects of individual compounds on TRPM7-mediated Ca^{2+} entry, we adapted an approach that was recently used to screen for TRPM7 inhibitors [11]. We employed an inducible HEK 293 cell line stably expressing mouse TRPM7 ($M7^{pIND}$ cell

line). M7^{pIND} cells had been generated using an ecdysone-inducible expression system (Invitrogen) as reported before [12]. The cell line was maintained at 37 °C and 5 % CO_2 in Dulbecco's Modified Eagle Medium (DMEM, Invitrogen) supplemented with 10 % fetal calf serum, 100 μg/ml streptomyci, 100 U/ml penicillin, 400 μg/ml hygromycin, and 400 μg/ml zeocin (Invitrogen). These cells cultured in 100-mm dishes were transiently transfected with a pG5A construct (2 μg/dish) encoding enhanced green fluorescent protein fused in-frame to *Aequorea victoria* apo-aequorin [4]. Four hours after transfection, the cell culture medium was replaced by fresh medium containing 10 μM ponasterone A. Twenty-four hours after induction, cells were washed two times with phosphate-buffered saline (PBS) and incubated with 0.05 % trypsin/1 mM EDTA in PBS for 1 min at room temperature. Cell suspensions were centrifuged two times at 600 g for 3 min and resuspended in Mg^{2+}-free 2-[4-(2-hydroxyethyl)piperazin-1-yl]ethanesulfonic acid (HEPES)-buffered saline (Mg^{2+}-free HBS: 140 mM NaCl, 6 mM KCl, 1 mM $CaCl_2$, 10 mM HEPES, 5 mM glucose, and 0.1 % BSA, pH 7.4). For reconstitution of aequorin, cell suspensions were incubated with 5 μM coelenterazin (Biaffin GmbH) in Mg^{2+}-free HBS for 30 min at room temperature. Cells were washed twice by centrifugation at 600 rpm for 3 min followed by resuspension of the pellet in Mg^{2+}-free HBS and placed in 96-well plates (Greiner Bio-one) at a density of 1×10^5 cells per well. For a negative control, M7^{pIND} cells were prepared identically except that ponasterone A was not added to the culture medium.

To monitor TRPM7-mediated Ca^{2+} influx, 30-μM test compounds in Mg^{2+}-free HBS were injected into the medium, and bioluminescence rates (counts/s) were measured using a FLUOstar OPTIMA microplate reader (BMG LABTECH) at 37 °C. Measurements were terminated by lysing cells with 0.1 % (*v*/*v*) Triton X-100 in HBS to record total bioluminescence. Bioluminescence rates (counts/s) were analyzed at 1-s intervals and calibrated as $[Ca^{2+}]_i$ using the following equation:

$$p\left[Ca^{2+}\right]_i = 0.332588\ (-\log(k)) + 5.5593$$

where k represents the rate of aequorin consumption, i.e., counts per second divided by the total number of counts.

Compounds that evoked Ca^{2+} rises ($\Delta[Ca^{2+}]_I>50$ nM) exclusively in induced M7^{pIND} cells were selected for further study, whereas substances that elicited responses in induced and control cells were considered as false positives and excluded from further analysis.

Secondary screen In order to assess potential off-target effects, we tested whether Ca^{2+} rises elicited at a final compound concentration of 50 μM could be suppressed by coapplication of 20 μM NS8593, a recently identified inhibitor of the TRPM7 channel [11] or 10 mM extracellular Mg^{2+}, a potent TRPM7 channel pore blocker. In these experiments, HEK 293 cells cultured in 35-mm dishes were transfected with a mixture of 20 μg/dish of wild-type (wt) or mutant TRPM7-pIRES-eGFP expression constructs and 2 μg/dish pG5A constructs using the Lipofectamine 2000 reagent (Invitrogen). Four hours after transfection, the cell culture medium was replaced by fresh medium, and Ca^{2+} measurements were performed 24 h after transfection analogous to measurements with M7^{pIND} cells.

To determine EC_{50} values, data were fit to the Hill equation:

$$E = E_0 + (E_{max}-E_0)c^h/\left(EC_{50}{}^h + c^h\right)$$

where E_{max} is denoting the maximally achievable effect, EC_{50} the half-maximal concentration, and h the Hill factor.

Electrophysiological techniques

HEK 293 cells grown in 35-mm dishes to about 70 % confluence were transfected with wt or mutant mouse TRPM7-pIRES-eGFP expression constructs (1–2 μg/dish) 20–30 h before analysis. Whole-cell patch-clamp recordings were carried out at room temperature (22 °C). Unless stated otherwise, cells were perfused with an external solution E1: 140 mM NaCl, 5 mM CsCl, 2 mM $CaCl_2$, 1 mM $MgCl_2$, 10 mM glucose, and 10 mM HEPES, pH 7.4 with NaOH. Whole-cell patch-clamp recordings were performed with an EPC10 patch-clamp amplifier (HEKA, Germany) using the Pulse software (HEKA). Patch pipettes were made of borosilicate glass (Science Products) and had resistances between 2 and 3.5 MΩ when filled with the standard Mg^{2+}-free intracellular solution P1: 120 mM CsCl, 10 mM NaCl, 10 mM HEDTA, 1 mM EGTA, and 10 mM HEPES, pH 7.4. In some experiments, the pipette solution was HEDTA-free and contained 0.5–2 mM Mg^{2+}. Series resistance compensation of 80 % was used to reduce voltage errors in all experiments. Data were acquired at a frequency of 5 kHz after filtering at 1.67 kHz.

For perforated patch recordings of TRPM7 currents, freshly prepared 200 μg/ml nystatin was added to the pipette solution (P1). After briefly dipping the already filled pipette into nystatin-free P1, seals were formed and series resistance was monitored until a resistance <50 MΩ developed (usually after 10–15 min), and experiments were started. Ramps were applied from −100 to +80 mV in order to reduce voltage errors at higher voltages due to higher series resistances.

Functional characterization of TRPM3 was carried out in HBS saline (140 mM NaCl, 5 mM KCl, 2 mM $CaCl_2$, 1 mM $MgCl_2$, 10 mM glucose, and 10 mM HEPES, pH 7.4). The

pipette solution contained 120 mM CsCl, 20 mM NaCl, 1 mM $MgCl_2$, 2 mM EGTA, and 10 mM HEPES, pH 7.4. TRPM3 currents were activated by external application of 10 μM pregnenolone sulphate. The extent of activation caused by PS was quantified by interpolation of currents at +100 mV.

Statistical analysis

Data are presented as means ± standard error of the mean (SEM). Unless stated otherwise, data were compared by an unpaired Student's *t* test. Significance was accepted at $P \leq 0.05$.

Results

Primary and secondary screens for small organic compounds capable of activating TRPM7 channel

In our primary screen, we used the LOPAC^{1280} compound library composed of 1,280 pharmacologically active synthetic and natural molecules. In our previous search for TRPM7 inhibitors, we used a bioluminescence-based assay [11, 40] to monitor Ca^{2+} influx in HEK 293 cells stably expressing mouse TRPM7 under the control of a ponasteron-A-inducible promoter [12]. In this study, we adapted the assay to screen for positive TRPM7 modulators based on the assumption that external application of an activator will lead to a fast and pronounced increase in aequorin bioluminescence in TRPM7-expressing (ponasteron-A-induced) cells without affecting control (uninduced) cells (data not shown). Based on these two criteria, we tested 1,280 substances and selected 29 candidates that were validated further.

In a secondary screen (Fig. 1), we reevaluated the effects of 29 compounds administered to HEK 293 cells transiently transfected with mouse TRPM7 cDNA testing two independent measures to suppress TRPM7 channels: external coapplication of either Mg^{2+} or the TRPM7 inhibitor NS8593. External Mg^{2+} works by means of competition with external Ca^{2+} for the channel pore whereas NS8593 affects the gating of TRPM7 [11, 45]. Figure 1a shows a characteristic response of TRPM7-expressing cells to external application of the positive modulator naltriben evoking a fast and sustained elevation of $[Ca^{2+}]_i$. Of note, the naltriben effect was abolished in the presence of either 20 μM NS8593 or 10 mM extracellular Mg^{2+}, indicating that TRPM7 was involved in the naltriben-induced $[Ca^{2+}]_i$ increase (Fig. 1a). Based on this experimental paradigm, we identified three groups of compounds (Figs. 1b and 2). The first group contained naltriben, clozapine, proadifen, doxepin, and A3 hydrochloride—compounds whose induction of $[Ca^{2+}]_i$ levels was fully ablated by NS8593 and Mg^{2+}. The second group contained a set of compounds (mibefradil, U-73343, CGP-74514A, metergoline, L-733,060, A-77636, ST-148, clemastine, and desipramine) that displayed a residual $[Ca^{2+}]_i$ response (≤50 nM) in the presence of NS8593 or Mg^{2+}, indicating that these substances eliceted minor TRPM7-independent (i.e., off-target or other nonspecific) effects on $[Ca^{2+}]_i$. The third group (sertraline, methiothepin, NNC 55-0396, prochlorperazine, nortriptyline, and loperamide) exhibited a moderate $[Ca^{2+}]_i$ response (>50 nM) in the presence of either NS8593 or Mg^{2+} (Fig. 1b). Those compounds that induced $[Ca^{2+}]_i$ rises despite the presence of NS8593 or external Mg^{2+} were excluded from the final list of 20 TRPM7 activators (Figs. 1b and 2).

Next, we took advantage of the patch-clamp technique to confirm that the identified modulators induced cognate whole-cell TRPM7 currents in HEK 293 cells overexpressing recombinant TRPM7. We observed that all 20 compounds activated currents conforming to all biophysical hallmarks of TRPM7 (data not shown) indicating that our previous screening steps were stringent enough to select bona fide TRPM7 agonists.

Characterization of naltriben as an activator of TRPM7 currents

We noted that with few exceptions, the identified modulators had different chemical structures (Fig. 2) suggesting that they exert their stimulatory action via different mechanisms. In the present study, we focused on the impact of naltriben on TRPM7, since the latter compound exhibited a high stimulatory effect on TRPM7-mediated Ca^{2+} entry without detectable off-target responses (Fig. 1a). In a first set of experiments, we determined the concentration-response relationship of naltriben and the maximum $[Ca^{2+}]_i$ increase in TRPM7-expressing HEK 293 cells (Fig. 3a, b). The naltriben-induced TRPM7-mediated Ca^{2+} entry was found to be concentration dependent with an EC_{50} value of 20.7±2.6 μM (Fig. 3a, b, n=5 experiments).

Next, we studied the ability of naltriben to activate TRPM7 whole-cell currents in HEK 293 cells transiently transfected with mouse TRPM7 cDNA. In particular, we intended to activate TRPM7 currents by naltriben under physiological intracellular conditions, i.e., without depletion of intracellular Mg^{2+} via the patch pipette solution—a commonly used approach to activate TRPM7 currents. We observed small constitutively active TRPM7 currents in nystatin-perforated patches. These currents were substantially increased by external application of naltriben (Fig. 3c). The effect of naltriben was fast, reversible, and symmetrically affected inward and outward currents (Fig. 3c). The current-voltage (I-V) relationships of TRPM7 currents after the application of naltriben exhibited characteristic TRPM7 features, i.e., small inward currents, pronounced outward rectification, and reversal potential around 0 mV, indicating that the effect of naltriben on the TRPM7 channel is voltage independent.

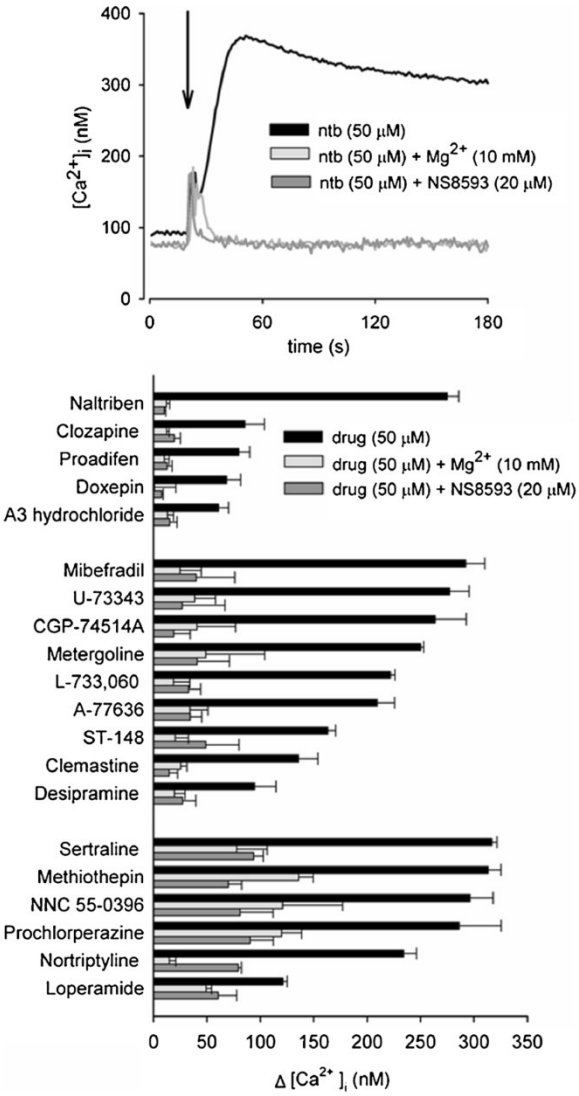

Fig. 1 Results of the secondary screen of TRPM7 activators using an aequorin bioluminescence-based assay. (**a**) Representative traces of $[Ca^{2+}]_i$ in HEK 293 cells overexpressing TRPM7 are shown. Naltriben (ntb) was applied at the time indicated by the *vertical arrow* in the absence and in the presence of 20 μM NS8593 or 10 mM Mg^{2+}. A naltriben-induced Ca^{2+} rise ($\Delta[Ca^{2+}]_i$) was calculated by subtraction of the resting $[Ca^{2+}]_i$ level from the maximal $[Ca^{2+}]_i$ before and after drug application. Consequently, the same time intervals were used to calculate $\Delta[Ca^{2+}]_i$ for the effects of naltriben in the presence of NS8593 and Mg^{2+}. Note that initial small $[Ca^{2+}]_i$ transients in the presence of NS8593 or Mg^{2+} represent a drug injection artifact that was also observed when naltriben was omitted. (**b**) Effects of the positive modulators on TRPM7-mediated Ca^{2+} entry. Mean values for $\Delta[Ca^{2+}]_i$ (±SEM) were calculated from three independent measurements similar to these illustrated in Fig. 1a

We next investigated whether naltriben interfered with pathways known to modulate TRPM7 activity in both physiological and experimental settings (Fig. 4). To this end, we fully induced whole-cell TRPM7 currents in HEK 293 cells using a Mg^{2+}-free intracellular solution in the patch pipette (Fig. 4a). When TRPM7 currents were fully developed, we applied naltriben externally. Under these conditions, we observed a moderate further increase of the TRPM7 current amplitude. In contrast, when cells were perfused with a pipette solution containing 2 mM Mg^{2+} (Fig. 4b)—a Mg^{2+} concentration that fully suppresses TRPM7 activity—the increase in current amplitude attributable to naltriben was substantially more pronounced. This finding indicated that naltriben counteracts the inhibitory effect of internal Mg^{2+} on TRPM7 channel activity and thus potentially functions as a positive modulator of TRPM7 channel gating.

In contrast to intracellular Mg^{2+}, extracellular divalent cations such as Mg^{2+} and Ca^{2+} are responsible for a permeation block of the TRPM7 channel pore [45]. Consequently, exposure of cells to a divalent cation-free solution entailed large monovalent cation currents with a characteristic linear I-V relationship (Fig. 4c). To investigate whether naltriben increases TRPM7 currents by altering permeation characteristics of the channel, we monitored the effect of naltriben on TRPM7 in the absence of divalent cations in the external solution. Under these conditions, naltriben caused an equal fractional increase of inward as well as outward monovalent currents (Fig. 4c), supporting the notion that naltriben most probably affects channel gating rather than permeation characteristics of the TRPM7 pore.

Activation of PLC-coupled GPCRs results in depletion of plasma membrane PIP_2, thus inhibiting TRPM7 channel activity even in the absence of internal Mg^{2+} [57]. In order to test whether naltriben would interfere with the permissive role of phospholipids for TRPM7 gating, we applied naltriben to cells in a state of PIP_2 depletion. Recombinant guinea pig H1 histamine receptor was coexpressed with TRPM7, and in accord with published reports [37], maximal stimulation of the receptor caused a fast and complete suppression of TRPM7 currents (Fig. 5a). However, subsequent perfusion of these cells with naltriben resuscitated TRPM7 activity in a reversible manner (Fig. 5a). These findings show that naltriben can at least partially compensate for the PIP_2 requirement for TRPM7 channel activity.

Recently, we identified a negative gating modulator of TRPM7 channels [12]. Conceptually, it is imaginable that NS8593 and naltriben may share the same or overlapping interaction site on the TRPM7 protein. Therefore, we asked if naltriben would be able to reverse the inhibitory effect of NS8593. Thus, we fully induced TRPM7 currents using Mg^{2+}-free internal pipette solutions and subsequently applied NS8593 to the bath (Fig. 5b). As expected, NS8593 inhibited TRPM7 currents. However, application of naltriben in addition to NS8593 partially and reversibly relieved TRPM7 currents from this inhibition. In order to further investigate the opposing effects of the latter two compounds on TRPM7

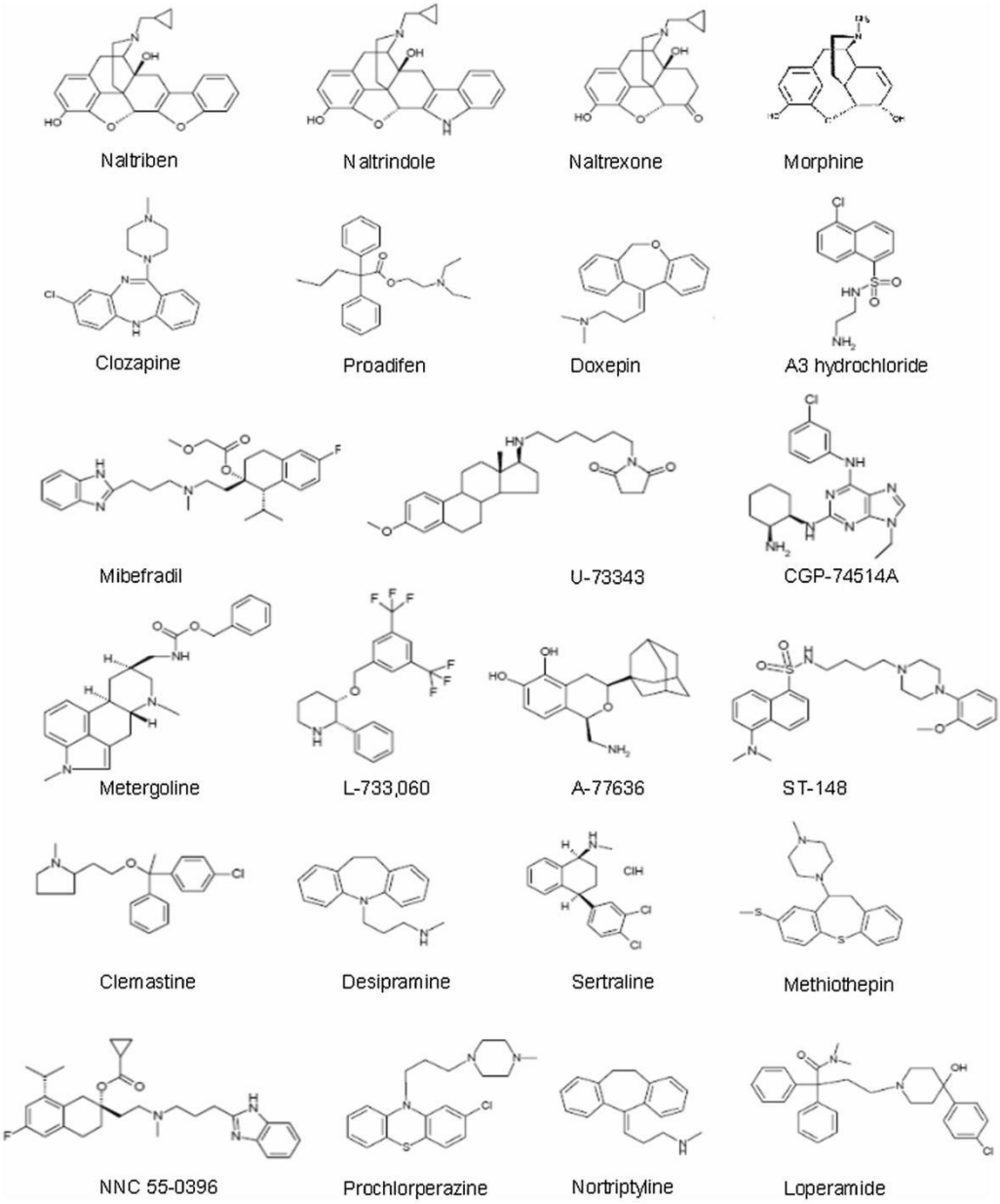

Fig. 2 Chemical structures of the compounds tested on TRPM7. Figure panels were obtained from the supplier of the drug library screened (LOPAC^{1280}, Sigma-Aldrich)

channel activity, we varied the concentrations of either drugs (Fig. 5c). For practical reasons, these experiments were carried out using the Ca^{2+} imaging approach as in Fig. 3b. We observed that application of increasing concentrations of NS8593 resulted in a rightward shift of the concentration-response curve to naltriben. The calculated EC_{50} values for naltriben in the presence of 0, 1, 2, and 5 μM N8593 were 20.7±2.26 (n=5), 51.6±5.9 (n=3), 85.8±16.7 (n=3), and 93.1±9 μM (n=3), respectively. For practical reasons (modest solubility of naltriben), we could not test whether high levels of naltriben can fully overcome the effects of 2 and 5 μM NS8593. Most straightforward explanations for these findings are that naltriben and NS8593 compete for a common binding site on TRPM7 and/or have opposite effects on a common gating mechanism. At this point, both options still await further experimental analysis.

Naltriben is a phenanthrene opioid known to function as an antagonist of δ opioid receptors [66]. It has a high structural

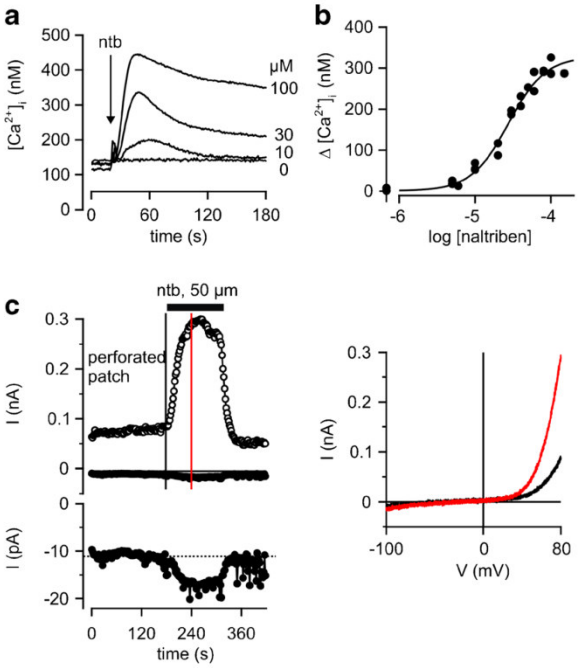

Fig. 3 Effects of naltriben on recombinant TRPM7 in HEK 293 cells. (**a**) Time course of $[Ca^{2+}]_i$ at different final concentrations of naltriben (ntb) applied at the time point indicated by the *vertical arrow*. (**b**) Concentration-response relationship of naltriben calculated from experiments similar to the ones shown in Fig. 3a. (**c**) Representative traces of TRPM7 currents induced by external application of naltriben to TRPM7-expressing HEK 293 cells measured by the nystatin perforated patch technique (n=5). (*left panel)* Whole cell currents at −100 mV (*filled symbols*) and +80 mV (*hollow symbols*) from voltage ramps applied at 2-s intervals. The *bottom figure* represents the −100-mV trace at a higher magnification in order to visualize the naltriben effect on small inward TRPM7 currents. (*right panel*) Current-voltage (I-V) relationship of TRPM7 currents obtained before (*black line*) and after (*red line*) application of naltriben at the time points indicated by the corresponding *vertical bars* in the *left panel*

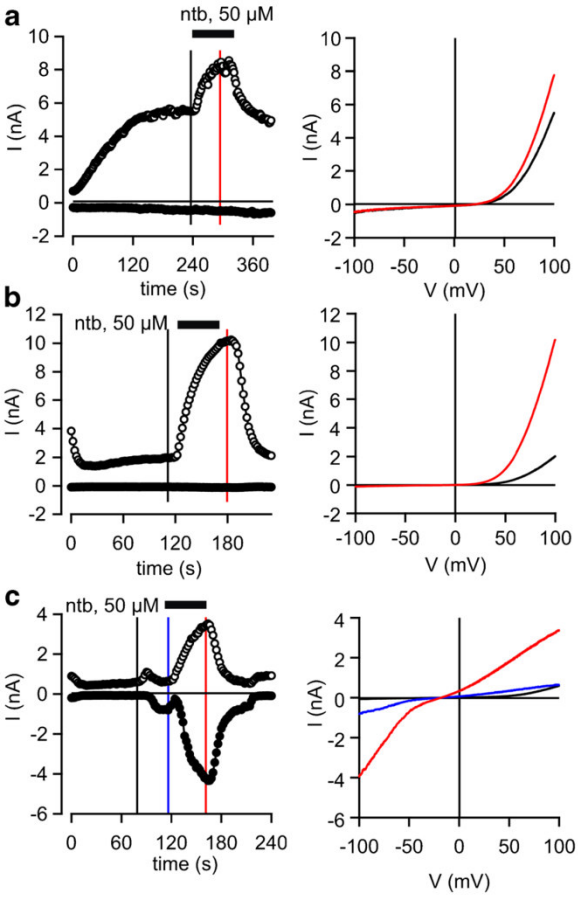

Fig. 4 Effects of intracellular and extracellular Mg^{2+} on naltriben-induced TRPM7 currents. (**a**) Representative recording (n=3) of whole-cell TRPM7 currents in HEK 293 cells perfused with Mg^{2+}-free intracellular solution. (*left panel*). Two traces representing the time course of ramp currents at −100 and +80 mV. (*Right panel*) I-V relationships obtained before (*black*) and after (*red*) application of naltriben (ntb) at the time points indicated by the corresponding *vertical bars* in *left panel*. (**b**) Measurements were performed analogous to Fig. 4a except that the cells (n=4) were perfused intracellularly with a pipette solution containing 2 mM Mg^{2+}. Note the initial decay of the current amplitude due to the high internal Mg^{2+} concentration and a pronounced increase of the currents upon application of naltriben. (**c**) Measurements (n=4) were performed analogous to Fig. 4b except that naltriben was applied after exchange of the external normal saline (*black bar*) for a divalent-free solution. Note that in the absence of the external Mg^{2+} block, the effect of naltriben was equally evident on both the inward and outward currents

similarity to other broadly used opioid receptor antagonists like naltrindole and naltrexone, with naltrindole most closely resembling naltriben in terms of substituent structure (only the oxygen atom of the benzofuran backbone of naltriben has been replaced with nitrogen) [66]. Of note, all three compounds share a common phenanthrene scaffold with morphine (Fig. 2). Therefore, we tested morphine, naltrindole, and naltrexone for their potency to activate TRPM7 (Fig. 6). We observed that neither naltrindole nor more distantly related analogs of naltriben were able to induce substantial TRPM7 currents (Fig. 6). Thus, naltrindole can be defined as an inactive analog of the TRPM7 agonist naltriben.

Finally, we asked whether naltriben could activate mouse TRPM3, a TRPM channel most closely related to TRPM7 and reliably expressible in HEK 293 cells (Fig. 6). Naltriben neither activated TRPM3 nor did it potentiate the moderate constitutive activity, whereas subsequent application of pregnenolone sulphate, a known TRPM3 activator [76], induced TRPM3 currents (Fig. 6). Additionally, we tested naltriben on a subset of TRP channels to ensure that this molecule does not act as a nonspecific channel modulator targeting the majority of TRPs, for instance, due to alterations of physical/chemical characteristics of the plasma membrane or cytosol. Specifically, human TRPM2, human TRPM8, and rat TRPV1 were probed by Ca^{2+} imaging experiments, and these channels were unaffected by naltriben (data not shown).

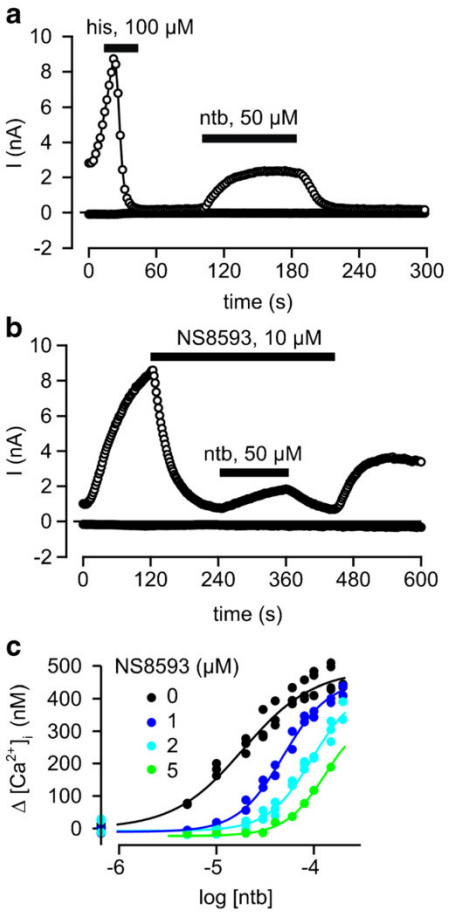

Fig. 5 Naltriben-mediated rescue of TRPM7 currents from the inhibitory effects of PIP_2 hydrolysis and NS8593. (**a**) Representative recording (n=4) of whole-cell TRPM7 currents in HEK 293 cells expressing both mTRPM7 and the H1 histamine receptor. Cells were perfused with Mg^{2+}-free intracellular solutions. Note that a brief histamine application caused an almost complete abrogation of TRPM7 currents. Subsequent application of naltriben (ntb) restituted TRPM7 currents in a reversible manner upon wash-out of the drug. (**b**) TRPM7 currents (n=4) were first allowed to develop to steady state by perfusion of the cell with Mg^{2+}-free pipette solution. Then, a nearly complete inhibition was achieved by application of NS8593. The inhibition by NS8593 could be partially and reversibly overcome by coapplication of naltriben. (**c**) Concentration-response relationship of naltriben on the maximal $\Delta[Ca^{2+}]_i$. Measurements were performed similar to Fig. 3a and b, except that NS8593 was coapplied with naltriben simultaneously. Data set for 0 μM NS8593 is the same as in Fig. 3. Note the rightward shift of the concentration-response curves of naltriben in the presence of increasing concentrations of NS8593

In aggregate, our findings lend credence to the notion that naltriben acts as a selective agonistic ligand of TRPM7 but does not target related TRPM channels. Furthermore, we propose that naltriben affects TRPM7 channel gating by delicate chemical structural requirements responsible for this effect.

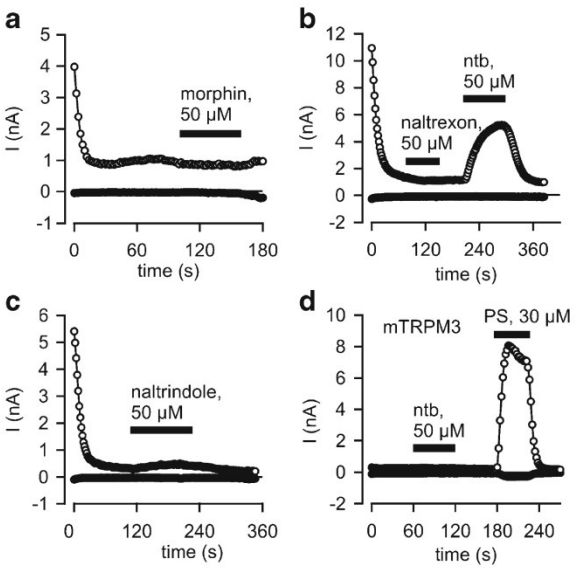

Fig. 6 Specificity of the TRPM7-naltriben interaction. (**a**–**c**) TRPM7-expressing HEK 293 cells were perfused with a pipette solution containing 2 mM Mg^{2+} and challenged with 50 μM each of various phenanthrene-based opioid compounds: morphine ((**a**), n=4), naltrexone ((**b**), n=6), and naltrindole ((**c**), n=4). (**d**) HEK 293 cells (n=5) expressing murine TRPM3 were challenged with naltriben as indicated by the *application bar*, followed by stimulation with the TRPM3 agonist, pregnenolone sulfate (PS)

Roles of the TRP domain, kinase, and pore-forming segments for naltriben effects on TRPM7 channel activity

In order to narrow down the localization of the domain responsible for the stimulatory effects of naltriben, we studied a set of TRPM7 constructs with deletions or point mutations in the pore region, the TRP domain, and the kinase domain of TRPM7 (Fig. 7). The "kinase-dead" TRPM7 variant harbors a K1646R point mutation ($TRPM7^{K1646R}$) in the catalytic ATP-binding site of the kinase domain resulting in complete loss of kinase activity [64]. We observed that, like wt TRPM7 (Fig. 4b), $TRPM7^{K1646R}$ was inhibited in the presence of 2 mM internal Mg^{2+} and fully sensitive to external application of naltriben (Fig. 7a). Next, we asked whether the kinase domain of TRPM7 per se was required for the effect of naltriben on channel activity. To this end, we studied a TRPM7 mutant truncated at the C terminus immediately downstream of the coiled-coil domain ($TRPM7^{\Delta C}$). We found that $TRPM7^{\Delta C}$ exhibited reduced channel activity but still was able to respond to external application of naltriben (Fig. 7b). We conclude that neither the kinase catalytic activity nor the protein C terminus is required for TRPM7 activation by naltriben.

Y1049P is located in a predicted "selectivity filter" of TRPM7 channel, and its mutation to proline ($TRPM7^{Y1049P}$)

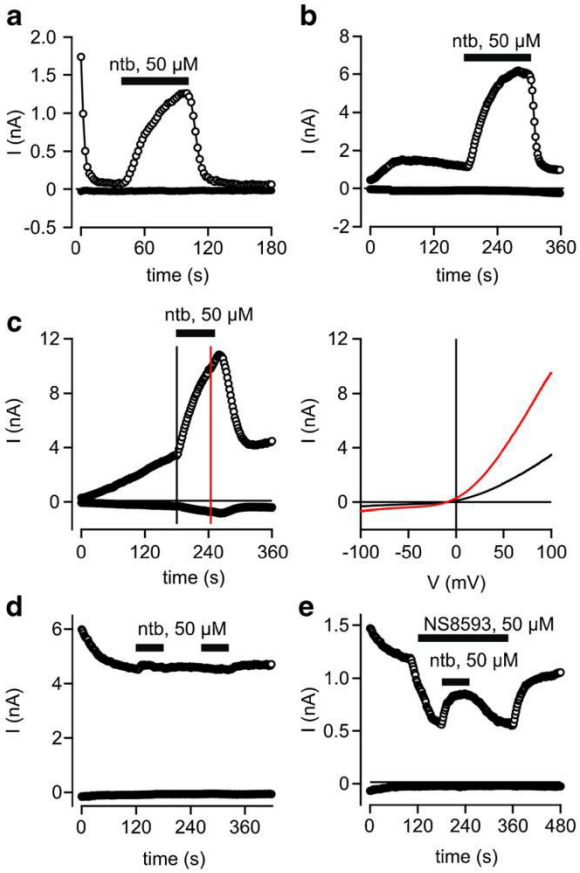

Fig. 7 Requirement of the TRP domain, but not the kinase domain and the pore-forming segment of TRPM7 for its sensitivity to naltriben. Representative recordings of the whole-cell currents in HEK 293 cells transiently transfected with **a** a kinase-dead TRPM7 point mutant ($TRPM7^{K1646R}$, n=9), **b** a TRPM7 variant lacking the entire C terminus beyond the coiled-coil domain ($TRPM7^{\Delta C}$, n=3), and **c** TRPM7 carrying a Y1049P mutation in the selectivity filter domain ($TRPM7^{Y1049P}$, n=6). **d** A constitutively active TRPM7 variant carrying the S1107E mutation in the TRP domain ($TRPM7^{S1107E}$, n=4) was challenged with naltriben. **e** Naltriben was applied during a partial inhibition of $TRPM7^{S1107E}$ by 50 μM NS8593 (n=4). Measurements were performed and analyzed analogous to Fig. 4. In Fig. 7a, d, e, HEK 293 cells were perfused with an intracellular solution containing 2 mM Mg^{2+}. In Fig. 7b, c, due to lower overall current amplitudes, cells were investigated with Mg^{2+}-free pipette solutions

results in an active channel that is poorly permeable to Mg^{2+} ions [40]. We used $TRPM7^{Y1049P}$ to test whether modification of the pore region would affect the channel's responsiveness to naltriben (Fig. 7b). We found that $TRPM7^{Y1049P}$ was sensitive to naltriben, supporting the notion that the stimulatory effect of this compound is not directly associated with the ion permeation path of the TRPM7 channel pore.

Recently, our systematic screen for domains and specific residues required for the regulation of TRPM7 by intracellular Mg^{2+} revealed that the TRP domain appears to play a key role in this process (manuscript to be published elsewhere). For instance, we found that mutation of serine at position 1107 to glutamate S1107E ($TRPM7^{S1107E}$) resulted in a constitutively active TRPM7 channel insensitive to high (2 mM) intracellular Mg^{2+} as illustrated in Fig. 7d. When we assessed the effect of naltriben on this mutant, we found that the $TRPM7^{S1107E}TRPM7^{S1111E}$ mutation rendered the channel insensitive to further activation by naltriben (Fig. 7d). However, $TRPM7^{S1107E}$ was inhibited by very high levels of NS8593 (Fig. 7d). Remarkably, coapplication of naltriben led to an immediate partial recovery of currents (Fig. 7d). Thus, in contrast to mutations affecting channel pore characteristics or kinase activity, modification of the Mg^{2+}-dependent gating of TRPM7 altered its sensitivity to naltriben, consistent with the idea that naltriben exerts its stimulatory effects by regulating the gating of TRPM7 most likely involving the TRP domain. At present, however, we cannot exclude the possibility that, like TRPM3 [75], TRPM7 has an additional ion permeation pathway affected by naltriben.

Effect of naltriben on endogenous TRPM7 currents

The composition of native TRPM7 channel kinase complexes is largely unknown. It is reasonable to assume that, like other TRP channels, endogenous TRPM7 is associated with accessory proteins, kinase substrates or cellular constituents such as PIP_2. Consequently, studies using overexpressed TRPM7 may not fully represent functional characteristics of native TRPM7 channel complexes including sensitivity to pharmacological compounds. In order to test whether native TRPM7 currents could be induced by naltriben, we performed patch-clamp experiments on RBL-1 cells—a cell model expressing high levels of TRPM7 and frequently used to study endogenous TRPM7-like currents [30, 36]. Using Mg^{2+}-free pipette solutions, we could induce characteristic TRPM7-like currents in all cells examined (Fig. 8a). Next, RBL-1 cells were perfused with a pipette solution containing near-physiological Mg^{2+} concentrations (0.5 mM) (Fig. 8b, c). Under these conditions, the baseline activity of endogenous TRPM7 currents remained stable, whereas external application of naltriben resulted in increased TRPM7 currents in all cells investigated (Fig. 8b, c). Interestingly, native TRPM7 current amplitudes elicited by Mg^{2+} depletion were higher than those resulting from naltriben administration. We also noted that the activation kinetics of TRPM7 currents in RBL cells by Mg^{2+} depletion and application of NTB were somewhat slower than that observed with overexpressed mouse or human TRPM7. These observations can be explained by species-specific differences of rat TRPM7 (RBL1 are rat cells) or by association of native TRPM7 with endogenous metabolites and accessory proteins. Collectively, we conclude that naltriben can activate

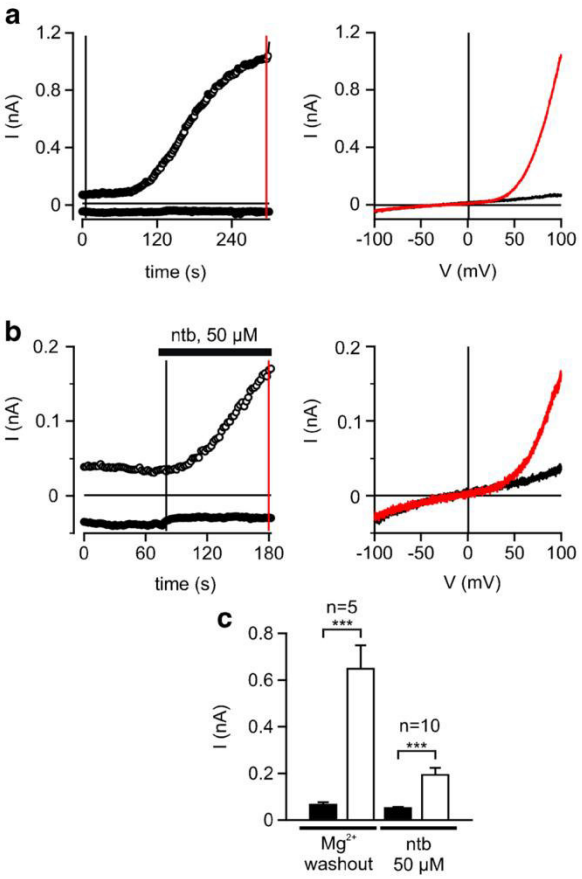

Fig. 8 Effect of naltriben on endogenous TRPM7-mediated currents in RBL-1 mast cells. **a** (*left panel*) Representative recording of whole-cell TRPM7 currents in RBL-1 cells induced by Mg^{2+}-free intracellular solution. (*right panel*) I-V relationships obtained before (*black*) and after (*red*) induction of TRPM7 currents at the time points indicated by the corresponding *vertical bars* in *left panel*. **b** Measurements were performed and analyzed like in Fig. 8a except that the cells were perfused intracellularly with near-physiological $[Mg^{2+}]_i$ (0.5 mM) in the pipette solution, and TRPM7 currents were induced upon application of naltriben (ntb) as indicated by the *application bar*. **c** Current amplitudes obtained at +80 mV before and after the respective activation treatments in experiments shown in Fig. 8a, b

recombinant and endogenous TRPM7 channels in the presence of physiological levels of intracellular Mg^{2+}.

Discussion and conclusions

Identification of TRPM7 activators

In another recent study, we identified a subset of synthetic inhibitors of the TRPM7 channel [12]. These findings prompted us to search for small molecules acting as positive modulators of TRPM7 channels. Our screening approach identified 20 substances that were able to activate the TRPM7 channel. The majority of identified TRPM7 modulators display heterogeneous chemical scaffolds that were previously used as templates to generate drug variants. For instance, naltriben has a morphinan backbone which is the base structure of many opioid analgesics [66, 70], whereas clozapine contains a benzodiazepine ring that is present in many psychoactive substances [79]. Thus, our study highlights an extensive array of scaffold structures that can be further employed to increase functional diversity and specificity of TRPM7 modulators.

Some of the TRPM7 activators found are in clinical use. For instance, clozapine is prescribed for the patients with schizophrenia [79]. Doxepin and desipramine are antidepressant drugs [20, 39], while clemastine is an antihistamine agent prescribed for the treatment of allergic complications [72]. Pharmacological effects of clozapine, doxepin, and desipramine are complex and incompletely understood. Therefore, ubiquitously expressed TRPM7 channels may play a hitherto unappreciated role as additional molecular targets of these drugs under certain circumstances, possibly imposing a critical revision of our current concepts of drug action.

Defining naltriben as a gating modulator of the TRPM7 channel

From the list of positive modulators of TRPM7 activity, we chose naltriben for further characterization. Naltriben exhibits a rather moderate potency for TRPM7 activation when compared to other TRP channel agonists. For example, the calculated EC_{50} value was about 20 μM for naltriben, 39 nM for capsaicin (TRPV1 agonist [7], 0.67 μM for 4alpha-PDD (TRPV4 agonists [77]), 11 μM for allyl isothiocyanate (TRPA1 agonist [33]), and 30–200 μM depending on temperature and membrane potential for menthol (TRPM8 agonist [51, 74]). Nevertheless, we are not aware of off-target effects on related TRP channels when naltriben was tested at 50 μM. The compound could be completely washed out, the effects were fully reversible, and naltriben was able to induce endogenous TRPM7 currents in RBL-1 cells. Furthermore, we found that naltriben acts both in a divalent or monovalent cation conduction mode of TRPM7. Naltriben was found to attenuate the inhibitory effects of $[Mg^{2+}]_i$, could compensate for PIP_2 depletion, and counteracted the inhibitory action of NS8593. Removal of the entire C terminus up to the coiled-coil domain of TRPM7 left the channel sensitive to naltriben, whereas a mutation that keeps the channel in a constitutively open state is insensitive to the action of naltriben as long as the channel is not deactivated by pretreatment with NS8593. In summary, these findings are compatible with the concept that naltriben is an allosteric positive gating modulator of TRPM7, most likely acting via the TRP domain.

Probing of naltriben as a new tool to study TRPM7 function

Our experiments with naltriben illustrated notable experimental advantages of using TRPM7 agonists. TRPM7 carries very small divalent cation selective inward currents at physiological negative voltages. Therefore, a commonly used method to quantify TRPM7 channel activity relies on fairly large outward monovalent cation currents measured at unphysiologically high positive membrane potentials upon a likewise completely unphysiological depletion of intracellular Mg^{2+}. The resulting data, however, are hard to correlate with actual TRPM7-mediated uptake of divalent cations at physiological membrane potentials and unaltered internal Mg^{2+} levels. In contrast, naltriben allows the measurement of TRPM7 currents without chelation of intracellular Mg^{2+}. In addition, naltriben is well suited to monitor TRPM7 activity using a Ca^{2+} imaging approach that is easily adaptable for experiments with genetic TRPM7 variants associated with human diseases [16, 27, 28], search for new TRPM7 antagonists, and for studies with cells that are difficult to approach by the patch-clamp technique, for instance, the classical TRPM7 model, DT-40 lymphocytes [64].

Taking advantage of naltriben, we could investigate an important aspect of TRPM7 function. So far, most studies on TRPM7 channel gating focused on negative channel regulators. It is commonly observed that high levels of internal Mg^{2+} entail a full suppression of TRPM7 currents. The plasma membrane phospholipid PIP_2 is believed to be required for TRPM7 channel activity, since PLC-mediated depletion of PIP_2 results in full inhibition of TRPM7 currents even in the absence of intracellular Mg^{2+}. However, it is very difficult to distinguish whether physiological variations of these two factors in native cells really exert the control of TRPM7 channel activity or whether they represent rather unspecific switch-off constraints. Interestingly, we found that naltriben offsets the sensitivity of TRPM7 to internal Mg^{2+} and is able to activate TRPM7 channel even if PIP_2 is depleted. These findings argue that variations in levels of Mg^{2+} or PIP_2 would not prevent TRPM7 channel activation induced by hitherto unknown endogenous or exogenous stimuli. Of note, in a library of just 1,280 small molecules, we could identify 20 compounds that activate TRPM7. This high-success rate is in line with the concept that TRPM7 harbors a still unidentified putative ligand-binging site that can be exploited by a variety of synthetic molecular structures. Accordingly, we speculate that endogenous positive gating modulators of TRPM7 do exist, for instance intracellular metabolites such as ADP-ribose as shown for TRPM2 [53] or hormones like pregnenolone sulfate as worked out for TRPM3 [76].

Acknowledgments This study was supported by the Deutsche Forschungsgemeinschaft (DFG), including an Emmy-Noether-Fellowship to T.H. (DFG-Ho-3869). S.S. was supported by the Förderprogramm für Forschung und Lehre Fellowship (FöFoLe) of the LMU, Munich. We thank Renate Heilmair for excellent technical assistance and Moritz Meißner and Anna Erbacher for their help with the primary screen.

Conflict of interest None

References

1. Aarts M, Iihara K, Wei WL, Xiong ZG, Arundine M, Cerwinski W, MacDonald JF, Tymianski M (2003) A key role for TRPM7 channels in anoxic neuronal death. Cell 115(7):863–877
2. Abed E, Martineau C, Moreau R (2011) Role of melastatin transient receptor potential 7 channels in the osteoblastic differentiation of murine MC3T3 cells. Calcif Tissue Int 88(3):246–253. doi:10.1007/s00223-010-9455-z
3. Bates-Withers C, Sah R, Clapham DE (2011) TRPM7, the Mg(2+) inhibited channel and kinase. Adv Exp Med Biol 704:173–183. doi:10.1007/978-94-007-0265-3_9
4. Baubet V, Le Mouellic H, Campbell AK, Lucas-Meunier E, Fossier P, Brulet P (2000) Chimeric green fluorescent protein-aequorin as bioluminescent Ca^{2+} reporters at the single-cell level. Proc Natl Acad Sci U S A 97(13):7260–7265
5. Brauchi S, Krapivinsky G, Krapivinsky L, Clapham DE (2008) TRPM7 facilitates cholinergic vesicle fusion with the plasma membrane. Proc Natl Acad Sci U S A 105(24):8304–8308. doi:10.1073/pnas.0800881105
6. Cao E, Liao M, Cheng Y, Julius D (2013) TRPV1 structures in distinct conformations reveal activation mechanisms. Nature 504(7478):113–118. doi:10.1038/nature12823
7. Caterina MJ, Schumacher MA, Tominaga M, Rosen TA, Levine JD, Julius D (1997) The capsaicin receptor: a heat-activated ion channel in the pain pathway. Nature 389(6653):816–824. doi:10.1038/39807
8. Chen YF, Chen YT, Chiu WT, Shen MR (2013) Remodeling of calcium signaling in tumor progression. J Biomed Sci 20:23. doi:10.1186/1423-0127-20-23
9. Chen JP, Luan Y, You CX, Chen XH, Luo RC, Li R (2010) TRPM7 regulates the migration of human nasopharyngeal carcinoma cell by mediating Ca(2+) influx. Cell Calcium 47(5):425–432. doi:10.1016/j.ceca.2010.03.003
10. Chen KH, Xu XH, Liu Y, Hu Y, Jin MW, Li GR (2013) TRPM7 channels regulate proliferation and adipogenesis in 3T3-L1 preadipocytes. J Cell Physiol 229(1):60–67. doi:10.1002/jcp.24417
11. Chubanov V, Mederos y Schnitzler M, Meissner M, Schafer S, Abstiens K, Hofmann T, Gudermann T (2012) Natural and synthetic modulators of SK (K(ca)2) potassium channels inhibit magnesium-dependent activity of the kinase-coupled cation channel TRPM7. Br J Pharmacol 166(4):1357–1376. doi:10.1111/j.1476-5381.2012.01855.x
12. Chubanov V, Schlingmann KP, Waring J, Heinzinger J, Kaske S, Waldegger S, Mederos y Schnitzler M, Gudermann T (2007) Hypomagnesemia with secondary hypocalcemia due to a missense mutation in the putative pore-forming region of TRPM6. J Biol Chem 282(10):7656–7667. doi:10.1074/jbc.M611117200
13. Chubanov V, Waldegger S, Mederos y Schnitzler M, Vitzthum H, Sassen MC, Seyberth HW, Konrad M, Gudermann T (2004) Disruption of TRPM6/TRPM7 complex formation by a mutation in the TRPM6 gene causes hypomagnesemia with secondary hypocalcemia. Proc Natl Acad Sci U S A 101(9):2894–2899. doi:10.1073/pnas.0305252101
14. Clark K, Langeslag M, van Leeuwen B, Ran L, Ryazanov AG, Figdor CG, Moolenaar WH, Jalink K, van Leeuwen FN (2006) TRPM7, a novel regulator of actomyosin contractility and cell adhesion. EMBO J 25(2):290–301. doi:10.1038/sj.emboj.7600931

15. Clark K, Middelbeek J, Morrice NA, Figdor CG, Lasonder E, van Leeuwen FN (2008) Massive autophosphorylation of the Ser/Thr-rich domain controls protein kinase activity of TRPM6 and TRPM7. PLoS One 3(3):e1876. doi:10.1371/journal.pone.0001876
16. Dai Q, Shrubsole MJ, Ness RM, Schlundt D, Cai Q, Smalley WE, Li M, Shyr Y, Zheng W (2007) The relation of magnesium and calcium intakes and a genetic polymorphism in the magnesium transporter to colorectal neoplasia risk. Am J Clin Nutr 86(3):743–751
17. Deason-Towne F, Perraud AL, Schmitz C (2012) Identification of Ser/Thr phosphorylation sites in the C2-domain of phospholipase C gamma2 (PLCgamma2) using TRPM7-kinase. Cell Signal 24(11): 2070–2075. doi:10.1016/j.cellsig.2012.06.015
18. Demeuse P, Penner R, Fleig A (2006) TRPM7 channel is regulated by magnesium nucleotides via its kinase domain. J Gen Physiol 127(4):421–434. doi:10.1085/jgp.200509410
19. Desai BN, Krapivinsky G, Navarro B, Krapivinsky L, Carter BC, Febvay S, Delling M, Penumaka A, Ramsey IS, Manasian Y, Clapham DE (2012) Cleavage of TRPM7 releases the kinase domain from the ion channel and regulates its participation in Fas-induced apoptosis. Dev Cell 22(6):1149–1162. doi:10.1016/j.devcel.2012.04.006
20. Dharmshaktu P, Tayal V, Kalra BS (2012) Efficacy of antidepressants as analgesics: a review. J Clin Pharmacol 52(1):6–17. doi:10.1177/0091270010394852
21. Dorovkov MV, Kostyukova AS, Ryazanov AG (2011) Phosphorylation of annexin A1 by TRPM7 kinase: a switch regulating the induction of an alpha-helix. Biochemistry 50(12):2187–2193. doi:10.1021/bi101963h
22. Du J, Xie J, Zhang Z, Tsujikawa H, Fusco D, Silverman D, Liang B, Yue L (2010) TRPM7-mediated Ca^{2+} signals confer fibrogenesis in human atrial fibrillation. Circ Res 106(5):992–1003. doi:10.1161/CIRCRESAHA.109.206771
23. Elizondo MR, Arduini BL, Paulsen J, MacDonald EL, Sabel JL, Henion PD, Cornell RA, Parichy DM (2005) Defective skeletogenesis with kidney stone formation in dwarf zebrafish mutant for trpm7. Curr Biol 15(7):667–671. doi:10.1016/j.cub.2005.02.050
24. Gao H, Chen X, Du X, Guan B, Liu Y, Zhang H (2011) EGF enhances the migration of cancer cells by up-regulation of TRPM7. Cell Calcium 50(6):559–568. doi:10.1016/j.ceca.2011.09.003
25. Guilbert A, Gautier M, Dhennin-Duthille I, Haren N, Sevestre H, Ouadid-Ahidouch H (2009) Evidence that TRPM7 is required for breast cancer cell proliferation. Am J Physiol Cell Physiol 297(3): C493–C502. doi:10.1152/ajpcell.00624.2008
26. Hanano T, Hara Y, Shi J, Morita H, Umebayashi C, Mori E, Sumimoto H, Ito Y, Mori Y, Inoue R (2004) Involvement of TRPM7 in cell growth as a spontaneously activated Ca^{2+} entry pathway in human retinoblastoma cells. J Pharmacol Sci 95(4):403–419
27. Hara K, Kokubo Y, Ishiura H, Fukuda Y, Miyashita A, Kuwano R, Sasaki R, Goto J, Nishizawa M, Kuzuhara S, Tsuji S (2009) TRPM7 is not associated with amyotrophic lateral sclerosis-parkinsonism dementia complex in the Kii peninsula of Japan. Am J Med Genet B Neuropsychiatr Genet 153B(1):310–313. doi:10.1002/ajmg.b.30966
28. Hermosura MC, Nayakanti H, Dorovkov MV, Calderon FR, Ryazanov AG, Haymer DS, Garruto RM (2005) A TRPM7 variant shows altered sensitivity to magnesium that may contribute to the pathogenesis of two Guamanian neurodegenerative disorders. Proc Natl Acad Sci U S A 102(32):11510–11515. doi:10.1073/pnas.0505149102
29. Jiang J, Li MH, Inoue K, Chu XP, Seeds J, Xiong ZG (2007) Transient receptor potential melastatin 7-like current in human head and neck carcinoma cells: role in cell proliferation. Cancer Res 67(22):10929–10938. doi:10.1158/0008-5472.CAN-07-1121
30. Jiang J, Li M, Yue L (2005) Potentiation of TRPM7 inward currents by protons. J Gen Physiol 126(2):137–150. doi:10.1085/jgp.200409185
31. Jin J, Desai BN, Navarro B, Donovan A, Andrews NC, Clapham DE (2008) Deletion of Trpm7 disrupts embryonic development and thymopoiesis without altering Mg^{2+} homeostasis. Science 322(5902):756–760. doi:10.1126/science.1163493
32. Jin J, Wu LJ, Jun J, Cheng X, Xu H, Andrews NC, Clapham DE (2011) The channel kinase, TRPM7, is required for early embryonic development. Proc Natl Acad Sci U S A 109(5):E225–E233. doi:10.1073/pnas.1120033109
33. Jordt SE, Bautista DM, Chuang HH, McKemy DD, Zygmunt PM, Hogestatt ED, Meng ID, Julius D (2004) Mustard oils and cannabinoids excite sensory nerve fibres through the TRP channel ANKTM1. Nature 427(6971):260–265. doi:10.1038/nature02282nature02282
34. Julius D (2013) TRP channels and pain. Annu Rev Cell Dev Biol 29: 355–384. doi:10.1146/annurev-cellbio-101011-155833
35. Kim BJ, Park EJ, Lee JH, Jeon JH, Kim SJ, So I (2008) Suppression of transient receptor potential melastatin 7 channel induces cell death in gastric cancer. Cancer Sci 99(12):2502–2509. doi:10.1111/j.1349-7006.2008.00982.x
36. Kozak JA, Kerschbaum HH, Cahalan MD (2002) Distinct properties of CRAC and MIC channels in RBL cells. J Gen Physiol 120(2):221–235
37. Kozak JA, Matsushita M, Nairn AC, Cahalan MD (2005) Charge screening by internal pH and polyvalent cations as a mechanism for activation, inhibition, and rundown of TRPM7/MIC channels. J Gen Physiol 126(5):499–514. doi:10.1085/jgp.200509324
38. Kuras Z, Yun YH, Chimote AA, Neumeier L, Conforti L (2012) KCa3.1 and TRPM7 channels at the uropod regulate migration of activated human T cells. PLoS One 7(8):e43859. doi:10.1371/journal.pone.0043859PONE-D-11-17226
39. Leggio GM, Salomone S, Bucolo C, Platania C, Micale V, Caraci F, Drago F (2013) Dopamine D(3) receptor as a new pharmacological target for the treatment of depression. Eur J Pharmacol 719(1–3):25–33. doi:10.1016/j.ejphar.2013.07.022
40. Mederos y Schnitzler M, Waring J, Gudermann T, Chubanov V (2008) Evolutionary determinants of divergent calcium selectivity of TRPM channels. FASEB J 22(5):1540–1551. doi:10.1096/fj.07-9694com
41. Meng X, Cai C, Wu J, Cai S, Ye C, Chen H, Yang Z, Zeng H, Shen Q, Zou F (2013) TRPM7 mediates breast cancer cell migration and invasion through the MAPK pathway. Cancer Lett 333(1):96–102. doi:10.1016/j.canlet.2013.01.031
42. Middelbeek J, Kuipers AJ, Henneman L, Visser D, Eidhof I, van Horssen R, Wieringa B, Canisius SV, Zwart W, Wessels LF, Sweep FC, Bult P, Span PN, van Leeuwen FN, Jalink K (2012) TRPM7 is required for breast tumor cell metastasis. Cancer Res 72(16):4250–4261. doi:10.1158/0008-5472.CAN-11-3863
43. Monteilh-Zoller MK, Hermosura MC, Nadler MJ, Scharenberg AM, Penner R, Fleig A (2003) TRPM7 provides an ion channel mechanism for cellular entry of trace metal ions. J Gen Physiol 121(1):49–60
44. Mubagwa K, Gwanyanya A, Zakharov S, Macianskiene R (2007) Regulation of cation channels in cardiac and smooth muscle cells by intracellular magnesium. Arch Biochem Biophys 458(1):73–89. doi:10.1016/j.abb.2006.10.014
45. Nadler MJ, Hermosura MC, Inabe K, Perraud AL, Zhu Q, Stokes AJ, Kurosaki T, Kinet JP, Penner R, Scharenberg AM, Fleig A (2001) LTRPC7 is a Mg.ATP-regulated divalent cation channel required for cell viability. Nature 411(6837):590–595. doi:10.1038/3507909235079092
46. Nilius B, Owsianik G, Voets T, Peters JA (2007) Transient receptor potential cation channels in disease. Physiol Rev 87(1):165–217. doi:10.1152/physrev.00021.2006
47. Numata T, Shimizu T, Okada Y (2007) Direct mechano-stress sensitivity of TRPM7 channel. Cell Physiol Biochem 19(1–4):1–8. doi:10.1159/000099187

48. Oancea E, Wolfe JT, Clapham DE (2006) Functional TRPM7 channels accumulate at the plasma membrane in response to fluid flow. Circ Res 98(2):245–253. doi:10.1161/01.RES.0000200179.29375.cc
49. Paravicini TM, Chubanov V, Gudermann T (2012) TRPM7: a unique channel involved in magnesium homeostasis. Int J Biochem Cell Biol 44(8):1381–1384. doi:10.1016/j.biocel.2012.05.010
50. Patapoutian A, Tate S, Woolf CJ (2009) Transient receptor potential channels: targeting pain at the source. Nat Rev Drug Discov 8(1):55–68. doi:10.1038/nrd2757
51. Peier AM, Moqrich A, Hergarden AC, Reeve AJ, Andersson DA, Story GM, Earley TJ, Dragoni I, McIntyre P, Bevan S, Patapoutian A (2002) A TRP channel that senses cold stimuli and menthol. Cell 108(5):705–715
52. Penner R, Fleig A (2007) The Mg(2+) and Mg(2+)-nucleotide-regulated channel-kinase TRPM7. Handb Exp Pharmacol 179:313–328. doi:10.1007/978-3-540-34891-7_19
53. Perraud AL, Fleig A, Dunn CA, Bagley LA, Launay P, Schmitz C, Stokes AJ, Zhu Q, Bessman MJ, Penner R, Kinet JP, Scharenberg AM (2001) ADP-ribose gating of the calcium-permeable LTRPC2 channel revealed by Nudix motif homology. Nature 411(6837):595–599. doi:10.1038/3507910035079100
54. Perraud AL, Zhao X, Ryazanov AG, Schmitz C (2010) The channel-kinase TRPM7 regulates phosphorylation of the translational factor eEF2 via eEF2-k. Cell Signal 23(3):586–593. doi:10.1016/j.cellsig.2010.11.011
55. Runnels LW (2010) TRPM6 and TRPM7: A Mul-TRP-PLIK-cation of channel functions. Curr Pharm Biotechnol 12(1):42–53
56. Runnels LW, Yue L, Clapham DE (2001) TRP-PLIK, a bifunctional protein with kinase and ion channel activities. Science 291(5506):1043–1047. doi:10.1126/science.10585191058519
57. Runnels LW, Yue L, Clapham DE (2002) The TRPM7 channel is inactivated by PIP(2) hydrolysis. Nat Cell Biol 4(5):329–336. doi:10.1038/ncb781ncb781
58. Ryazanov AG, Pavur KS, Dorovkov MV (1999) Alpha-kinases: a new class of protein kinases with a novel catalytic domain. Curr Biol 9(2):R43–R45
59. Ryazanova LV, Rondon LJ, Zierler S, Hu Z, Galli J, Yamaguchi TP, Mazur A, Fleig A, Ryazanov AG (2010) TRPM7 is essential for Mg(2+) homeostasis in mammals. Nat Commun 1:109. doi:10.1038/ncomms1108
60. Rybarczyk P, Gautier M, Hague F, Dhennin-Duthille I, Chatelain D, Kerr-Conte J, Pattou F, Regimbeau JM, Sevestre H, Ouadid-Ahidouch H (2012) Transient receptor potential melastatin-related 7 channel is overexpressed in human pancreatic ductal adenocarcinomas and regulates human pancreatic cancer cell migration. Int J Cancer 131(6):E851–E861. doi:10.1002/ijc.27487
61. Sah R, Mesirca P, Mason X, Gibson W, Bates-Withers C, Van den Boogert M, Chaudhuri D, Pu WT, Mangoni ME, Clapham DE (2013) Timing of myocardial trpm7 deletion during cardiogenesis variably disrupts adult ventricular function, conduction, and repolarization. Circulation 128(2):101–114. doi:10.1161/CIRCULATIONAHA.112.000768
62. Sah R, Mesirca P, Van den Boogert M, Rosen J, Mably J, Mangoni ME, Clapham DE (2013) Ion channel-kinase TRPM7 is required for maintaining cardiac automaticity. Proc Natl Acad Sci U S A 110(32):E3037–E3046. doi:10.1073/pnas.1311865110
63. Sahni J, Scharenberg AM (2008) TRPM7 ion channels are required for sustained phosphoinositide 3-kinase signaling in lymphocytes. Cell Metab 8(1):84–93. doi:10.1016/j.cmet.2008.06.002
64. Schmitz C, Perraud AL, Johnson CO, Inabe K, Smith MK, Penner R, Kurosaki T, Fleig A, Scharenberg AM (2003) Regulation of vertebrate cellular Mg^{2+} homeostasis by TRPM7. Cell 114(2):191–200
65. Siddiqui TA, Lively S, Vincent C, Schlichter LC (2012) Regulation of podosome formation, microglial migration and invasion by Ca(2+)-signaling molecules expressed in podosomes. J Neuroinflammation 9:250. doi:10.1186/1742-2094-9-250
66. Sofuoglu M, Portoghese PS, Takemori AE (1991) Differential antagonism of delta opioid agonists by naltrindole and its benzofuran analog (NTB) in mice: evidence for delta opioid receptor subtypes. J Pharmacol Exp Ther 257(2):676–680
67. Su LT, Agapito MA, Li M, Simonson WT, Huttenlocher A, Habas R, Yue L, Runnels LW (2006) TRPM7 regulates cell adhesion by controlling the calcium-dependent protease calpain. J Biol Chem 281(16):11260–11270. doi:10.1074/jbc.M512885200
68. Su LT, Liu W, Chen HC, Gonzalez-Pagan O, Habas R, Runnels LW (2011) TRPM7 regulates polarized cell movements. Biochem J 434(3):513–521. doi:10.1042/BJ20101678
69. Suh BC, Hille B (2008) PIP_2 is a necessary cofactor for ion channel function: how and why? Annu Rev Biophys 37:175–195. doi:10.1146/annurev.biophys.37.032807.125859
70. Takemori AE, Sultana M, Nagase H, Portoghese PS (1992) Agonist and antagonist activities of ligands derived from naltrexone and oxymorphone. Life Sci 50(20):1491–1495
71. Touyz RM (2008) Transient receptor potential melastatin 6 and 7 channels, magnesium transport, and vascular biology: implications in hypertension. Am J Physiol Heart Circ Physiol 294(3):H1103–H1118. doi:10.1152/ajpheart.00903.2007
72. Tramer MR, von Elm E, Loubeyre P, Hauser C (2006) Pharmacological prevention of serious anaphylactic reactions due to iodinated contrast media: systematic review. BMJ 333(7570):675. doi:10.1136/bmj.38905.634132.AE
73. Tseveleki V, Rubio R, Vamvakas SS, White J, Taoufik E, Petit E, Quackenbush J, Probert L (2010) Comparative gene expression analysis in mouse models for multiple sclerosis, Alzheimer's disease and stroke for identifying commonly regulated and disease-specific gene changes. Genomics 96(2):82–91. doi:10.1016/j.ygeno.2010.04.004
74. Voets T, Owsianik G, Janssens A, Talavera K, Nilius B (2007) TRPM8 voltage sensor mutants reveal a mechanism for integrating thermal and chemical stimuli. Nat Chem Biol 3(3):174–182. doi:10.1038/nchembio862
75. Vriens J, Held K, Janssens A, Toth BI, Kerselaers S, Nilius B, Vennekens R, Voets T (2014) Opening of an alternative ion permeation pathway in a nociceptor TRP channel. Nat Chem Biol. doi:10.1038/nchembio.1428
76. Wagner TF, Loch S, Lambert S, Straub I, Mannebach S, Mathar I, Dufer M, Lis A, Flockerzi V, Philipp SE, Oberwinkler J (2008) Transient receptor potential M3 channels are ionotropic steroid receptors in pancreatic beta cells. Nat Cell Biol 10(12):1421–1430. doi:10.1038/ncb1801
77. Watanabe H, Davis JB, Smart D, Jerman JC, Smith GD, Hayes P, Vriens J, Cairns W, Wissenbach U, Prenen J, Flockerzi V, Droogmans G, Benham CD, Nilius B (2002) Activation of TRPV4 channels (hVRL-2/mTRP12) by phorbol derivatives. J Biol Chem 277(16):13569–13577. doi:10.1074/jbc.M200062200M200062200
78. Wei C, Wang X, Chen M, Ouyang K, Song LS, Cheng H (2009) Calcium flickers steer cell migration. Nature 457(7231):901–905. doi:10.1038/nature07577
79. Wenthur CJ, Lindsley CW (2013) Classics in chemical neuroscience: clozapine. ACS Chem Neurosci 4(7):1018–1025. doi:10.1021/cn400121z
80. Yamaguchi H, Matsushita M, Nairn AC, Kuriyan J (2001) Crystal structure of the atypical protein kinase domain of a TRP channel with phosphotransferase activity. Mol Cell 7(5):1047–1057
81. Zhang Z, Wang M, Fan XH, Chen JH, Guan YY, Tang YB (2012) Upregulation of TRPM7 channels by angiotensin II triggers phenotypic switching of vascular smooth muscle cells of ascending aorta. Circ Res 111(9):1137–1146. doi:10.1161/CIRCRESAHA.112.273755
82. Zierler S, Yao G, Zhang Z, Kuo WC, Porzgen P, Penner R, Horgen FD, Fleig A (2011) Waixenicin A inhibits cell proliferation through magnesium-dependent block of transient receptor potential melastatin 7 (TRPM7) channels. J Biol Chem 286(45):39328–39335. doi:10.1074/jbc.M111.264341

Natural and synthetic modulators of SK (K(ca)2) potassium channels inhibit magnesium-dependent activity of the kinase-coupled cation channel TRPM7

BJP British Journal of Pharmacology

DOI:10.1111/j.1476-5381.2012.01855.x
www.brjpharmacol.org

RESEARCH PAPER

Natural and synthetic modulators of SK ($K_{ca}2$) potassium channels inhibit magnesium-dependent activity of the kinase-coupled cation channel TRPM7

V Chubanov[1]*, M Mederos y Schnitzler[1]*, M Meißner[1], S Schäfer[1], K Abstiens[1], T Hofmann[2] and T Gudermann[1]

[1]*Walther-Straub-Institute of Pharmacology and Toxicology, University of Munich, Munich, Germany, and* [2]*Institute of Pharmacology, University of Marburg, Marburg, Germany*

Correspondence
V Chubanov,
Walther-Straub-Institute of Pharmacology and Toxicology,
University of Munich,
Goethestrasse 33, 80336 Munich,
Germany. E-mail:
vladimir.chubanov@
lrz.uni-muenchen.de

*These authors contributed equally.

Keywords
transient receptor potential; TRPM7; SK channels; $K_{Ca}2.1$–2.3 channels; magnesium; cell motility

Received
24 May 2011
Revised
15 December 2011
Accepted
4 January 2012

BACKGROUND AND PURPOSE

Transient receptor potential cation channel subfamily M member 7 (TRPM7) is a bifunctional protein comprising a TRP ion channel segment linked to an α-type protein kinase domain. TRPM7 is essential for proliferation and cell growth. Up-regulation of TRPM7 function is involved in anoxic neuronal death, cardiac fibrosis and tumour cell proliferation. The goal of this work was to identify non-toxic inhibitors of the TRPM7 channel and to assess the effect of blocking endogenous TRPM7 currents on the phenotype of living cells.

EXPERIMENTAL APPROACH

We developed an aequorin bioluminescence-based assay of TRPM7 channel activity and performed a hypothesis-driven screen for inhibitors of the channel. The candidates identified were further assessed electrophysiologically and in cell biological experiments.

KEY RESULTS

TRPM7 currents were inhibited by modulators of small conductance Ca^{2+}-activated K^+ channels ($K_{Ca}2.1$–2.3; SK) channels, including the antimalarial plant alkaloid quinine, CyPPA, dequalinium, NS8593, SKA31 and UCL 1684. The most potent compound NS8593 (IC_{50} 1.6 μM) specifically targeted TRPM7 as compared with other TRP channels, interfered with Mg^{2+}-dependent regulation of TRPM7 channel and inhibited the motility of cultured cells. NS8593 exhibited full and reversible block of native TRPM7-like currents in HEK 293 cells, freshly isolated smooth muscle cells, primary podocytes and ventricular myocytes.

CONCLUSIONS AND IMPLICATIONS

This study reveals a tight overlap in the pharmacological profiles of TRPM7 and $K_{Ca}2.1$–2.3 channels. NS8593 acts as a negative gating modulator of TRPM7 and is well-suited to study functional features and cellular roles of endogenous TRPM7.

Abbreviations

BK channels, high-conductance Ca^{2+}-activated K^+ channels; IK channels, intermediate conductance Ca^{2+}-activated K^+ channels; $K_{Ca}2.1$–2.3 (SK) channels, small conductance Ca^{2+}-activated K^+ channels; TRPM7, melastatin-related TRP cation channel 7

Introduction

TRPM7 (transient receptor potential cation channel, subfamily M, member 7) is a bifunctional protein comprising two distinct functional moieties: an ion channel segment and a protein kinase domain. The channel segment of TRPM7 displays high homology to other melastatin-related TRP (TRPM) channels (reviewed in Chubanov *et al.*, 2005), whereas the kinase domain is a member of the family of α-type serine/threonine protein kinases with structural similarity to PKA (Ryazanov *et al.*, 1999; Yamaguchi *et al.*, 2001). Although TRPM channels are highly conserved throughout the animal kingdom (Mederos y Schnitzler *et al.*, 2008; Hofmann *et al.*, 2010), only in TRPM7 and a genetically related protein, TRPM6, the ion pore-forming subunits are covalently linked to α-kinase domains.

In heterologous expression systems, TRPM7 behaves as a constitutively active cation channel that is highly permeable to a broad range of divalent cations, including Ca^{2+} and Mg^{2+} (Nadler *et al.*, 2001; Runnels *et al.*, 2001; Monteilh-Zoller *et al.*, 2003). Intracellular and extracellular Mg^{2+} tightly regulates TRPM7 channel activity. External Mg^{2+} is a permeant blocker of TRPM7 (Nadler *et al.*, 2001; Monteilh-Zoller *et al.*, 2003; Kozak *et al.*, 2005). Internal Mg^{2+} (as well as Mg^{2+}-ATP) inhibits TRPM7 via a nucleotide-binding site in the kinase domain synergistically with another as yet unidentified Mg^{2+} binding site extrinsic to the kinase domain (Nadler *et al.*, 2001; Demeuse *et al.*, 2006). Native TRPM7-like currents have been detected in all cell types examined so far (Kozak *et al.*, 2002; Aarts *et al.*, 2003; Gwanyanya *et al.*, 2004; Kim *et al.*, 2007; Numata *et al.*, 2007b; Mishra *et al.*, 2009), indicating that this channel type plays a role indispensable for cell function. It has been suggested that TRPM7-mediated cation entry regulates many essential cellular functions such as cellular Mg^{2+} homeostasis (Schmitz *et al.*, 2003; Chubanov *et al.*, 2004; Sahni and Scharenberg, 2008; Ryazanova *et al.*, 2010), cell spreading (Clark *et al.*, 2006; Su *et al.*, 2006; Wei *et al.*, 2009), proliferation (Nadler *et al.*, 2001; Schmitz *et al.*, 2003; Sahni and Scharenberg, 2008), mechanosensitivity (Oancea *et al.*, 2006; Numata *et al.*, 2007a; Wei *et al.*, 2009) and exocytosis (Brauchi *et al.*, 2008). TRPM7 was found to play a role in anoxic neuronal death (Aarts *et al.*, 2003), hypertension (Touyz, 2008), neurodegenerative disorders (Hermosura *et al.*, 2005; Tseveleki *et al.*, 2010), cardiac fibrosis (Du *et al.*, 2010) and tumour cell proliferation (Hanano *et al.*, 2004; Jiang *et al.*, 2007; Kim *et al.*, 2008; Guilbert *et al.*, 2009)

Despite the physiological and clinical importance of TRPM7, only a few modulators of TRPM7 channel are currently available (Table 1), including a subset of non-specific ion channel blockers like spermine and 2-aminoethoxydiphenyl borate (2-APB) (Kerschbaum *et al.*, 2003; Monteilh-Zoller *et al.*, 2003; Jiang *et al.*, 2005; Parnas *et al.*, 2009; Chen *et al.*, 2010a,b). However, as TRPM7 null mice are embryonic lethal (Jin *et al.*, 2008; Ryazanova *et al.*, 2010), an indiscriminate pharmacological inactivation of TRPM7 will be most probably toxic and, therefore, is not a preferable option. In contrast, similar to the situation with voltage-gated sodium channel inhibitors, drugs acting as 'use-dependent' or 'state-dependent' TRPM7 channel inhibitors may be particularly valuable. Accordingly, organic compounds that would interfere with Mg^{2+}-dependent gating of TRPM7 are of particular interest since they might be instrumental in developing this type of TRPM7 drugs.

The gating mechanisms of TRPM7 as well as its high sensitivity to internal Mg^{2+} are poorly understood and any relevant results are controversial (Nadler *et al.*, 2001; Runnels *et al.*, 2001; 2002; Kozak and Cahalan, 2003; Kozak *et al.*, 2005). It is possible that intracellular Mg^{2+} regulates TRPM7 via one of the mechanisms described for a subset of K^+ channels. For instance, intracellular Mg^{2+} blocks small conductance Ca^{2+}-activated K^+ (SK1-3 or $K_{Ca}2.1$–2.3 according to Alexander *et al.*, 2011) channels in a voltage-dependent manner, resulting in a rectified current–voltage relationship (Soh and Park, 2002). A corresponding divalent cation-binding site in $K_{Ca}2.1$–2.3 channels was identified in a pore-forming loop similar to that in TRPM7 (Figure 1A). The phenomenon of inward rectification in inward rectifier K^+ channels type 2.1–2.4 ($K_{ir}2.1$–2.4) channels is a result of

Table 1

Organic compounds inhibiting TRPM7 currents

Compound	IC_{50} (μM)*	Description of the block	Reference
2-APB	178	Reversible	Prakriya and Lewis, 2002, Li *et al.*, 2006
Spermine	2.3†	Reversible, voltage dependent	Kozak *et al.*, 2002
Carvacrol	306	Reversible	Parnas *et al.*, 2009
NDGA	n.d.	Tested only at 10 and 20 μM	Chen *et al.*, 2010b
AA861	n.d.	Tested only at 10 and 40 μM	Chen *et al.*, 2010b
MK886	n.d.	Tested only at 20 μM	Chen *et al.*, 2010b
Nafamostat mesylate	617	Reversible, voltage and extracellular divalents dependent	Chen *et al.*, 2010a
Waixenicin A	7.0	Irreversible, $[Mg^{2+}]_i$ dependent	Zierler *et al.*, 2011
NS8593	1.6	Reversible, $[Mg^{2+}]_i$ dependent	Present study

*IC_{50} values were determined for recombinant TRPM7 in patch-clamp measurements in the absence of internal Mg^{2+}.
†The dose-dependent effect of spermine was evaluated on endogenous MIC currents in divalent-free external solution.
n.d., not determined.

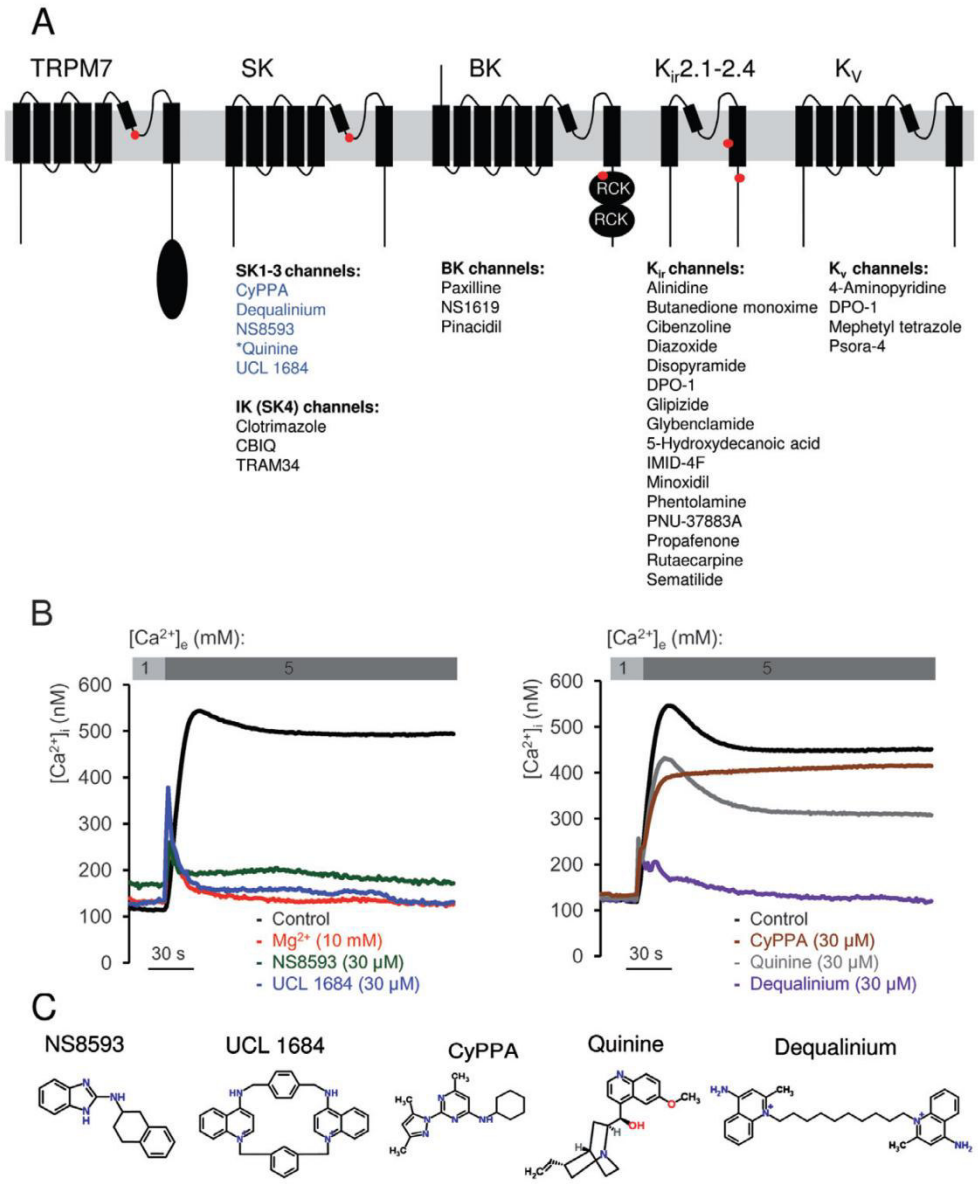

Figure 1

Identification of TRPM7 channel inhibitors among known modulators of Mg^{2+} sensitive K^+ channels. (A) Domain architecture of TRPM7, K_{Ca}2.1–2.3 (SK), K_{Ca}3.1 (IK, SK4), K_{Ca}1.1 (BK), K_{IR} and K_V channels. Locations of Mg^{2+}-binding sites in TRPM7 (formed by E1047 and Y1049 in mouse TRPM7 (Mederos y Schnitzler *et al.*, 2008), K_{Ca}2.1–2.3 channels [S359 in rat K_{Ca}2.2 (Soh and Park, 2002)], K_{Ca}1.1 channels (formed by E374 and E399 in human BK1) (Wu *et al.* 2010; Yang *et al.*, 2008), K_{IR} channels (D172 and E224 in mouse K_{IR}2.1) (Stanfield *et al.*, 1994; Wible *et al.*, 1994; Taglialatela *et al.*, 1995) are indicated by red dots. KD, Ser/Thr kinase domain in TRPM7; RCK, 'regulating the conductance of K^+' domain in K_{Ca}1.1 channels. The modulators of K^+ channels tested in a primary screen for TRPM7 inhibitors are listed below their known targets. Compounds labelled in blue were found to be inhibitors of TRPM7, while modulators in black showed no inhibitory effect on TRPM7. *Quinine blocks K_{Ca}1.1 and K_{Ca}3.1 channels. (B) Primary assessment of modulators using a bioluminescence-based assay of TRPM7 channel activity. Representative traces are shown from two independent experiments with similar results. The indicated compounds (30 µM) or Mg^{2+} (10 mM) were applied to ponasterone A-induced HEK 293 cells, and the measurements were performed in the presence of 1 or 5 mM external Ca^{2+} ($[Ca^{2+}]_e$) as indicated. (C) Chemical structures of TRPM7 inhibitors identified.

voltage-dependent block by internal polyamines and Mg^{2+} acting via a site located in one of the transmembane helices and in the C-terminus of the ion channel (Figure 1A) (Stanfield *et al.*, 1994; Wible *et al.*, 1994; Taglialatela *et al.*, 1995). High-conductance Ca^{2+}-activated K^+ (BK or $K_{Ca}1.1$) channels are also sensitive to intracellular Mg^{2+} (Shi and Cui, 2001; Yang *et al.*, 2008; Wu *et al.* 2010). Unlike $K_{Ca}2.1$–2.3 and $K_{IR}2.1$–2.4, Mg^{2+} binds to a C-terminal domain to positively modulate $K_{Ca}1.1$ channels (Figure 1A).

In a hypothesis-driven chemical screen to identify novel modulators of TRPM7 channel activity, we discovered that TRPM7 is the target of commonly used activators and inhibitors of $K_{Ca}2.1$–2.3 channels. We noted that the antimalarial plant alkaloid quinine as well as synthetic $K_{Ca}2.1$–2.3 modulators, such as CyPPA, dequalinium, NS8593, SKA31 and UCL 1684 (reviewed in Weatherall *et al.*, 2010), are potent inhibitors of TRPM7. The most efficient compound, NS8593, acts as a gating modulator of the TRPM7 channel, similar to the situation with $K_{Ca}2.1$–2.3 channels (Strobaek *et al.*, 2006; Jenkins *et al.*, 2011). These findings suggest that genetically unrelated TRPM7 and $K_{Ca}2.1$–2.3 channels harbour a similar drug-binding site functionally linked to divalent cation-dependent gating of the channels. Accordingly, existing drugs targeting $K_{Ca}2.1$–2.3 channels may be applied to test their potential towards TRPM7.

Methods

Compounds

Alinidine, 2-aminobenzimidazole (ABI), 4-aminopyridine, butanedione monoxime, benzimidazol-1-methylethyl-benzimidazole (BMB), CBIQ, 2-chlorobenzimidazole (CBI), clotrimazole, cibenzoline, dequalinium, diazoxide, disopyramide, DPO-1, glipizide, glybenclamide, 5-hydroxydecanoic acid, IMID-4F, nimodipin, mephetyl tetrazole, minoxidil, phentolamine, pinacidil, PNU-37883A, pregnenolone sulfate (PS), propafenone, rutaecarpine, sematilide, psora-4, paxilline, NS1619, NS8593, quinine, quinidine and 1,2,3,4-tetrahydro-1-naphthylamine (THT) were purchased from Sigma-Aldrich (Taufkirchen, Germany). Synthetic apamin, CyPPA, icilin, NS309, SKA31, TRAM 34, UCL 1684 and tetrodotoxin (TTX) were procured from Tocris Bioscience (Bristol, UK). Synthetic tamapin was from Alomone Labs (Jerusalem, Israel). The molecular target nomenclature was according to Alexander *et al.* (2011).

Molecular biology, cell culture and immunofluorescence staining

Mouse TRPM7, in pIRES-eGFP vector (Clontech Laboratories Mountain View, CA, USA), was generated as described previously (Chubanov *et al.*, 2004; 2007; Mederos y Schnitzler *et al.*, 2008). Mouse TRPM3 cDNA (JF706722) was cloned from kidney mRNA by an RT-PCR approach and inserted into the pcDNA3.1-TOPO vector (Invitrogen, Darmstadt, Germany).

HEK 293 cells were maintained at 37°C and 5% CO_2 in Earl's minimal essential medium supplemented with 10% fetal calf serum, 100 $\mu g \cdot mL^{-1}$ streptomycin and 100 $U \cdot mL^{-1}$ penicillin (Invitrogen). Cells were transiently transfected using the Lipofectamine 2000 reagent (Invitrogen) according to the manufacturer's instructions.

A stable HEK 293 cell line expressing mouse TRPM7 was generated using an ecdysone-inducible expression system (Invitrogen) as reported previously (Chubanov *et al.*, 2007). The cell line was maintained at 37°C and 5% CO_2 in Dulbecco's modified Earl's medium (DMEM, Invitrogen) supplemented with 10% fetal calf serum, 100 $\mu g \cdot mL^{-1}$ streptomycin and 100 $U \cdot mL^{-1}$ penicillin, 400 $\mu g \cdot mL^{-1}$ hygromycin and 400 $\mu g \cdot mL^{-1}$ zeocin (Invitrogen). To induce the expression of recombinant mouse TRPM7, 10 μM ponasterone A (Invitrogen) was added to the cell culture medium.

A stable HEK 293 cell line expressing human TRPM7 was obtained from Carsten Schmitz (Schmitz *et al.*, 2003). The cell line was maintained at 37°C and 5% CO_2 in DMEM (Invitrogen) supplemented with 10% fetal calf serum, 100 $\mu g \cdot mL^{-1}$ streptomycin and 100 $U \cdot mL^{-1}$ penicillin, 400 $\mu g \cdot mL^{-1}$ zeocin and 10 $\mu g \cdot mL^{-1}$ blasticidin (Invitrogen). To confirm tetracyclin-dependent expression of recombinant TRPM7 protein, cells were examined by immunofluorescence microscopy using a TRPM7-specific antibody as described previously (Chubanov *et al.*, 2007).

Smooth muscle cells were enzymatically isolated from cerebellar and basilar arteries of C57Bl/J mice as described previously (Dietrich *et al.*, 2005) and were used immediately for patch-clamp experiments. Primary human ventricular cardiomyocytes were purchased (Promocell, Heidelberg, Germany) and cultured according to the manufacturer's instructions. The experiments with cardiomyocytes were performed with the fourth passage of cells.

Primary podocytes were isolated from the kidneys of 4–8-week-old C57Bl/J mice using a conventional sieving approach (Schlondorff, 1990), with some modifications. Kidneys (four organs per batch) were mechanically disrupted in 200 mL Ham's F12 medium containing 10% FCS and 100 $U \cdot mL^{-1}$ penicillin (Invitrogen) using a set of steel sieves with a pore size of 100, 75, 50 and 36 μm (Retsch, Haan, Germany) coated by Ham's F12 medium containing 50% FCS (Invitrogen) at room temperature. Freshly isolated cells from the final fraction were centrifuged for 5 min at 200× *g* and cultured in Ham's F12 medium supplemented with 10% FCS, 2 mM glutamine, 100 $U \cdot mL^{-1}$ penicillin, 100 $\mu g \cdot mL^{-1}$ streptomycin, 100 $\mu g \cdot mL^{-1}$ normocin, 5 $\mu g \cdot mL^{-1}$ transferrin, 5 $ng \cdot mL^{-1}$ natriumselenite, 100 nM hydrocortisone and 5 $\mu g \cdot mL^{-1}$ recombinant human insulin (Sigma, Taufkirchen, Germany). Enrichment of podocytes was over 95% as assessed by cell morphology and staining with an anti-podocin antibody (Sigma). Primary podocytes were analysed after the second cell passage.

Imaging of living cells, wound healing and viability assay

Wild-type or tetracycline-inducible HEK 293 cells were grown in 35 mm dishes (1×10^4 cells per dish) in the absence or presence of NS8593 for 24–36 h as indicated in the figure legends. Images from living cells were acquired using an Axiovert 40 CFL inverted microscope equipped with an LD-A-plan 20×/0.30PhI objective and an AxioCam ICc 1 CCD camera (Carl Zeiss, Göttingen, Germany). To evaluate effects of NS8593 on cellular viability, cells were washed twice with PBS and incubated at 37°C and 5% CO_2 in 1 mL of 0.05% trypsin/EDTA solution (Invitrogen). The incubation was terminated by addition of 1 mL of the corresponding cell

culture medium. Cells were vigorously resuspended and counted using a Neubauer chamber.

For the wound healing assay, confluent wild-type HEK 293 cells grown in 35 mm dishes were scratched by a yellow pipette tip, washed three times with PBS and supplemented with fresh culture medium with or without NS8593. The wound areas (~600 µm) were imaged immediately or after 24 h as described above. To quantify the effect of NS8593 on cell motility, the ImageJ software (http://rsbweb.nih.gov/ij/index.html) was used to outline the wound area and calculate the percentage of closure.

Aequorin-based $[Ca^{2+}]_i$ measurements

In initial screening experiments, the HEK 293 cell line stably expressing mouse TRPM7 was used. Cells cultured in 100 mm dishes were transfected with 2 µg·per dish of plasmid DNAs containing a pG5A construct encoding enhanced green fluorescent protein fused in-frame to *Aequorea victoria* apo-aequorin (Baubet *et al.*, 2000). Four hours after transfection, the cell culture medium was replaced by fresh medium containing 10 µM ponasterone A. Then 24 h after induction, cells were washed twice with PBS and incubated with 0.05% trypsin, 1 mM EDTA in PBS for 1 min at room temperature. Cell suspensions were centrifuged twice at 600× *g* for 3 min and resuspended in Mg^{2+}-free HEPES-buffered saline (HBS; Mg^{2+}-free HBS: 140 mM NaCl, 6 mM KCl, 1 mM $CaCl_2$, 10 mM HEPES, 5 mM glucose and 0.1% BSA, pH 7.4). For reconstitution of aequorin, cell suspensions were incubated with 5 µM coelenterazin (Biaffin GmbH, Kassel, Germany) in Mg^{2+}-free HBS for 30 min at room temperature. Cells were washed twice by centrifugation at 200× *g* for 3 min followed by resuspension of the pellet in Mg^{2+}-free HBS and placed in 96-well plates (1×10^5 cells per well). Luminescence was detected using a FLUOstar OPTIMA microplate reader at 37°C (BMG LABTECH GmbH, Ortenberg, Germany). To monitor TRPM7-mediated Ca^{2+} influx, extracellular Ca^{2+} was increased by injection of Mg^{2+}-free HBS containing 5 mM $CaCl_2$ (final concentration). Experiments were terminated by lysing cells with 0.1% (v v^{-1}) Triton X-100 in HBS to record total bioluminescence. Bioluminescence rates (counts·s^{-1}) were analysed at 1 s intervals and calibrated as $[Ca^{2+}]_i$ values using the following equation:

$$p[Ca^{2+}]_i = 0.332588[-\log(k)] + 5.5593$$

where k represents the rate of aequorin consumption (i.e. counts·s^{-1} divided by total number of counts).

Determination of Ca^{2+} and Ba^{2+} influx in HEK 293 cells with Fura-2

HEK 293 cells grown on 25 mm glass coverslips in 35 mm dishes were transiently transfected with 2 µg per dish mTRPM7 cDNA in pIRES2-eGFP vector. Ba^{2+} entry was measured 18–24 h after transfection. Cells were loaded with 5 µM fura-2 acetoxymethyl ester (Sigma) in HBS (140 mM NaCl, 6 mM KCl, 1 mM $MgCl_2$, 2 mM $CaCl_2$, 10 mM HEPES, 5 mM glucose, 0.1% BSA, pH 7.4) at room temperature for 45 min. After an additional 10 min incubation in HBS, coverslips were placed in a perfusion chamber, washed three times by Ca^{2+} and Mg^{2+} free HBS (140 mM NaCl, 6 mM KCl, 10 mM HEPES, 5 mM glucose, pH 7.4) and immediately used for measurements at room temperature. Fura-2 fluorescence was recorded from eGFP-positive cells at an 340/380 nm excitation wavelength with 1 s intervals using a Polychrome V monochromator (TILL Photonics, Gräfelfing, Germany) and 14-Bit EMCCD; XON3 885 Andor camera (Andor Technology, South Windsor, CT, USA) coupled to an inverted IX71 microscope equipped with an UApo 340 40×/1.35 oil objective (Olympus, Hamburg, Germany).

Electrophysiological techniques

HEK 293 cells grown in 35 mm dishes to about 70% confluence were transfected with mouse TRPM7 cDNA in pIRES2-eGFP vector (Clontech Laboratories) (1–2 µg per dish) 20–30 h before analysis. Whole-cell patch-clamp recordings were carried out at room temperature (22°C).

Unless stated otherwise, cells were superfused with a standard physiological solution: 140 mM NaCl, 5 mM CsCl, 2 mM $CaCl_2$, 1 mM $MgCl_2$, 10 mM glucose, 10 mM HEPES, pH 7.4 with NaOH. The Cs^+-based external bath solution contained 130 mM CsCl, 50 mM mannitol, 10 mM HEPES, pH 7.4 with CsOH. In experiments with primary human ventricular cardiomyocytes, the external solution contained 10 µM TTX und 10 µM nimodipin in order to fully inhibit voltage-gated Na^+ and Ca^{2+} currents, respectively. Whole-cell patch-clamp recordings were performed with an EPC10 patch-clamp amplifier (HEKA, Lambrecht, Germany) using the PatchMaster v2x52 software (HEKA). Patch pipettes were made of borosilicate glass (Science Products, Hofheim, Germany) and had resistances between 1.2 to 2.3 MΩ when filled with the standard Mg^{2+} free intracellular solution: 130 mM CsCl, 0.635 mM $CaCl_2$ [5.5 nM calculated free $[Ca^{2+}]$ calculated with CaBuf programme (ftp.cc.kuleuven.ac.be/pub/droogmans/cabuf.zip)], 10 mM BAPTA, 1 mM HEDTA, 10 mM HEPES, pH 7.2. The Mg^{2+}-containing pipette solution was adjusted to 300 µM calculated free $[Mg^{2+}]$. The liquid junction potential was +5.1 or +4.7 mV, respectively, and corrected by the PatchMaster software. Series resistance compensation of 80% was used to reduce voltage errors in all experiments. Data were acquired at a frequency of 5 kHz after filtering at 1.67 kHz. The osmolality of all solutions was controlled by the vapour osmometer Vapro 5520 (Wescor Inc., Logan, UT, USA) and was 298 ± 3 mOsm·kg^{-1}.

To determine IC_{50} values, data were fitted with the Hill equation:

$$E(c) = E_{max} \times [c^n / (IC_{50}{}^n + c^n)]$$

with E being the effect/current at a given concentration c of activator/inhibitor, E_{max} the maximally achievable effect, IC_{50} the half-maximal concentration and n the Hill factor, being negative in the case of inhibitory action.

For cell-attached recordings of TRPM7 currents, HEK 293 cells were transfected with TRPM7 in pIRES-eGFP for 24 h. Prior to recording, cells were perfused 3–20 min with bath solution containing 140 mM NaCl, 5 mM CsCl, 1 mM $MgCl_2$, 2 mM $CaCl_2$ 10 mM HEPES (pH 7.4), 10 mM glucose with or without 10 µM NS8593. Continuous gap-free cell-attached recordings at pipette potentials of +60 mV (corresponding to –60 mV transmembrane potential) were performed for 1.5 min after gigaseal formation using ~8 MΩ borosilicale pipettes filled with a divalent cation free solution containing 145 mM CsCl, 5 mM NMDG-HEPES (pH 7.4) and 200 µM

Cs-HEDTA. A recording was considered positive when at least 1 burst of TRPM7 activity could be observed.

Functional characterization of TRPM3 was carried out in HBS (140 mM NaCl, 5 mM KCl, 2 mM $CaCl_2$, 1 mM $MgCl_2$, 10 mM glucose, 10 mM HEPES, pH 7.4). The pipette solution contained 120 mM CsCl, 20 mM NaCl, 1 mM $MgCl_2$, 2 mM EGTA and 10 mM HEPES, pH 7.4. Cells were activated by 10 μM PS. The extent of inhibition caused by NS8593 was quantified by interpolation of currents at +100 mV before the addition of the inhibitor and after complete wash-out.

Statistical analysis

Data are presented as means ± SEM. Unless stated otherwise, data were compared by Student's unpaired *t*-test. Significance was accepted at $P \leq 0.05$.

Results

Modulators of K_{Ca}2.1–2.3 (SK) channels inhibit TRPM7 activity

In light of the functional and structural similarity between pore-forming segments of TRPM7 and tetrameric K^+ channels (Chubanov *et al.*, 2007; Mederos y Schnitzler *et al.*, 2008), we wondered whether known modulators of K^+ channels would also affect TRPM7. To this end, we employed a 'chemical genomics' approach by investigating a subset of small compounds that have been shown to target distinct types of K^+ channels, that is, K_{IR}, K_V, K_{Ca}2.1–2.3, K_{Ca}1.1 (BK) and intermediate conductance K^+ (IK or K_{Ca}3.1) channels (Figure 1A). In these experiments, we took advantage of a recently developed bioluminescent assay that allows monitoring of Ca^{2+} influx mediated by recombinant TRPM7 stably expressed in HEK 293 cells under the control of a ponasteron A-inducible promoter sequence (Chubanov *et al.*, 2007). As shown in Figure 1B, in the absence of Mg^{2+} in the external bath solution, a one-step elevation of the external Ca^{2+} level ($[Ca^{2+}]_e$) from 1 to 5 mM elicited a fast and sustained rise of intracellular Ca^{2+} in stimulated HEK 293 cells. Intracellular Ca^{2+} levels ($[Ca^{2+}]_i$) were not increased in unstimulated cells or if external Ca^{2+} was constantly maintained at 1 mM (data not shown). TRPM7-mediated Ca^{2+} entry was abolished when 5 mM Ca^{2+} was co-applied with 10 mM Mg^{2+}, due to Mg^{2+}-dependent channel block (Nadler *et al.*, 2001). Furthermore, we observed that a select array of compounds targeting K_{Ca}2.1–2.3 channels (CyPPA, Dequalinium, NS8593, Quinine, and UCL 1684) inhibited TRPM7 to various degrees when applied externally at 30 μM (Figure 1B, C). In contrast, numerous modulators of K_{IR}, K_V, K_{Ca}1.1 and K_{Ca}3.1 channels (listed in Figure 1A) had no effect on TRPM7-mediated Ca^{2+} influx (data not shown). Since the sensitivity of TRPM7 to only one group of modulators was unexpected, we extended our screen to compounds affecting more distantly related channels, such as epithelial Na^+ (ENaC) channels (amiloride, triamterene), voltage-gated Na^+ (Na_V) channels (BIA 2–093, disopyramide, lidocaine, mexiletine, phenytoin, prilocaine, procainamide, procaine, R(-)-Me5, tetracaine, tocainide) and voltage-gated Ca^{2+} (Ca_V) channels (amiodarone, bepridil, cilnidipine, cinnarizine, diltiazem, ethosuximide, felodipine, gabapentin, FPL 64176, lercanidipine, nemadipine-A, nifedipine, nimodipine, nitrendipine, methoxyverapamil, plunarizine, SKF 96365, verapamil). We found that TRPM7 is insensitive to these compounds (30 μM) (data not shown). Thus, beyond inhibitors of K_{Ca}2.1–2.3 channels, TRPM7 displays a rather low cross-sensitivity to modulators targeting different channel groups.

NS8593 directly blocks the TRPM7 channel

In order to investigate if K_{Ca}2.1–2.3 inhibitors had direct effects on TRPM7 currents, we employed the patch-clamp technique. Figure 2 illustrates whole-cell currents measured in HEK 293 cells transiently transfected with TRPM7 cDNA. Removal of internal Mg^{2+} using a divalent-free pipette solution induced large currents with a current–voltage relationship, reflecting the typical signature of TRPM7: steep outward rectification, a reversal potential of about 0 mV, minute inward currents with divalent cations in the bath solution (Figure 2A, B). After currents had activated to saturation, we perfused cells with either 1 or 30 μM NS8593. We found that 1 μM NS8593 effectively reduced TRPM7 currents (Figure 2A). Of note, the suppression of TRPM7 currents was fully reversible and reproducible. The current–voltage (*I–V*) relationship of TRPM7 currents in the presence of 1 μM NS8593 was indistinguishable from *I–V* characteristics of TRPM7 in untreated cells (Figure 2A), indicating that under the experimental conditions chosen, the inhibitory effect of NS8593 does not appear to be voltage-dependent. This notion was further supported by recordings of voltage ramps up to 200 mV, thus ruling out substantial voltage-dependence of the NS8593 block (Supporting Information Figure S1, Appendix S1 and Appendix S2). In line with the Ca^{2+} imaging experiments, we observed that 30 μM NS8593 attenuated TRPM7 whole-cell currents in transfected HEK 293 cells (Figure 2B).

External divalent cations (Mg^{2+} and Ca^{2+}) are permeant blockers of TRPM7 resulting in very small inward currents at physiological membrane potentials carried by divalent cations. However, in the presence of divalent cation-free external solutions, TRPM7 is well permeable to monovalent cations such as Na^+ and Cs^+, giving rise to large inward currents. Consequently, we asked whether NS8593 would be equally effective in blocking such inward currents. However, our measurements performed in Na^+-based external saline revealed that initial monovalent cation currents exhibited a fast run-down, suggesting that under these experimental conditions Na^+ behaves as a blocker of TRPM7 similar to its effect on the genetically related TRPM3 channel (Oberwinkler *et al.*, 2005) (Supporting Information Figure S2). By contrast, whole-cell recordings in the presence of Cs^+-based external bath solutions yielded sustained inward and outward TRPM7 currents, allowing for a reliable analysis of NS8593 effects (Figure 2C). We found that 30 μM NS8593 completely suppressed both the inward and outward component of monovalent TRPM7 currents. Analogous to recordings with divalents in the bath solution (Figure 2A), NS8593 had no influence on the shape of the *I–V* relationship of Cs^+ currents (Figure 2C), supporting the notion that NS8593 acts by targeting the gating process of the channel rather than the permeation properties of the channel pore.

Next, we determined the concentration-dependence of the NS8593 effect under standard experimental conditions (i.e. Mg^{2+}-free internal solutions) (Figure 2D). Fitting of

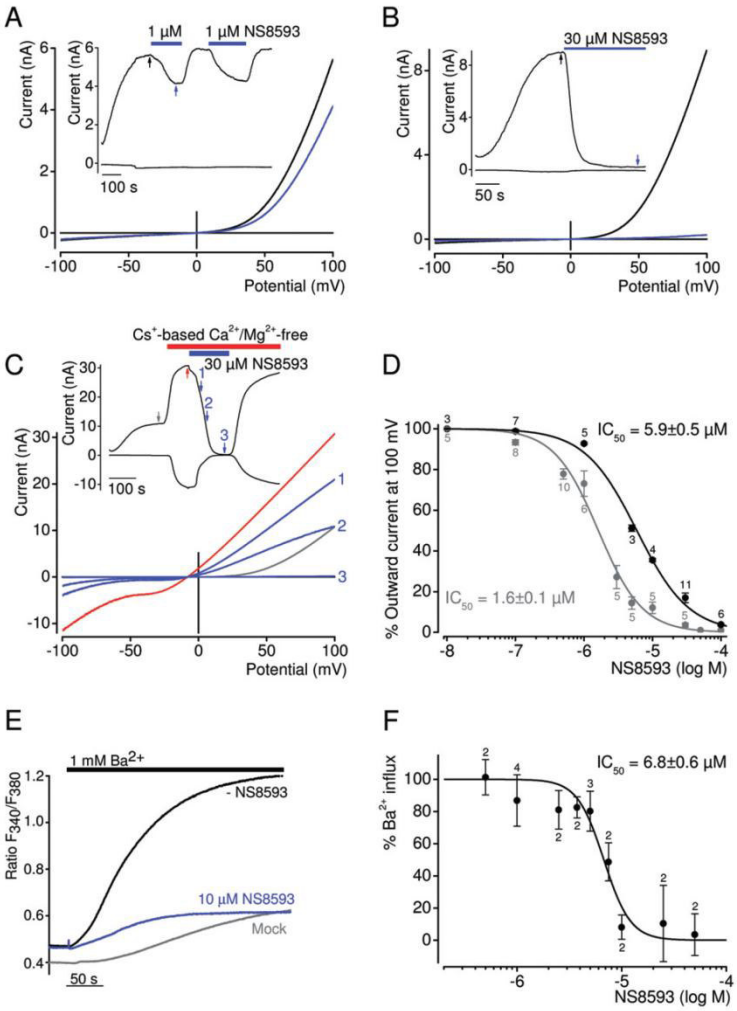

Figure 2

Inhibition of TRPM7 channel by NS8593. (A–B) Whole-cell TRPM7 currents measured in HEK 293 cells transiently expressing TRPM7. Representative current–voltage (*I–V*) relationships of TRPM7 currents were acquired before and after external application of 1 µM (A) or 30 µM (B) NS8593 as indicated by arrows in the corresponding currents over time recordings (shown in inserts) at −100 and 100 mV. (C) Representative traces of whole-cell currents measured as in (A–B) except that 30 µM NS8593 were applied when cells were perfused with divalent cation-free bath solution. (D) Concentration-dependent suppression of TRPM7 currents measured with internal solutions containing 0 or 300 µM Mg^{2+}. Numbers above dots indicate the number of cells measured. (E–F) The effect of NS8593 on Ba^{2+} influx in TRPM7-transfected HEK 293 cells. (E) Representative measurements of fura-2 fluorescence (ratio $F_{340/380}$) in cells incubated in divalent cation-free external bath solution followed by addition of 1 mM Ba^{2+} without or with 10 µM NS8593. Traces obtained with mock-transfected cells are shown. (F) Concentration-dependent effect of NS8593 on TRPM7-mediated Ba^{2+} entry. Measurements were performed as in (E), and Δ ratio $F_{340/380}$ values (calculated from datasets acquired at 25 and 250 s) were used to evaluate the inhibitory effect of NS8593. Numbers above dots indicate independent measurements.

experimental data with the Hill equation resulted in an IC_{50} value of 1.6 ± 0.1 µM. Previously, NS8593 was described as a 'negative gating modulator' of $K_{Ca}2.1$–2.3 channels, because channel inhibition was prominent at low internal Ca^{2+} concentrations and undetectable at 30 µM $[Ca^{2+}]_i$ (Jenkins *et al.*, 2011). Therefore, we tested whether internal Mg^{2+} would effect the sensitivity of TRPM7 to NS8593. Thus, we investigated the concentration-dependent suppression of TRPM7 activity by NS8593 in the presence of 300 µM internal Mg^{2+}, a subphysiological concentration that causes approximately

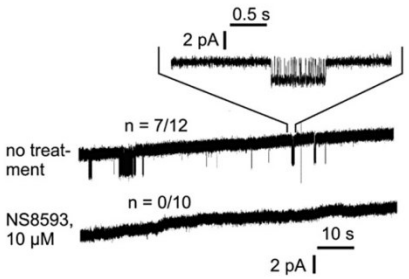

Figure 3

Cell-attached recordings of TRPM7 currents in HEK 293 cells. Before as well as during recording, cells were superfused with normal bath solution or bath solution supplemented with 10 µM NS8593. Inward monovalent currents through recombinant TRPM7 are visible as intermittent deflections from baseline level in 7 out of 12 untreated patches, but in 0 out of 10 patches from NS8593-pretreated cells.

half-maximal inhibition of TRPM7 currents (Mederos y Schnitzler *et al.*, 2008). Under these conditions, we observed a 3.7-fold rightward shift of the IC_{50} value (5.9 ± 0.5 µM), suggesting that NS8593 has a lower apparent affinity to the inactive (closed) channel; that is, the compound interferes with Mg^{2+}-dependent gating of the channel.

To investigate the inhibitory effect of NS8592 under more physiological conditions, we chose an imaging approach such that $[Mg^{2+}]_i$ was not modified by patch pipette solutions. It has previously been shown that TRPM7 is well permeable to Ba^{2+} (Monteilh-Zoller *et al.*, 2003; Mederos y Schnitzler *et al.*, 2008). Therefore, we measured Ba^{2+} influx into TRPM7-expressing HEK 293 labelled with the fluorescent dye fura-2 (Figure 2E, F). Addition of 1 mM Ba^{2+} to the bath resulted in fast and sustained Ba^{2+} influx (Figure 2E). NS8593 10 µM suppressed Ba^{2+} entry to levels observed in untransfected HEK 293 cells. Consequently, we systematically monitored concentration-dependent inhibition of TRPM7-mediated Ba^{2+} entry and determined an IC_{50} value of 6.5 ± 0.6 µM (Figure 2F), similar to the IC_{50} value obtained in patch-clamp experiments with 300 µM $[Mg^{2+}]_i$ (Figure 2D).

Next, we aimed to evaluate the inhibitory effect of NS8593 on TRPM7 at the single channel level using experimental conditions employed to study properties of endogenous TRPM7-like currents in Jurkat T-lymphocytes and RBL cells (referred to as Mg^{2+} inhibited currents or MIC) (Kerschbaum and Cahalan, 1999; Braun *et al.*, 2001; Kozak *et al.*, 2002). Accordingly, we performed continuous cell-attached recordings of monovalent cation currents at transmembrane potentials of –60 mV for 1.5 min after gigaseal formation (Figure 3). In TRPM7-transfected HEK 293 cells, we observed characteristic bursts of channel activity strikingly resembling MIC in RBL cells (Braun *et al.*, 2001; Prakriya and Lewis, 2002; Kerschbaum *et al.*, 2003). These bursts were not detectable in mock-transfected HEK 293 cells. Since under these experimental conditions the opening of TRPM7 was infrequent and short, we have compared the burst frequency in patches recorded from control and treated cells (Figure 3). We noted that characteristic single channel activities were not detectable when cells had been pre-exposed to 10 µM NS8593.

Table 2

Apparent affinity of wild-type and mutant TRPM7 channels to NS8593

TRPM7 variants	IC_{50} (µM) $[Mg^{2+}]_i$ free	300 µM $[Mg^{2+}]_i$
Wild type	1.6 ± 0.1	5.9 ± 0.6
Y1049P	0.47 ± 0.03	1.9 ± 0.2

Next, we performed a set of experiments to uncover the binding site of NS8593. It was shown that the kinase domain regulates the sensitivity of TRPM7 channel to $[Mg^{2+}]_i$. Therefore, we investigated whether the kinase domain is required for the NS8593 block of TRPM7 currents. In these experiments, we used two mutant cDNA variants: TRPM7 carrying the point mutation K1646R resulting in complete loss of kinase activity (TRPM7-K1646R) (Schmitz *et al.*, 2003; Matsushita *et al.*, 2005) and TRPM7 containing yellow fluorescent protein (YFP) instead of the kinase domain (residues 1464–1863 of mouse TRPM7, TRPM7-Δkinase-YFP). We found that TRPM7-K1646R and TRPM7-Δkinase-YFP gave rise to characteristic TRPM7 currents that could be suppressed by 10 µM NS8593 (data not shown), indicating that the kinase domain is not required for the action of NS8593 on TRPM7.

It was demonstrated that in the case of $K_{Ca}2.1$–2.3 channels, NS8593 directly interacts with serine and alanine residues located in the pore-forming loop and the S6 helix, implying that NS8593 occupies the inner pore vestibule near the selectivity filter, thus blocking the gate of $K_{Ca}2.1$–2.3 channels (Jenkins *et al.*, 2011). Therefore, we determined whether NS8593 would interact with TRPM7 in a similar fashion. We have recently shown (Mederos y Schnitzler *et al.*, 2008) that the putative pore-forming loop of mouse TRPM7 harbours conserved residues (E1047 and Y1049) essential for the permeability of divalent cations. While the E1047Q mutant was as sensitive to NS8593 as wild-type TRPM7 (data not shown), TRPM7-Y1049P displayed a substantially increased apparent affinity of the channel to NS8593 (Table 2). The Y1049P mutation resulted in an approximately fourfold reduction of IC_{50} values obtained either with 0 or 300 µM Mg^{2+} in the patch pipette when compared with wild-type TRPM7 (Table 2). These results suggest that the TRPM7 pore loop is involved in the interaction of TRPM7 and NS8593.

Taken together, we conclude that NS8593 directly and reversibly interacts with the pore-forming segment of activated TRPM7 channels resulting in a complete block.

Effect of modulators of $K_{Ca}2.1$–2.3 channels on TRPM7 currents

Our primary screening experiments suggested that chemically unrelated modulators of $K_{Ca}2.1$–2.3 channels are able to suppress TRPM7-mediated Ca^{2+} influx, in contrast to numerous modulators of other K^+ channel types (Figure 1B). In order to further substantiate these findings, we performed patch-clamp experiments to monitor the effects of com-

monly used inhibitors of $K_{Ca}2.1$–2.3, $K_{Ca}3.1$ and $K_{Ca}1.1$ channels on TRPM7 currents (Figure 4A, Supporting Information Figure S3). Analogous to experiments with NS8593, we assessed the modulators in the presence (Figure 4A) and absence (Figure 4B) of divalent cations in the external bath solution. These experiments confirmed that external (30 μM) quinine, dequalinium, CyPPA and UCL 1684 are able to suppress TRPM7 currents with different efficacies (Figure 4). We also observed that quinidine (stereoisomer of quinine) and clotrimazole exerted only modest inhibitory effects (5.6% and 7.5%, respectively) on TRPM7 currents. Interestingly, a peptide toxin of the Indian red scorpion, tamapin, that specifically blocks the pore of $K_{Ca}2.1$–2.3 channels by binding to an external site of the channel subunits (Pedarzani *et al.*, 2002), elicited a modest, but reproducible suppression of TRPM7 currents. In contrast, apamin, the bee venom peptide toxin, failed to inhibit TRPM7 activity, neither did paxilline and TRAM 34 (Figure 4A), known modulators of $K_{Ca}1.1$ and $K_{Ca}3.1$ channels, respectively.

Assessment of NS8593-related compounds

Structure–activity relationships (SAR) provide critical information for drug improvement. NS8593 contains benzimidazole and naphthylamine groups (Figure 5A). In order to get initial insights into SAR of NS8593, we tested several small compounds representing distinct chemical moieties of NS8593, such as 1,2,3,4-tetrahydro-1-naphthylamine (THN) and ABI. Patch-clamp experiments revealed that 30 μM ABI significantly (21%) suppressed TRPM7 currents, while THN had no influence on channel activity (Figure 5B), indicating that the aminobenzimidazole moiety is critical for the activity of NS8593. This conclusion was further supported by the observation that 30 and 100 μM BMB, containing two covalently linked aminobenzimidazole groups, inhibited TRPM7 (Figure 5B). Furthermore, we found that CBI is as effective as ABI, suggesting that an amino group at position 2 of benzimidazole is not essential for the sensitivity of TRPM7 to benzimidazoles.

The benzimidazole group is present in several compounds with known biological activity such as ABT 724 (dopamine D_4 receptor antagonist), clemizole (histamine H_1 receptor antagonist), DMAT (casein kinase 2 inhibitor 2), D-ribofuranosylbenzimidazole (inhibitor of RNA synthesis), droperidol (dopamine D_2 receptor antagonist), IRAK-1/4 Inhibitor I (inhibitor of interleukin-1 receptor-associated kinases 1/4), rabenzazole (fungicide), Ro 90-7501 (inhibitor of amyloid β42 fibril formation) and TBBz (inhibitor of casein kinase 2). To test the potential cross-reactivity of these molecules, we employed the bioluminescent assay of TRPM7 channel activity. We found no detectable effects of the latter compounds at 30 μM on TRPM7 (data not shown) and, therefore, excluded them from further biophysical analysis. We conclude that the benzimidazole group of NS8593 is primarily required for targeting of TRPM7 channels. Nevertheless, the overall structure of benzimidazole-derived compounds also appears to play a role in the inhibitory effect on TRPM7.

We noted that the benzimidazole group of NS8593 resembles known positive modulators of $K_{Ca}2.1$–2.3 channels such as NS309 and SKA31 (Figure 5A). Therefore, we tested

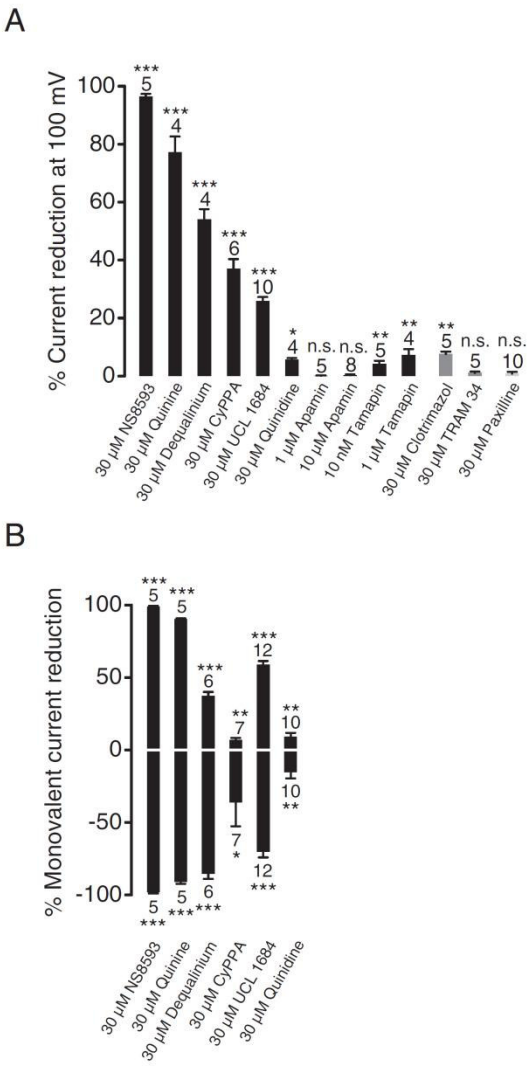

Figure 4

Assessment of effects of the $K_{Ca}2.1$–2.3 (SK) inhibitors on TRPM7 currents. (A) Whole-cell TRPM7 currents were measured in the presence of divalent cations in the same bath solutions as in Figure 2A. Inhibitory effects (%) were quantified by means of current amplitudes acquired at +100 mV before and after application of the indicated compounds. Effects of the compounds acting on $K_{Ca}3.1$ (IK) and $K_{Ca}1.1$ (BK) channels are illustrated. Numbers above columns indicate the number of cells measured. (B) Outward (upper panel) and inward (lower panel) monovalent cation currents were measured at +100 and −100 mV, respectively, in divalent cation-free bath solutions as in Figure 2C. $^{***}P \leq 0.001$; $^{**}P \leq 0.01$; $^{*}P \leq 0.05$; n.s., not significantly different (*t*-test).

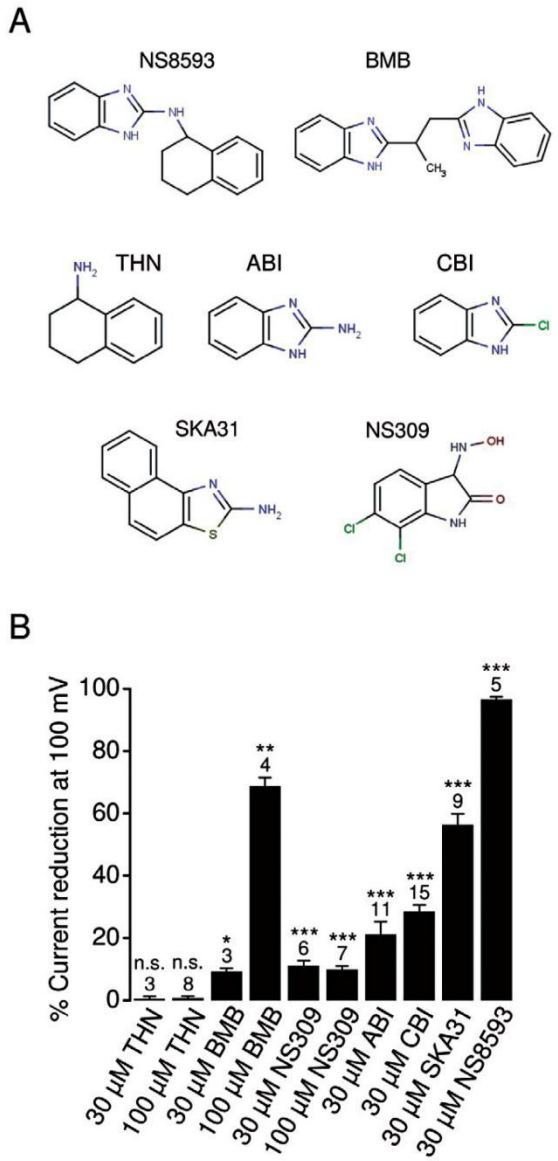

Figure 5

Characterization of NS8593-related compounds. (A) Chemical structures of the compounds examined. (B) Whole-cell TRPM7 currents were measured in the presence of divalent cations in bath solutions as in Figure 2A. Inhibitory effects (%) were quantified by means of current amplitudes acquired at +100 mV before and after the application of the indicated compounds. Numbers above columns indicate the number of cells measured. ***$P \leq 0.001$; **$P \leq 0.01$; *$P \leq 0.05$; n.s., not significantly different (*t*-test).

whether these compounds (30 µM) were able to positively modulate TRPM7. However, we found that SKA31 suppressed TRPM7 currents (56%), whereas NS309 caused only a minor reduction (11%) of channel activity (Figure 5B).

Effect of NS8593 on other TRP channels

We determined whether NS8593 can discriminate between TRPM7 and other genetically related TRP channels. TRPM7 and TRPM6 are paralogues sharing ~64% amino acid sequence similarity within their channel segments (Chubanov *et al.*, 2004). However, we were unable to monitor the effect of NS8593 on TRPM6, since our previous efforts (Chubanov *et al.*, 2004; 2007) to express recombinant functional TRPM6 channels either in mammalian cells or *Xenopus* oocytes failed and attempts to measure endogenous TRPM6 currents were not successful so far (Li *et al.*, 2006; Ryazanova *et al.*, 2010).

TRPM3, the closest non-kinase-bearing relative of TRPM7 within the TRPM family, is a constitutively active cation channel highly permeable to Ca^{2+} and can further be potentiated by sulfated steroids like PS (Wagner *et al.*, 2008). To this end, we performed whole-cell measurements of PS-induced currents in HEK 293 cells transiently transfected with TRPM3 cDNA (Figure 6). In line with previous publications (Wagner *et al.*, 2008), external application of 10 µM PS induced large cation currents. At ramp potentials of +100 mV, coapplication of NS8593 in the range of 10–100 µM resulted in suppression of PS-induced TRPM3 currents with an IC_{50} value of 26.7 ± 3.9 µM. During voltage ramps from −100 to +200 mV, we observed an increase in current suppression at highly positive potentials (Supporting Information Figure S1B). This behaviour was only rudimentarily seen in analogous experiments with TRPM7. To assess whether this phenomenon would reduce the ability of the compound to discriminate between the two related ion channels at more physiological membrane potentials, we performed fluorescence-based Ca^{2+} entry experiments with fura-2 loaded cells (Supporting Information Figure S4A). NS8593 at 10 µM has no measurable influence on PS-induced Ca^{2+} influx in TRPM3-expressing cells. We conclude that moderate concentrations of NS8593 are selective for TRPM7.

Next, we investigated the effect of NS8593 on TRPM channels more distantly related to TRPM7 in terms of primary sequence similarity and function. TRPM8 is Ca^{2+} -permeable cation channel activated by cold temperatures and several agonists such as menthol and icilin (Peier *et al.*, 2002). TRPM2 is activated by free intracellular ADP-ribose in synergy with free intracellular Ca^{2+} (Perraud *et al.*, 2001; Starkus *et al.*, 2007). TRPM2 also acts as a sensor for reactive oxygen species including H_2O_2 (Hara *et al.*, 2002). Using a Ca^{2+} imaging approach, we tested whether 10 µM NS8593 would negatively modulate H_2O_2-activated TRPM2 and icilin-activated TRPM8 channels (Supporting Information Figure S4B, C). These experiments demonstrated that NS8593 does not suppress TRPM8 and TRPM2 channel activity. TRPM5 is a monovalent-selective cation channel, directly gated by intracellular calcium that rises upon stimulation of GPCRs linked to PLC (Hofmann *et al.*, 2003). We observed that 10 µM NS8593 has no effect on TRPM5 currents (Supporting Information Figure S5A). TRPC6 is a Ca^{2+}-permeable cation channel directly gated by diacylglycerol produced by PLC after activation of GPCR such as histamine H_1 receptors (Hofmann *et al.*, 1999). We found that TRPC6 currents induced by stimulation of H_1 receptors are insensitive to externally applied 10 µM NS8593 (Supporting Information Figure S5B).

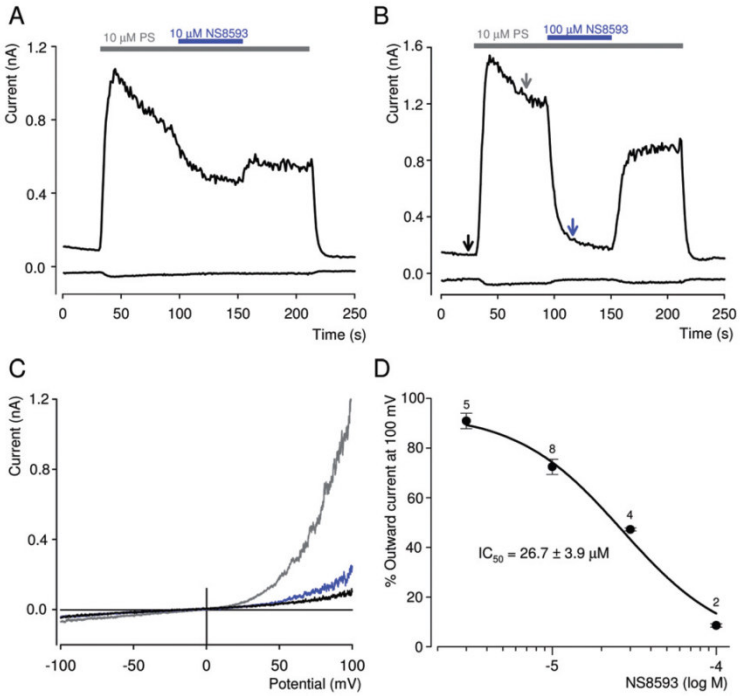

Figure 6

Effect of NS8593 on PS-induced TRPM3 currents. (A, B) Representative traces of whole-cell TRPM3 currents measured at –100 and +100 mV over time induced by extracellular application of 10 μM PS. NS8593 10 μM (A) or 100 μM (B) were coapplied with PS as indicated. (C) Current–voltage relationships of PS-induced TRPM3 currents acquired from measurements before and after application of 100 μM NS8593 as indicated by arrows in (B). (D) Concentration-dependent suppression of PS-induced TRPM3 currents by NS8593. Numbers above symbols indicate the number of cells measured.

Finally, we studied the effects of NS8593 on TRPV1 and TRPA1, which are receptive to a very broad range of natural and synthetic compounds (Vriens *et al.*, 2008) (Supporting Information Figure S6). We observed that Ca^{2+} entry in HEK 293 cells mediated by capsaicin-induced TRPV1 as well as allyl isothiocyanate (AITC)-stimulated TRPA1 is not affected by 10–30 μM NS8593. Thus, NS8593 specifically targets the TRPM7 channel among TRP channels representing distinct genetic and functional branches of TRP channels.

Assessment of long-term effects of NS8593

So far, we had studied short-term pharmacological properties of NS8593. In order to clarify if NS8593 was a useful suppressor of TRPM7 function in a cell biological context, we performed additional experiments addressing long-term effects of NS8593. Overexpression of human TRPM7 in a tetracycline-inducible HEK 293 cell line results in detachment and consequently cell death (Nadler *et al.*, 2001). Therefore, we wondered whether NS8593 would be able to forestall this cellular phenotype (Figure 7). We induced TRPM7 expression in a HEK 293 cell line with tetracycline and confirmed channel expression using a TRPM7-specific antibody (Figure 7A). In line with previous reports, we found that after 18 h of induction with 1 μM tetracycline, TRPM7-expressing cells developed a rounded morphology (Figure 7A), while patch-clamp measurements revealed at the same time that stimulated cells exhibited very large TRPM7 currents (Figure 7B). Most of the cells stimulated for 36 h lost adherence to the substratum and formed floating cell clusters (Figure 7C, D). Next, we added different concentrations of NS8593 to the culture medium and noted that 5–10 μM NS8593 preserved cell adherence and viability, thus completely reversing the cellular phenotype caused by TRPM7 overexpression (Figure 7C, D). Thus, application of NS8593 for a longer time period allows for the suppression of TRPM7 function without any obvious cell toxicity. Finally, we tested whether other TRPM7 inhibitors, like quinine and UCL 1684 (Figure 4, Supporting Information Figure S3), were able to rescue the phenotype of stimulated HEK 293 cells. We found that the application of both compounds (10 μM) to the cell culture medium prevented detachment of tetracycline-induced cells (Supporting Information Figure S7). Thus, structurally unrelated inhibitors of TRPM7 currents were able to protect HEK 293 cells overexpressing recombinant TRPM7 from resultant morphological changes.

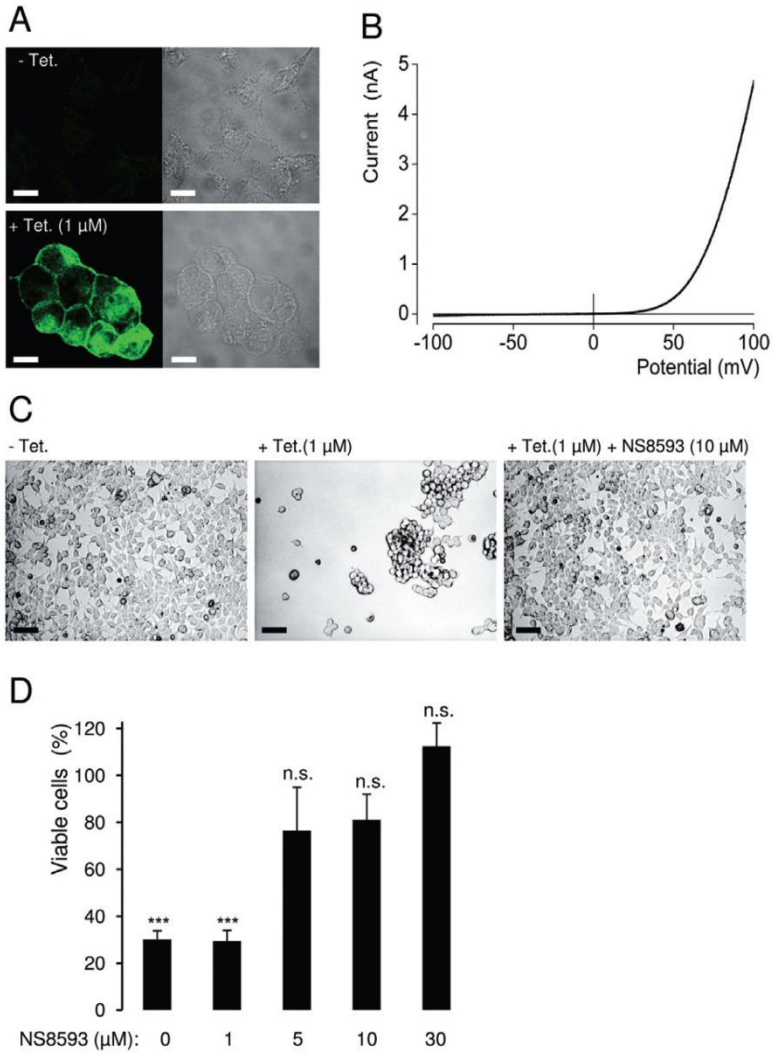

Figure 7

Effect of NS8593 on the viability of HEK 293 cells overexpressing recombinant TRPM7. (A) Tetracyclin(Tet)-induced (1 µM, 18 h) expression of the human TRPM7 protein as assessed by immunofluorescence staining using anti-TRPM7 antibody. Scale bars – 10 µm. (B) Representative *I–V* relationship of fully developed whole-cell TRPM7 currents measured in stimulated HEK 293 cells (1 µM tetracycline, 18–24 h). (C) Effect of NS8593 (10 µM) on the morphology of tetracycline-induced (1 µM, 36 h) HEK 293 cells. Scale bars – 50 µm. (D) Viability of HEK 293 cells expressing TRPM7 in the presence of different concentrations of NS8593. Experiments were performed as in (C), and the total number of viable cells was compared with that of unstimulated cells (– tetracycline). Data from three independent experiments are shown. ***$P \leq 0.001$; n.s., not significantly different (*t*-test).

Targeting of endogenous TRPM7 currents by NS8593

We determined whether NS8593 is able to inhibit endogenous TRPM7 channels. TRPM7 is a ubiquitously expressed protein and, consistently, patch-clamp experiments showed that native TRPM7-like currents are present in all cells examined so far, including HEK 293 cells (Nadler *et al.*, 2001; Chubanov *et al.*, 2007). Figure 8 illustrates the effect of NS8593 on native cation currents with an *I–V* relationship very similar to that of recombinant TRPM7. Currents were induced by removal of cytosolic Mg^{2+} as shown in Figure 2. We found that 10 or 30 µM NS8593 effectively suppressed whole-cell currents to background levels measured immediately after establishment of the whole-cell configuration (Figure 8A). We next studied the affect of 10 µM NS8593 on

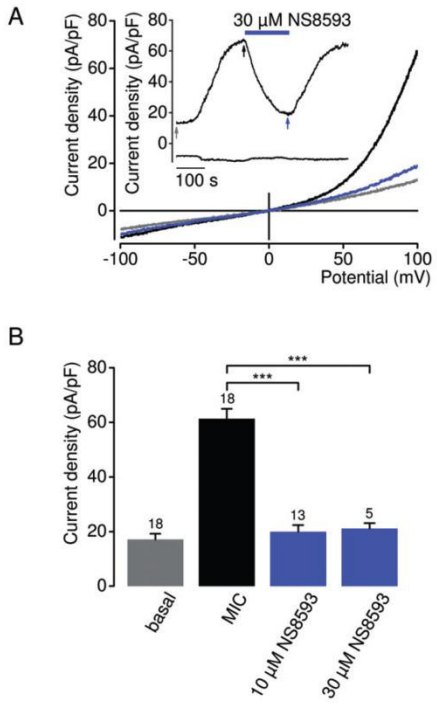

Figure 8

Inhibition of native TRPM7-like currents in HEK 293 cells by NS8593. (A) Representative current density–voltage relationships of native whole-cell currents (MIC) induced by depletion of internal Mg^{2+} in HEK 293 cells. Measurements were performed as in Figure 2A. The insert shows the corresponding currents over time measured at −100 and +100 mV. Current density–voltage relationships were acquired at time points as indicated by arrows. (B) Analysis of current density amplitudes at +100 mV acquired before and after current induction or after application of NS8593 as indicated by arrows in (A). Numbers above columns indicate the number of cells measured; $***P \leq 0.001$ (*t*-test).

endogenous TRPM7 currents in mouse smooth muscle cells freshly isolated from brain arteries, primary mouse podocytes and primary human ventricular myocytes (Figure 9). TRPM7-like currents were persistently detectable in all cell types examined. We observed that – like in HEK 293 cells – 10 µM NS8593 caused a full and reversible suppression of native TRPM7-like currents (Figure 9). Thus, NS8593 appears to be equally efficient in targeting recombinant and native TRPM7 channels.

Subsequently, we determined whether pharmacological inhibition of the native TRPM7 protein by NS8593 would affect TRPM7-dependent cellular processes such as cell motility (Clark *et al.*, 2006; Su *et al.*, 2006; 2011) and proliferation (Nadler *et al.*, 2001; Schmitz *et al.*, 2003; Sahni and Scharenberg, 2008), which are affected by a depletion of TRPM7 or by RNAi approaches. Specifically, we investigated if NS8593

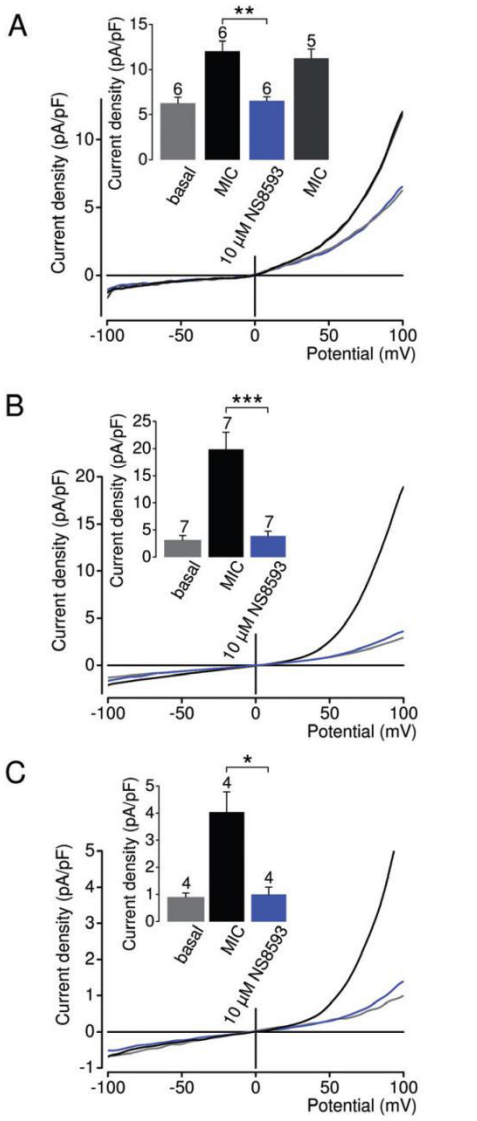

Figure 9

Inhibition of native TRPM7-like currents in vascular smooth muscle cells, podocytes and ventricular myocytes by NS8593. Representative current density–voltage relationships of native whole-cell currents (MIC) induced by depletion of internal Mg^{2+} in mouse smooth muscle cells freshly isolated from brain arteries (A), primary mouse podocytes (B) and primary human ventricular myocytes (C). Measurements were performed as in Figure 2A. The insert shows corresponding current densities at +100 mV acquired before and during current induction or in the presence of NS8593. The insert in (A) shows recovered currents, if pretreated cells were reperfused with NS8593-free solution. Numbers above columns indicate the number of cells measured; $***P \leq 0.001$; $**P \leq 0.01$; $*P \leq 0.05$ (*t*-test).

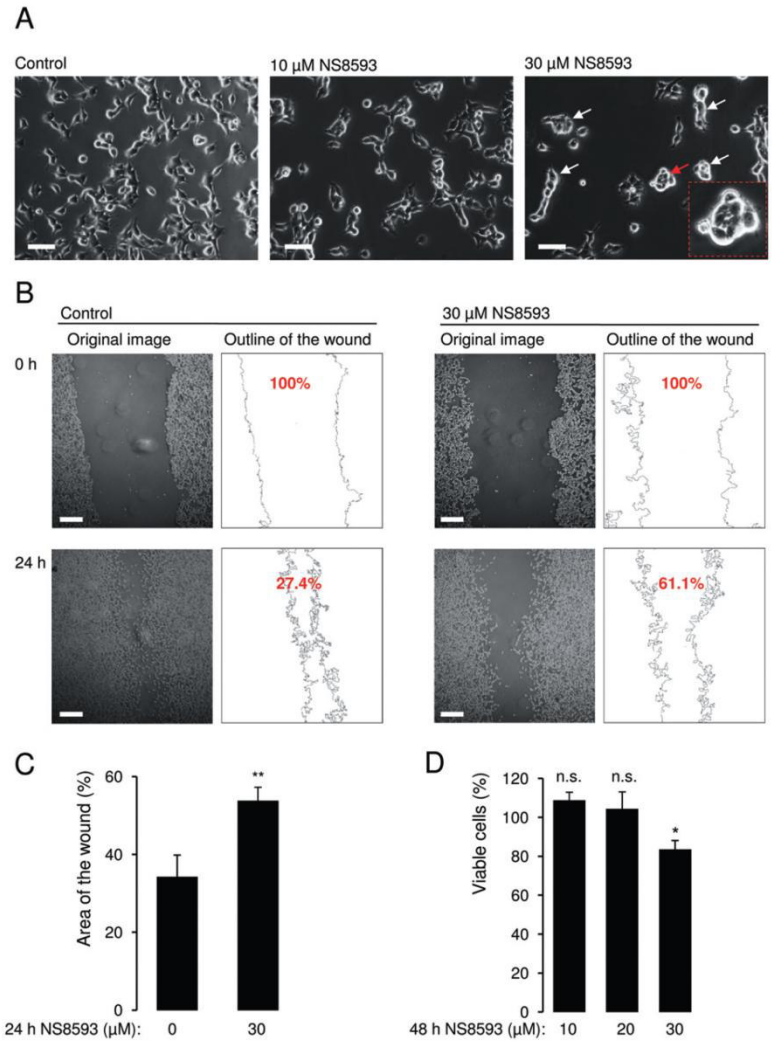

Figure 10

Effects of NS8593 on motility and proliferation of HEK 293 cells. (A) Images of living HEK 293 cells cultured without or with indicated concentrations of NS8593 (24 h). In the presence of 30 μM NS8593, cell colonies frequently displayed a tight and round shape. Insert illustrates at a higher magnification the colony indicated by the red arrow. Scale bars – 30 μm. (B, C) Effect of 30 μM NS8593 on cell motility as assessed by a wound healing assay. (B) Representative images of HEK 293 cells acquired either immediately or 24 h after wounding. Outline of the wound and percentage of the closure area (%) were determined using ImageJ. Scale bars – 200 μm. (C) Data from six independent assays are shown; $^{**}P \leq 0.01$ (*t*-test). (D) Viability of HEK 293 cells cultured (48 h) in the presence of indicated concentrations of NS8593. The total number of viable cells was compared with that of untreated cells (100%). Data from three independent experiments are shown, $^{*}P \leq 0.05$; n.s., not significantly different (*t*-test).

would influence growth and motility of HEK 293 cells displaying the highest level of native TRPM7 currents (compare Figure 8 and Figure 9). Figure 10A depicts HEK 293 cells cultured for 24 h without or with 10–30 μM NS8593. Under control conditions, we observed groups of cells with characteristic protrusions as well as numerous single spreading cells. We noted that 10 μM NS8593 suppressed motility of HEK 293 cells, because most treated cells remained in colonies and displayed either shorter protrusions or a round shape. Furthermore, cells cultured in the presence of 30 μM NS8593 often formed very tight round colonies (Figure 10A, insert), which were never observed in control cells. These morphological changes were not found, when 1 μM apamin was added to the culture medium, strongly arguing against an

involvement of $K_{Ca}2.1–2.3$ channels (Supporting Information Figure S8). Next we investigated whether benzimidazol derivatives, like BMB (Figure 5B), might suppress the motility of HEK 293 cells as well. Previously, we found that 30 μM BMB elicited only a minor (~10%) inhibitory effect on TRPM7 currents (Figure 5B). Consistently, application of 10–30 μM BMB to the cell culture medium had no influence on cell morphology (Supporting Information Figure S8), indicating that the effect of NS8593 on HEK 293 cells was due to inactivation of TRPM7 currents rather than $K_{Ca}2.1–2.3$ channels.

In order to further evaluate the influence of NS8593 on the motility of HEK 293 cells, we performed a wound healing assay (Figure 10B, C). In line with our previous experiments, wound closure was substantially more efficient in control cells as compared with cells cultured for 24 h in the presence of 30 μM of NS8593 ($P \leq 0.01$, Figure 10C). Finally, we examined whether NS8593 would influence the proliferation of HEK 293 cells, because numerous studies reported that TRPM7 deficiency profoundly interferes with cell viability (Nadler *et al.*, 2001; Schmitz *et al.*, 2003; Sahni and Scharenberg, 2008; Ryazanova *et al.*, 2010). NS8539 10–30 μM did not significantly reduce the total number of HEK 293 cells cultured for 24 h (data not shown), ruling out the possibility that the reduced motility of NS8593-treated cells (Figure 10A–C) is secondary to cellular toxicity of the drug. However, after 48 h, cell proliferation was reduced (17%, $P \leq 0.05$) in the presence of 30 μM NS8593 (Figure 10D). Thus, NS8593 has a rather modest influence on the proliferation of HEK 293 cells, which is fully compatible with the aforementioned concept that NS8593 preferentially targets active TRPM7 channels. However, we cannot exclude the possibility that inhibition of both the channel and kinase moieties of TRPM7 would impart a more pronounced effect on the proliferation of HEK 293 cells.

Overall, our cell biological experiments demonstrate that moderate concentrations of NS8593, at which the drug discriminates well amongst TRPM channels and is non-toxic to cells in culture, selectively inhibit native TRPM7 channels and elicit characteristic cellular phenotypes. Consequently, NS8593 may be a promising compound to pharmacologically target TRPM7 *in vivo*.

Discussion and conclusions

We present the results of a hypothesis-driven 'chemical genomics' approach to identify non-toxic inhibitors of the ubiquitously expressed Mg^{2+}-sensitive TRPM7 cation channel. Our data indicate that structurally unrelated modulators of $K_{Ca}2.1–2.3$ channels are able to suppress TRPM7 currents, in stark contrast to numerous compounds targeting other channel types. Thus, the broad array of known $K_{Ca}2.1–2.3$ modulators opens up the possibility for a pharmacological assessment of still poorly understood aspects of TRPM7 function. As a proof-of-concept, we further investigated NS8593. This drug turned out to be specific for TRPM7 when compared with other TRP channels, interfered with Mg^{2+} dependent activation of TRPM7 most probably due to interaction with the channel pore, and is capable of modulating cell motility.

Identification of new TRPM7 modulators

There is mounting evidence that TRPM channels share several structural and functional characteristics with tetrameric K^+ channels. For instance, intrinsic voltage-dependence of temperature-sensitive TRPM8 and TRPM5 was found to be mediated by positively charged residues located in the fourth transmembrane helix, analogous to a voltage sensor of voltage-gated K^+ channels (Nilius *et al.*, 2007). Due to a homology of the pore-forming regions of TRPM and K^+ channels, ion permeation mechanisms of several TRPM channels have recently been uncovered (Mederos y Schnitzler *et al.*, 2008). Furthermore, the control of TRPM7 channel activity by Mg^{2+} and, ATP and PIP_2 (Nadler *et al.*, 2001; Runnels *et al.*, 2002; Kerschbaum *et al.*, 2003) is also a functional hallmark of several types of K^+ channels (Figure 1) (Stanfield *et al.*, 1994; Wible *et al.*, 1994; Taglialatela *et al.*, 1995).

Against this background, we investigated whether known inhibitors and activators of Mg^{2+}-sensitive K^+ channels would target TRPM7. We tested a subset of compounds targeting different types of cation channels and identified several organic compounds exhibiting inhibitory effects on TRPM7 activity when applied at 30 μM. The identified inhibitors can be grouped into three different classes according to their chemical structure. Quinine, dequalinium and UCL 1684 contain quinolinium groups; NS8593, SKA31, THN and ABI are benzimidazole derivates; finally, CyPPA represents a third scaffold – this molecule comprises cyclohexyl, dimethylpyrazol and methylpyrimidin groups. Previous SAR studies concentrating on these three scaffolds (Sorensen *et al.*, 2008) yielded dozens of related compounds, which can be used in future to improve the affinity and specificity of TRPM7 inhibitors (reviewed in Weatherall *et al.*, 2010). Interestingly, some of these compounds are known therapeutic agents. For instance, quinine is a plant alkaloid known as the first effective antimalaria drug, which is still employed to treat the disease in certain critical situations

In addition to the identification of new organic modulators of TRPM7, our screening experiments highlight an unexpected relationship between TRPM7 and $K_{Ca}2.1–2.3$ channels. Thus, we observed that TRPM7 is not sensitive to numerous modulators targeting K_{IR}, K_V, $K_{Ca}1.1$, $K_{Ca}3.1$, ENaC, Na_V, Ca_V channels, arguing that TRPM7 has a rather low cross-sensitivity to these types of cation channel modulators. By contrast, chemically unrelated inhibitors of $K_{Ca}2.1–2.3$ channels were able to inactivate TRPM7. The most straightforward mechanistic explanation for this finding is that despite the low degree of primary amino acid sequence homology, the channel segments of TRPM7 and $K_{Ca}2.1–2.3$ harbour a similar drug binding site interfering with the gating of these channels. We cannot exclude the possibility that common endogenous metabolites regulate $K_{Ca}2.1–2.3$ and TRPM7 channels, thereby causing cross-sensitivity of $K_{Ca}2.1–2.3$ and TRPM7 to the same synthetic ligands.

NS8593 as a negative gating modulator of TRPM7

The mechanism underlying the Mg^{2+}-dependent regulation of TRPM7 channel activity is still incompletely understood, unlike the Ca^{2+}-dependent gating of $K_{Ca}2.1–2.3$ channels, which occurs via a 'chemical-coupling' mechanism. The

C-terminus of $K_{Ca}2.1–2.3$ channels is constitutively attached to calmodulins. Interaction of Ca^{2+} with calmodulin induces a conformational rearrangement of the C-terminus and, subsequently, of the channel gate (Berkefeld *et al.*, 2010). In addition, intracellular Mg^{2+} negatively regulates $K_{Ca}2.1–2.3$ channels acting via a conserved serine pore loop residue (S359 in rat $K_{Ca}2.2$, Figure 1) (Soh and Park, 2002). It has been shown recently that this serine residue directly interacts with NS8593 (Jenkins *et al.*, 2011). It was postulated that NS8593 acts as negative gating modulator of $K_{Ca}2.1–2.3$ channels, since the inhibitory potential of NS8593 was highly dependent on intracellular Ca^{2+}: inhibition was prominent at low Ca^{2+} concentrations and abolished at 30 μM Ca^{2+} (Strobaek *et al.*, 2006).

A similar scenario may also underlie the inhibitory effects of NS8593 on TRPM7. Our experiments revealed that the effect of NS8593 on TRPM7 is modulated by internal Mg^{2+}: the IC_{50} value of NS8593 was increased by 3.7-fold when the pipette solution was supplemented with 300 μM Mg^{2+}. The inhibition of TRPM7 currents by NS8593 was voltage-independent and equally potent for monovalent and divalent cation currents carried by TRPM7. Furthermore, we were able to detect the inhibitory effect of NS8593 on TRPM7 channels at the single channel level. We also determined a possible NS8593 interaction site within TRPM7. Apparently, the kinase domain of TRPM7 is not required for targeting of TRPM7 by NS8593, since two kinase deficient mutants, TRPM7-K1646R and TRPM7-Δkinase-YFP, were fully suppressed by NS8592. However, we observed that a point mutation in the pore-forming loop (Y1049P) of TRPM7 increased sensitivity of the channel to NS8593 since TRPM7-Y1049P elicited a fourfold smaller IC_{50} value. Finally, we performed an initial SAR analysis of NS8593, suggesting that the benzimidazole group is required for the pharmacological action of NS8593 on TRPM7. However, TRPM7 was found to be insensitive to a subset of biologically active compounds containing the benzimidazole group, arguing that interaction of TRPM7 with NS8593 is relatively specific.

Taken together, we hypothesize that similar to $K_{Ca}2.1–2.3$ channels NS8593 occupies the inner pore vestibule distally to the predicted selectivity filter of TRPM7. The molecular interaction is most probably mediated by the pore-forming loop of TRPM7 and the imidazole ring of NS8593 and is critically dependent on intracellular Mg^{2+}. A plausible explanation for the observed Mg^{2+} dependence is that the inactive (closed) TRPM7 channel (high concentration of intracellular Mg^{2+}) is less accessible to NS8593 than the active (open) channel (low intracellular Mg^{2+}).

Recently, Zierler *et al.* (2011) showed that a natural compound, waixenicin A, inhibits TRPM7-mediated entry of divalent cations (IC_{50} = 12 μM) as assessed by Fura 2. Interestingly, patch-clamp experiments revealed that waixenicin A irreversibly blocks TRPM7 currents (IC_{50} = 7 μM and 16 nM at 0 and 700 μM $[Mg^{2+}]_i$). Thus, unlike other TRPM7 inhibitors (Table 1), NS8593 and waixenicin A act on TRPM7 in a $[Mg^{2+}]_i$-dependent manner, which may be instrumental in differentiating gating mechanisms.

Pharmacological potential of NS8593

TRPM7 plays a crucial role in several pathological conditions. For instance, TRPM7 regulates proliferation and survival of several types of tumour cells (Hanano *et al.*, 2004; Jiang *et al.*, 2007; Kim *et al.*, 2008; Guilbert *et al.*, 2009; Mishra *et al.*, 2009). Furthermore, a role of TRPM7 was postulated in hypertension (Touyz, 2008), neuronal cell death following ischaemic injury (Aarts *et al.*, 2003), multiple sclerosis and Alzheimer's disease (Tseveleki *et al.*, 2010). More recently, up-regulation of TRPM7 function was found to be associated with fibrogenesis leading to atrial fibrillation in the failing heart (Du *et al.*, 2010). These findings highlight TRPM7 as a promising drug target. However, since ubiquitously expressed TRPM7 plays an indispensible role in the cell cycle, an indiscriminate pharmacological inactivation of TRPM7 will most likely be toxic implying that use-dependent TRPM7 blockers would have a better therapeutic perspective. In the present study, we present data to support the notion that the development of this type of organic compounds is feasible. Specifically, we found that NS8593 reversibly inhibits recombinant TRPM7 channels in a Mg^{2+}-dependent manner, allowing for preferential suppression of active TRPM7 channels. Our results indicate that NS8593 at concentrations (10 μM) sufficient to fully suppress TRPM7 activity does not affect other TRP channels, like TRPM2, TRPM3, TRPM5, TRPM8, TRPC6, TRPV1 and TRPA1. We have also shown that NS8593 is able to elicit a sustained effect on TRPM7, since addition of NS8593 to the cell culture medium completely reversed the cell toxic effect of TRPM7 overexpression in HEK 293 cells. In addition, we showed that 10 μM NS8593 fully inhibit native TRPM7 currents in HEK 293 cells, resulting in a substantial inhibition of cell motility, indicating that inactivation of the channel activity of the bifunctional TRPM7 protein is sufficient to induce this phenotype. Finally, we demonstrated that 10 μM NS8593 block endogenous TRPM7 currents in mouse smooth muscle cells freshly isolated from brain arteries, primary mouse podocytes and primary human ventricular myocytes. Together, our findings suggest that NS8593 is well-suited to study recombinant and native TRPM7 channels *in vitro* and may be a first step towards the development of non-toxic drugs targeting TRPM7 *in vivo*.

NS8593 was originally described as a reversible inhibitor of apamin-sensitive Ca^{2+}-activated potassium channels with IC_{50} values 0.42, 0.60 and 0.73 μM at 0.5 μM Ca^{2+} for $K_{Ca}2.1–2.3$ subtypes (Strobaek *et al.*, 2006). Interestingly, the inhibitory effects of NS8593 on $K_{Ca}2.1–2.3$ were undetectable at 30 μM $[Ca^{2+}]_i$ (Jenkins *et al.*, 2011). In excitable cells, $K_{Ca}2.1–2.3$ channels mediate hyperpolarizing K^+ currents to modulate repetitive electrical activity and firing patterns (Berkefeld *et al.*, 2010). In nonexcitable cells, such as endothelial cells, hyperpolarizing $K_{Ca}2.1–2.3$ currents maintain the driving force for Ca^{2+} influx (Taylor *et al.*, 2003; Berkefeld *et al.*, 2010). The pharmacological potential of NS8593 *in vivo* has already been demonstrated for the modulation of the firing rate of dopaminergic neurons (Herrik *et al.*, 2010) and the termination of atrial fibrillation (Diness *et al.*, 2010). Of note, the cross-reactivity of NS8593 might be beneficial for these pharmacological actions: The suppression of ubiquitously present TRPM7 by NS8593 may reduce intracellular concentrations of divalent cations including Ca^{2+}, which in turn may further enhance the NS8593-induced block of $K_{Ca}2.1–2.3$ channels. Future studies will have to specifically address this issue.

Acknowledgements

This study was supported by the Deutsche Forschungsgemeinschaft, Wissenschaftliches Herausgeberkollegium der Münchener Medizinischen Wochenschrift e.V and Friedrich-Baur-Stiftung Muenchen. TH was supported by the Emmy-Noether-Programm of the DFG (DFG-Ho-3869). We thank Anna-Lena Forst for preparation of podocytes, Renate Heilmair and Joanna Zaißerer for excellent technical assistance and Ursula Storch for critical discussion. We thank Carsten Schmitz, National Jewish Health and University of Colorado Denver, for providing a HEK 293 cell line stably expressing human TRPM7.

Conflicts of interest

None.

References

Aarts M, Iihara K, Wei WL, Xiong ZG, Arundine M, Cerwinski W *et al.* (2003). A key role for TRPM7 channels in anoxic neuronal death. Cell 115: 863–877.

Alexander SPH, Mathie A, Peters JA (2011). Guide to Receptors and Channels (GRAC), 5th Edition. Br J Pharmacol 164 (Suppl. 1): S1–S324.

Baubet V, Le Mouellic H, Campbell AK, Lucas-Meunier E, Fossier P, Brulet P (2000). Chimeric green fluorescent protein-aequorin as bioluminescent Ca^{2+} reporters at the single-cell level. Proc Natl Acad Sci U S A 97: 7260–7265.

Berkefeld H, Fakler B, Schulte U (2010). Ca^{2+}-activated K^+ channels: from protein complexes to function. Physiol Rev 90: 1437–1459.

Brauchi S, Krapivinsky G, Krapivinsky L, Clapham DE (2008). TRPM7 facilitates cholinergic vesicle fusion with the plasma membrane. Proc Natl Acad Sci U S A 105: 8304–8308.

Braun FJ, Broad LM, Armstrong DL, Putney JW Jr (2001). Stable activation of single Ca^{2+} release-activated Ca^{2+} channels in divalent cation-free solutions. J Biol Chem 276: 1063–1070.

Chen HC, Xie J, Zhang Z, Su LT, Yue L, Runnels LW (2010b). Blockade of TRPM7 channel activity and cell death by inhibitors of 5-lipoxygenase. PLoS ONE 5: e11161.

Chen X, Numata T, Li M, Mori Y, Orser BA, Jackson MF *et al.* (2010a). The modulation of TRPM7 currents by nafamostat mesilate depends directly upon extracellular concentrations of divalent cations. Mol Brain 3: 38.

Chubanov V, Waldegger S, Mederos y Schnitzler M, Vitzthum H, Sassen MC, Seyberth HW *et al.* (2004). Disruption of TRPM6/TRPM7 complex formation by a mutation in the TRPM6 gene causes hypomagnesemia with secondary hypocalcemia. Proc Natl Acad Sci U S A 101: 2894–2899.

Chubanov V, Mederos y Schnitzler M, Waring J, Plank A, Gudermann T (2005). Emerging roles of TRPM6/TRPM7 channel kinase signal transduction complexes. Naunyn Schmiedebergs Arch Pharmacol 371: 334–341.

Chubanov V, Schlingmann KP, Waring J, Heinzinger J, Kaske S, Waldegger S *et al.* (2007). Hypomagnesemia with secondary hypocalcemia due to a missense mutation in the putative pore-forming region of TRPM6. J Biol Chem 282: 7656–7667.

Clark K, Langeslag M, van Leeuwen B, Ran L, Ryazanov AG, Figdor CG *et al.* (2006). TRPM7, a novel regulator of actomyosin contractility and cell adhesion. EMBO J 25: 290–301.

Demeuse P, Penner R, Fleig A (2006). TRPM7 channel is regulated by magnesium nucleotides via its kinase domain. J Gen Physiol 127: 421–434.

Dietrich A, Mederos y Schnitzler M, Gollasch M, Gross V, Storch U, Dubrovska G *et al.* (2005). Increased vascular smooth muscle contractility in $TRPC6^{-/-}$ mice. Mol Cell Biol 25: 6980–6989.

Diness JG, Sorensen US, Nissen JD, Al-Shahib B, Jespersen T, Grunnet M *et al.* (2010). Inhibition of small-conductance Ca^{2+}-activated K^+ channels terminates and protects against atrial fibrillation. Circ Arrhythm Electrophysiol 3: 380–390.

Du J, Xie J, Zhang Z, Tsujikawa H, Fusco D, Silverman D *et al.* (2010). TRPM7-mediated Ca^{2+} signals confer fibrogenesis in human atrial fibrillation. Circ Res 106: 992–1003.

Guilbert A, Gautier M, Dhennin-Duthille I, Haren N, Sevestre H, Ouadid-Ahidouch H (2009). Evidence that TRPM7 is required for breast cancer cell proliferation. Am J Physiol Cell Physiol 297: C493–C502.

Gwanyanya A, Amuzescu B, Zakharov SI, Macianskiene R, Sipido KR, Bolotina VM *et al.* (2004). Magnesium-inhibited, TRPM6/7-like channel in cardiac myocytes: permeation of divalent cations and pH-mediated regulation. J Physiol 559: 761–776.

Hanano T, Hara Y, Shi J, Morita H, Umebayashi C, Mori E *et al.* (2004). Involvement of TRPM7 in cell growth as a spontaneously activated Ca^{2+} entry pathway in human retinoblastoma cells. J Pharmacol Sci 95: 403–419.

Hara Y, Wakamori M, Ishii M, Maeno E, Nishida M, Yoshida T *et al.* (2002). LTRPC2 Ca^{2+}-permeable channel activated by changes in redox status confers susceptibility to cell death. Mol Cell 9: 163–173.

Hermosura MC, Nayakanti H, Dorovkov MV, Calderon FR, Ryazanov AG, Haymer DS *et al.* (2005). A TRPM7 variant shows altered sensitivity to magnesium that may contribute to the pathogenesis of two Guamanian neurodegenerative disorders. Proc Natl Acad Sci U S A 102: 11510–11515.

Herrik KF, Christophersen P, Shepard PD (2010). Pharmacological modulation of the gating properties of small conductance Ca^{2+}-activated $^{K+}$ channels alters the firing pattern of dopamine neurons in vivo. J Neurophysiol 104: 1726–1735.

Hofmann T, Obukhov AG, Schaefer M, Harteneck C, Gudermann T, Schultz G (1999). Direct activation of human TRPC6 and TRPC3 channels by diacylglycerol. Nature 397: 259–263.

Hofmann T, Schaefer M, Schultz G, Gudermann T (2002). Subunit composition of mammalian transient receptor potential channels in living cells. Proc Natl Acad Sci U S A 99: 7461–7466.

Hofmann T, Chubanov V, Gudermann T, Montell C (2003). TRPM5 is a voltage-modulated and Ca^{2+}-activated monovalent selective cation channel. Curr Biol 13: 1153–1158.

Hofmann T, Chubanov V, Chen X, Dietz AS, Gudermann T, Montell C (2010). Drosophila TRPM channel is essential for the control of extracellular magnesium levels. PLoS ONE 5: e10519.

Jenkins DP, Strobaek D, Hougaard C, Jensen ML, Hummel R, Sorensen US *et al.* (2011). Negative gating modulation by (R)-N-(Benzimidazol-2-yl)-tetrahydro-1-naphtylamine (NS8593) depends on residues in the inner pore vestibule: pharmacological evidence of deep-pore gating of $K_{Ca}2$ channels. Mol Pharmacol 79: 899–909.

Jiang J, Li M, Yue L (2005). Potentiation of TRPM7 inward currents by protons. J Gen Physiol 126: 137–150.

Jiang J, Li MH, Inoue K, Chu XP, Seeds J, Xiong ZG (2007). Transient receptor potential melastatin 7-like current in human head and neck carcinoma cells: role in cell proliferation. Cancer Res 67: 10929–10938.

Jin J, Desai BN, Navarro B, Donovan A, Andrews NC, Clapham DE (2008). Deletion of Trpm7 disrupts embryonic development and thymopoiesis without altering Mg^{2+} homeostasis. Science 322: 756–760.

Kerschbaum HH, Cahalan MD (1999). Single-channel recording of a store-operated Ca^{2+} channel in Jurkat T lymphocytes. Science 283: 836–839.

Kerschbaum HH, Kozak JA, Cahalan MD (2003). Polyvalent cations as permeant probes of MIC and TRPM7 pores. Biophys J 84: 2293–2305.

Kim BJ, Jeon JH, Kim SJ, So I, Kim KW (2007). Regulation of transient receptor potential melastatin 7 (TRPM7) currents by mitochondria. Mol Cells 23: 363–369.

Kim BJ, Park EJ, Lee JH, Jeon JH, Kim SJ, So I (2008). Suppression of transient receptor potential melastatin 7 channel induces cell death in gastric cancer. Cancer Sci 99: 2502–2509.

Kozak JA, Cahalan MD (2003). MIC channels are inhibited by internal divalent cations but not ATP. Biophys J 84: 922–927.

Kozak JA, Kerschbaum HH, Cahalan MD (2002). Distinct properties of CRAC and MIC channels in RBL cells. J Gen Physiol 120: 221–235.

Kozak JA, Matsushita M, Nairn AC, Cahalan MD (2005). Charge screening by internal pH and polyvalent cations as a mechanism for activation, inhibition, and rundown of TRPM7/MIC channels. J Gen Physiol 126: 499–514.

Li M, Jiang J, Yue L (2006). Functional characterization of homo- and heteromeric channel kinases TRPM6 and TRPM7. J Gen Physiol 127: 525–537.

Matsushita M, Kozak JA, Shimizu Y, McLachlin DT, Yamaguchi H, Wei FY *et al.* (2005). Channel function is dissociated from the intrinsic kinase activity and autophosphorylation of TRPM7/ChaK1. J Biol Chem 280: 20793–20803.

Mederos y Schnitzler M, Waring J, Gudermann T, Chubanov V (2008). Evolutionary determinants of divergent calcium selectivity of TRPM channels. FASEB J 22: 1540–1551.

Mishra R, Rao V, Ta R, Shobeiri N, Hill CE (2009). Mg^{2+}- and MgATP-inhibited and Ca^{2+}/calmodulin-sensitive TRPM7-like current in hepatoma and hepatocytes. Am J Physiol Gastrointest Liver Physiol 297: G687–G694.

Monteilh-Zoller MK, Hermosura MC, Nadler MJ, Scharenberg AM, Penner R, Fleig A (2003). TRPM7 provides an ion channel mechanism for cellular entry of trace metal ions. J Gen Physiol 121: 49–60.

Nadler MJ, Hermosura MC, Inabe K, Perraud AL, Zhu Q, Stokes AJ *et al.* (2001). LTRPC7 is a Mg.ATP-regulated divalent cation channel required for cell viability. Nature 411: 590–595.

Nilius B, Mahieu F, Karashima Y, Voets T (2007). Regulation of TRP channels: a voltage-lipid connection. Biochem Soc Trans 35: 105–108.

Numata T, Shimizu T, Okada Y (2007a). Direct mechano-stress sensitivity of TRPM7 channel. Cell Physiol Biochem 19: 1–8.

Numata T, Shimizu T, Okada Y (2007b). TRPM7 is a stretch- and swelling-activated cation channel involved in volume regulation in human epithelial cells. Am J Physiol Cell Physiol 292: C460–C467.

Oancea E, Wolfe JT, Clapham DE (2006). Functional TRPM7 channels accumulate at the plasma membrane in response to fluid flow. Circ Res 98: 245–253.

Oberwinkler J, Lis A, Giehl KM, Flockerzi V, Philipp SE (2005). Alternative splicing switches the divalent cation selectivity of TRPM3 channels. J Biol Chem 280: 22540–22548.

Parnas M, Peters M, Dadon D, Lev S, Vertkin I, Slutsky I *et al.* (2009). Carvacrol is a novel inhibitor of Drosophila TRPL and mammalian TRPM7 channels. Cell Calcium 45: 300–309.

Pedarzani P, D'Hoedt D, Doorty KB, Wadsworth JD, Joseph JS, Jeyaseelan K *et al.* (2002). Tamapin, a venom peptide from the Indian red scorpion (Mesobuthus tamulus) that targets small conductance Ca^{2+}-activated K^+ channels and afterhyperpolarization currents in central neurons. J Biol Chem 277: 46101–46109.

Peier AM, Moqrich A, Hergarden AC, Reeve AJ, Andersson DA, Story GM *et al.* (2002). A TRP channel that senses cold stimuli and menthol. Cell 108: 705–715.

Perraud AL, Fleig A, Dunn CA, Bagley LA, Launay P, Schmitz C *et al.* (2001). ADP-ribose gating of the calcium-permeable LTRPC2 channel revealed by Nudix motif homology. Nature 411: 595–599.

Prakriya M, Lewis RS (2002). Separation and characterization of currents through store-operated CRAC channels and Mg^{2+}-inhibited cation (MIC) channels. J Gen Physiol 119: 487–507.

Runnels LW, Yue L, Clapham DE (2001). TRP-PLIK, a bifunctional protein with kinase and ion channel activities. Science 291: 1043–1047.

Runnels LW, Yue L, Clapham DE (2002). The TRPM7 channel is inactivated by PIP_2 hydrolysis. Nat Cell Biol 4: 329–336.

Ryazanov AG, Pavur KS, Dorovkov MV (1999). Alpha-kinases: a new class of protein kinases with a novel catalytic domain. Curr Biol 9: R43–R45.

Ryazanova LV, Rondon LJ, Zierler S, Hu Z, Galli J, Yamaguchi TP *et al.* (2010). TRPM7 is essential for Mg^{2+} homeostasis in mammals. Nat Commun 1: 109.

Sahni J, Scharenberg AM (2008). TRPM7 ion channels are required for sustained phosphoinositide 3-kinase signaling in lymphocytes. Cell Metab 8: 84–93.

Schlondorff D (1990). Preparation and study of isolated glomeruli. Methods Enzymol 191: 130–140.

Schmitz C, Perraud AL, Johnson CO, Inabe K, Smith MK, Penner R *et al.* (2003). Regulation of vertebrate cellular Mg^{2+} homeostasis by TRPM7. Cell 114: 191–200.

Shi J, Cui J (2001). Intracellular Mg^{2+} enhances the function of BK-type Ca^{2+}-activated K^+ channels. J Gen Physiol 118: 589–606.

Soh H, Park CS (2002). Localization of divalent cation-binding site in the pore of a small conductance Ca^{2+}-activated K^+ channel and its role in determining current-voltage relationship. Biophys J 83: 2528–2538.

Sorensen US, Strobaek D, Christophersen P, Hougaard C, Jensen ML, Nielsen EO *et al.* (2008). Synthesis and structure-activity relationship studies of 2-(N-substituted)-aminobenzimidazoles as potent negative gating modulators ofsmall conductance Ca^{2+}-activated K^+ channels. J Med Chem 51: 7625–7634.

Stanfield PR, Davies NW, Shelton PA, Sutcliffe MJ, Khan IA, Brammar WJ *et al.* (1994). A single aspartate residue is involved in both intrinsic gating and blockage by Mg^{2+} of the inward rectifier, IRK1. J Physiol 478 (Pt 1): 1–6.

Starkus J, Beck A, Fleig A, Penner R (2007). Regulation of TRPM2 by extra- and intracellular calcium. J Gen Physiol 130: 427–440.

Strobaek D, Hougaard C, Johansen TH, Sorensen US, Nielsen EO, Nielsen KS *et al.* (2006). Inhibitory gating modulation of small conductance Ca^{2+}-activated K^+ channels by the synthetic compound (R)-N-(benzimidazol-2-yl)-1,2,3,4-tetrahydro-1-naphtylamine (NS8593) reduces afterhyperpolarizing current in hippocampal CA1 neurons. Mol Pharmacol 70: 1771–1782.

Su LT, Agapito MA, Li M, Simonson WT, Huttenlocher A, Habas R *et al.* (2006). TRPM7 regulates cell adhesion by controlling the calcium-dependent protease calpain. J Biol Chem 281: 11260–11270.

Su LT, Liu W, Chen HC, Gonzalez-Pagan O, Habas R, Runnels LW (2011). TRPM7 regulates polarized cell movements. Biochem J 434: 513–521.

Taglialatela M, Ficker E, Wible BA, Brown AM (1995). C-terminus determinants for Mg^{2+} and polyamine block of the inward rectifier K+ channel IRK1. EMBO J 14: 5532–5541.

Taylor MS, Bonev AD, Gross TP, Eckman DM, Brayden JE, Bond CT *et al.* (2003). Altered expression of small-conductance Ca^{2+}-activated K^+ (SK3) channels modulates arterial tone and blood pressure. Circ Res 93: 124–131.

Touyz RM (2008). Transient receptor potential melastatin 6 and 7 channels, magnesium transport, and vascular biology: implications in hypertension. Am J Physiol Heart Circ Physiol 294: H1103–H1118.

Tseveleki V, Rubio R, Vamvakas SS, White J, Taoufik E, Petit E *et al.* (2010). Comparative gene expression analysis in mouse models for multiple sclerosis, Alzheimer's disease and stroke for identifying commonly regulated and disease-specific gene changes. Genomics 96: 82–91.

Vriens J, Nilius B, Vennekens R (2008). Herbal compounds and toxins modulating TRP channels. Curr Neuropharmacol 6: 79–96.

Wagner TF, Loch S, Lambert S, Straub I, Mannebach S, Mathar I *et al.* (2008). Transient receptor potential M3 channels are ionotropic steroid receptors in pancreatic beta cells. Nat Cell Biol 10: 1421–1430.

Weatherall KL, Goodchild SJ, Jane DE, Marrion NV (2010). Small conductance calcium-activated potassium channels: from structure to function. Prog Neurobiol 91: 242–255.

Wei C, Wang X, Chen M, Ouyang K, Song LS, Cheng H (2009). Calcium flickers steer cell migration. Nature 457: 901–905.

Wible BA, Taglialatela M, Ficker E, Brown AM (1994). Gating of inwardly rectifying K^+ channels localized to a single negatively charged residue. Nature 371: 246–249.

Wu Y, Yang Y, Ye S, Jiang Y (2010). Structure of the gating ring from the human large-conductance Ca^{2+}-gated K^+ channel. Nature 466: 393–397.

Yamaguchi H, Matsushita M, Nairn AC, Kuriyan J (2001). Crystal structure of the atypical protein kinase domain of a TRP channel with phosphotransferase activity. Mol Cell 7: 1047–1057.

Yang H, Shi J, Zhang G, Yang J, Delaloye K, Cui J (2008). Activation of Slo1 BK channels by Mg^{2+} coordinated between the voltage sensor and RCK1 domains. Nat Struct Mol Biol 15: 1152–1159.

Zierler S, Yao G, Zhang Z, Kuo WC, Poerzgen P, Penner R *et al.* (2011). Waixenicin A inhibits cell proliferation through magnesium-dependent block of TRPM7. J Biol Chem 286: 39328–39335.

Supporting information

Additional Supporting Information may be found in the online version of this article:

Figure S1 Voltage dependence of the NS8593 block of TRPM7 and TRPM3 channels. Representative current–voltage (*I–V*) relationships of whole-cell currents measured in HEK 293 cells transiently transfected with TRPM7 or TRPM3 cDNAs. (A) TRPM7 currents acquired before and a few seconds after external application of 5 μM NS8593. Measurements were performed as in Figure 2B applying voltage ramps from −100 to 200 mV. (B) PS (10 μM) induced TRPM3 currents acquired before and a few seconds after external application of 30 μM NS8593. Measurements were performed as in Figure 6B applying voltage ramps from −100 to +200 mV.

Figure S2 Run-down of TRPM7 currents in Na^+-based external saline. Whole-cell TRPM7 currents measured in HEK 293 cells transiently transfected with TRPM7 cDNA. Representative currents over time acquired at −100 and 100 mV (*left*) and corresponding *I–V* relationships (*right*) are shown. (A) Effect of a Na^+-based external solution on fully induced TRPM7 currents. Note that perfusion of cells with a Na^+-based saline results in transient increases of inward and outward currents followed by their fast run-down, which was reversible if cells were perfused again by physiological saline (containing 1 mM Mg^{2+} and 2 mM Ca^{2+}). (B) Measurements were performed similar to (A) using a Cs^+-based saline. Monovalent TRPM7 cation currents were fully sustained during recordings in Cs^+-based saline.

Figure S3 Effects of SK inhibitors on TRPM7 currents in HEK 293 cells. Representative traces of TRPM7 currents from experiments shown in Figure 4A. Inhibitory effects of 30 μM quinine (A), dequalinium (B), CyPPA (C), UCL 1684 (D) and 10 nM and 1 μM tamapin (E, F) on TRPM7 whole-cell currents are illustrated.

Figure S4 Evaluation of NS8593 on Ca^{2+} influx mediated by TRPM3, TRPM8 and TRPM2 channels using fura-2. (A) (*Left*) Representative traces obtained with mock- and TRPM3 cDNA-transfected cells stimulated with 10 μM PS; (*right*) mean values of Ca^{2+} transients (Δ ratio F_{340}/F_{380} of fura-2) obtained from three independent transfections. (B) (*Left*) Representative traces obtained with mock- and TRPM8 cDNA-transfected cells stimulated with 10 μM icillin; (*right*) mean values of Ca^{2+} transients (Δ ratio F_{340}/F_{380} of fura-2) obtained from three independent transfections. (C) (*Left*) Representative traces (aequorin-based assay) obtained with mock- and TRPM2 cDNA-transfected cells stimulated with 1 mM H_2O_2; (*right*) mean values of Ca^{2+} transients obtained from three independent transfections.

Figure S5 Evaluation of NS8593 on TRPM5 and TRPC6 currents. HEK 293 cells were transfected with mouse TRPM5 (Hofmann *et al.*, 2003) or a YFP-labelled human TRPC6 (Hofmann *et al.*, 1999; 2002). Representative recordings are

shown. (A) TRPM5 cells were perfused with a pipette solution containing calculated 3 μM Ca^{2+}. In the right panel, cells were superfused with 10 μM NS8593 as indicated by the application bar (n = 12), in the left panel without the inhibitor (n = 4). (B) TRPC6-expressing cells were stimulated with a moderate concentration of histamine (1 μM) acting at a coexpressed H_1 histamine receptor, and superfused with 10 μM NS8593, as indicated by application bars (n = 3).

Figure S6 Evaluation of NS8593 on Ca^{2+} influx mediated by TRPA1 and TRPV1 channels in HEK 293 cells using an aequorin-based approach. (A) (*Left*) Representative traces obtained with TRPA1 cDNA-transfected cells stimulated with 10 μM AITC; (*right*) mean values of Ca^{2+} rises obtained from three independent transfections. (B) (*Left*) Representative traces obtained with TRPV1 cDNA-transfected cells stimulated with 1 μM capsaicin; (*right*) mean values of Ca^{2+} rises obtained from three independent transfections.

Figure S7 Impact of NS8593, Quinine and UCL 1684 on the viability of HEK 293 cells overexpressing recombinant TRPM7. Experiments with tetracycline-induced (1 μM, 40 h) expression of human TRPM7 were performed as described in Methods. Scale bars – 60 μm

Figure S8 Effects of NS8593, BMB and apamin on the morphology of HEK 293 cells. The images show living HEK 293 cells cultured with or without the compounds indicated for 48 h. Note that in the presence of 30 μM NS8593, HEK 293 cells form tight colonies. Scale bars represent 30 μm each.

Appendix S1 Supplementary methods.

Appendix S2 Supplementary References.

Please note: Wiley-Blackwell are not responsible for the content or functionality of any supporting materials supplied by the authors. Any queries (other than missing material) should be directed to the corresponding author for the article.

Suppl. Figure 1

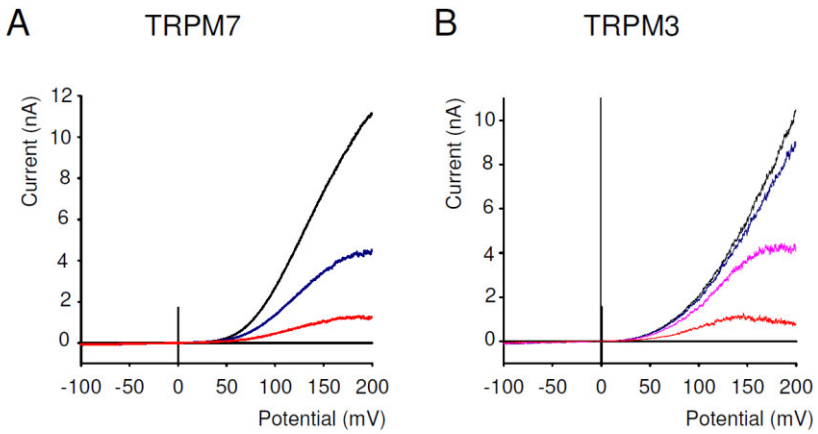

Suppl. Figure 2

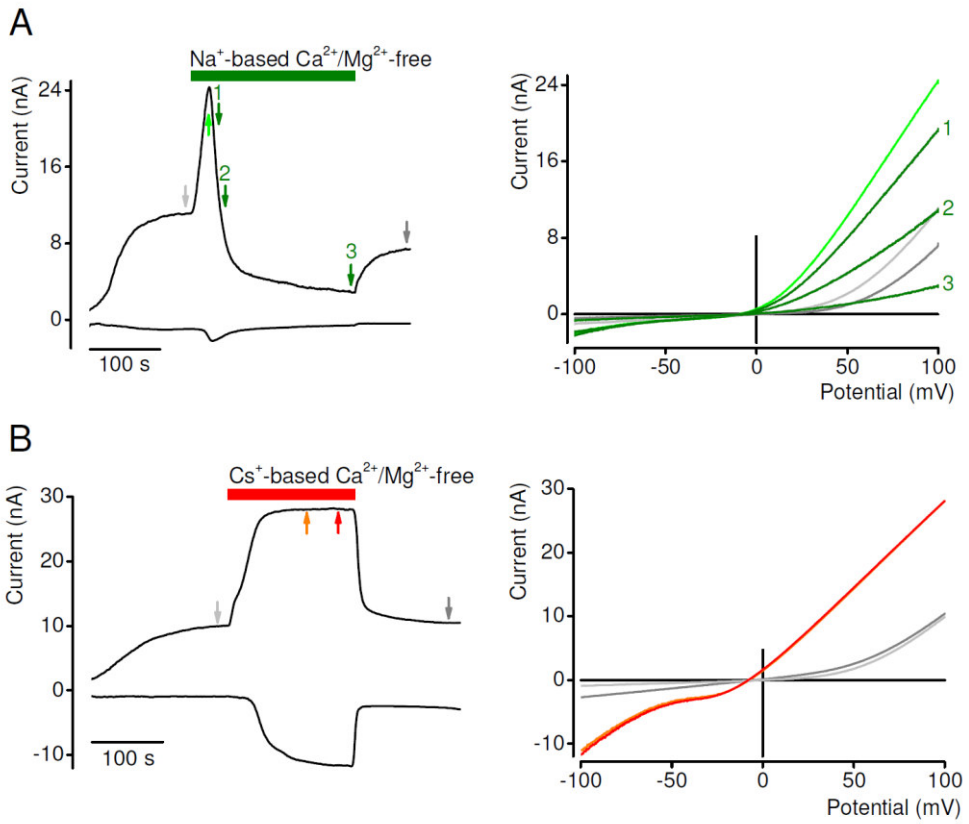

Suppl. Figure 3

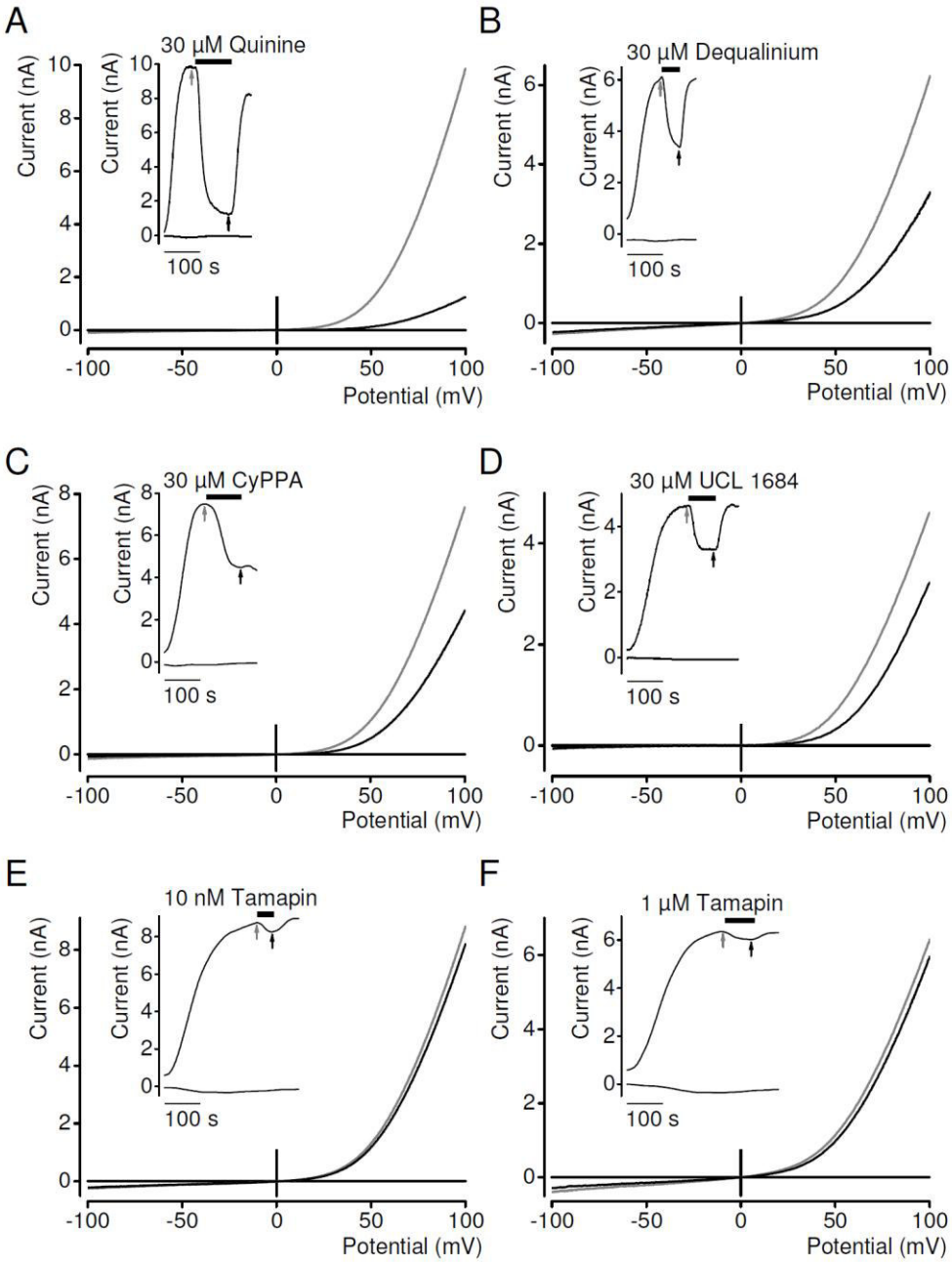

Suppl. Figure 4

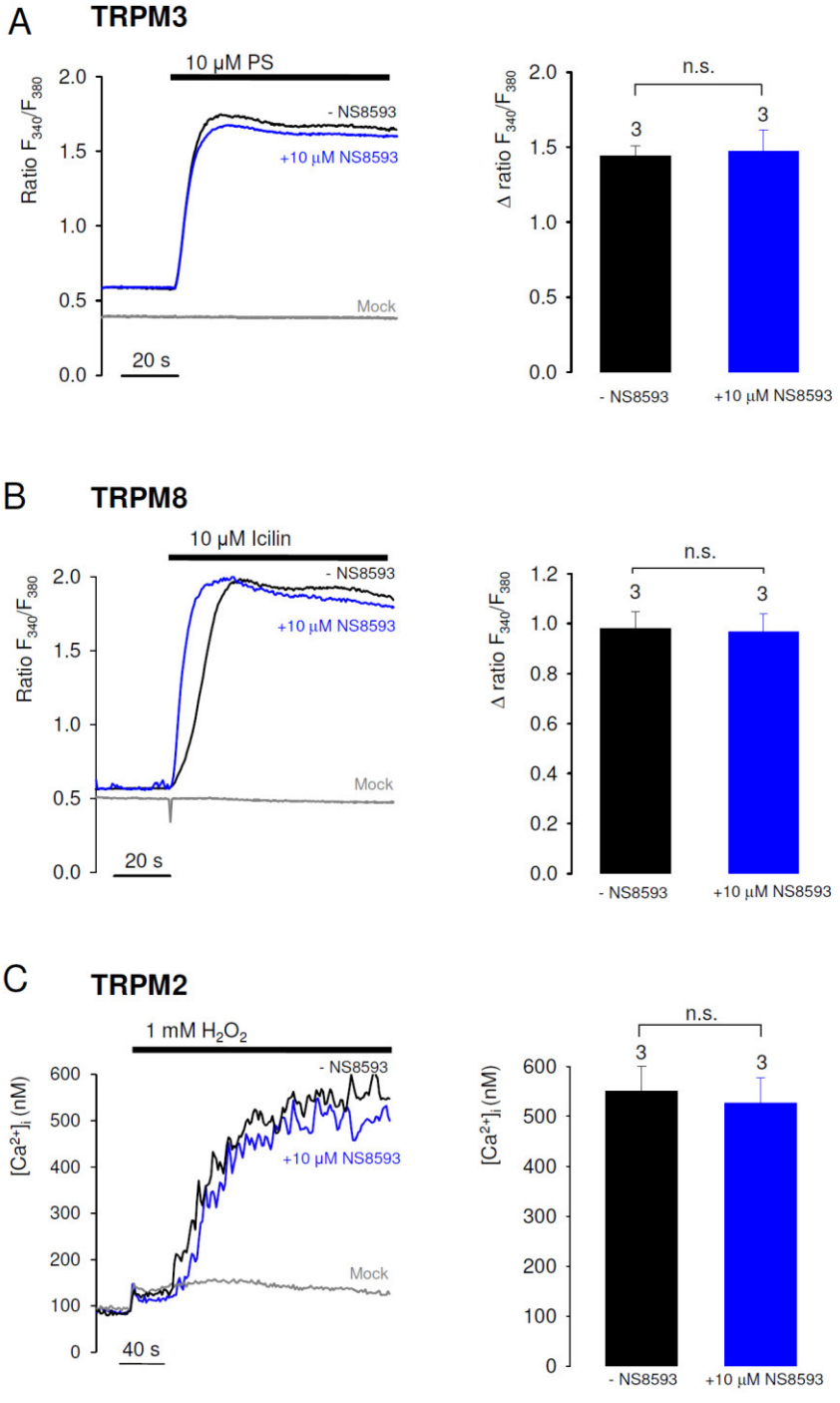

Suppl. Figure 5

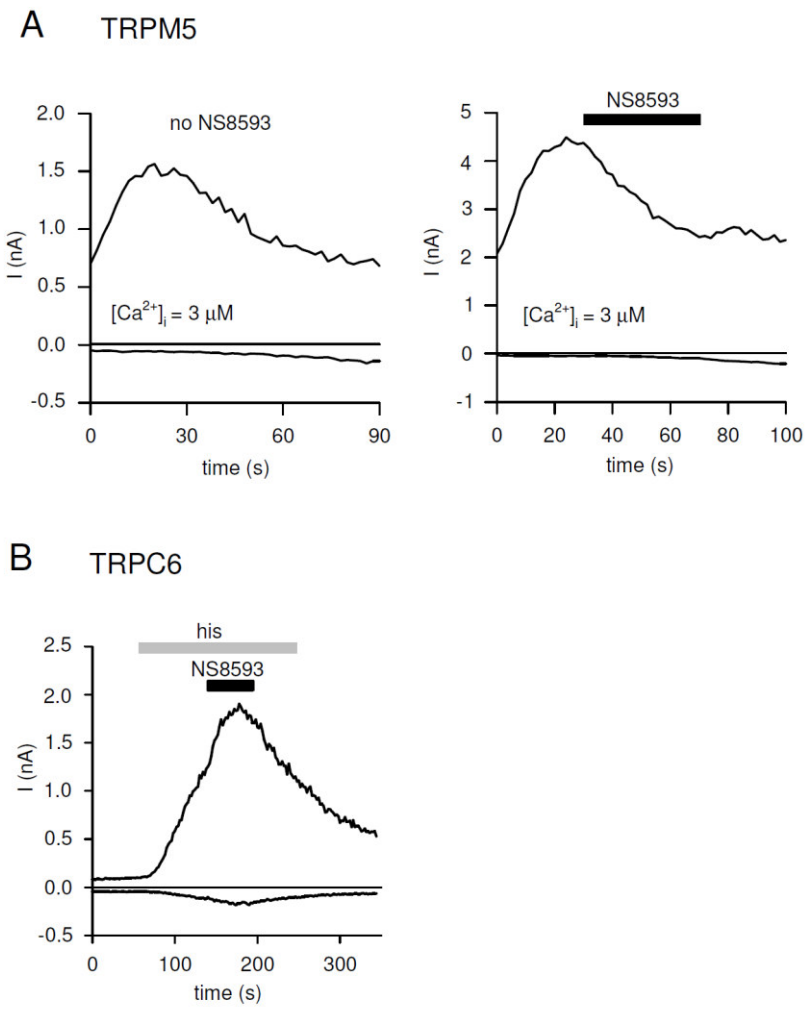

Suppl. Figure 6

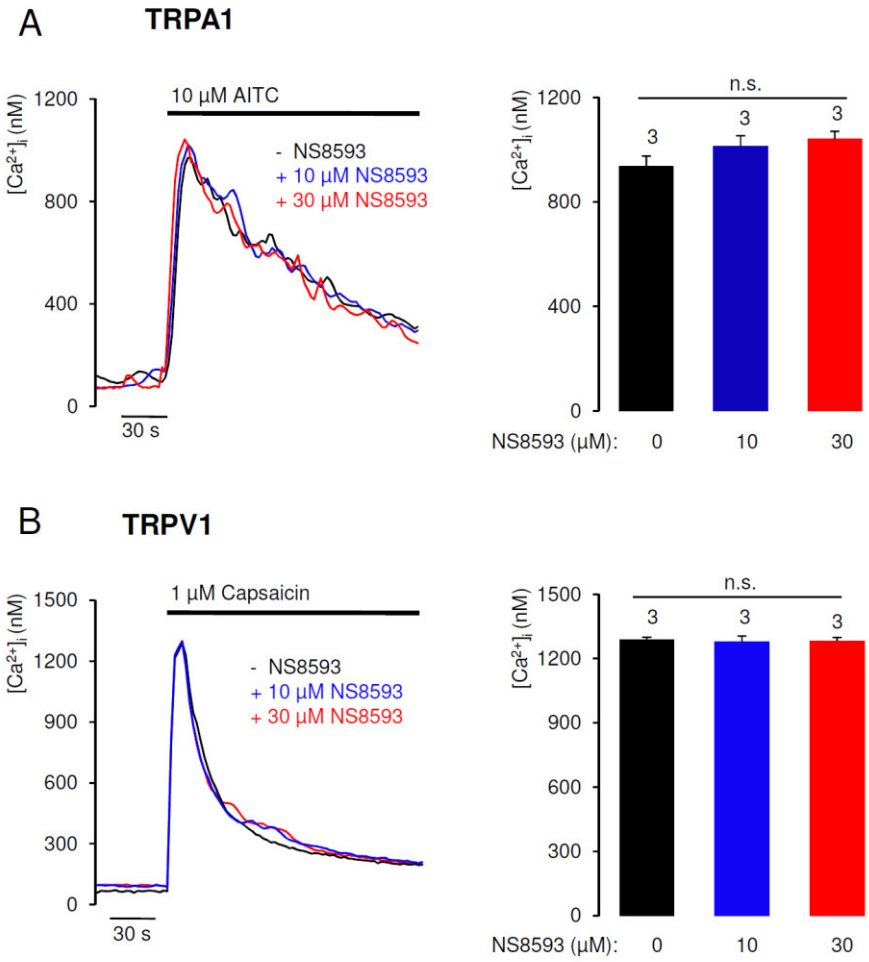

Suppl. Figure 7

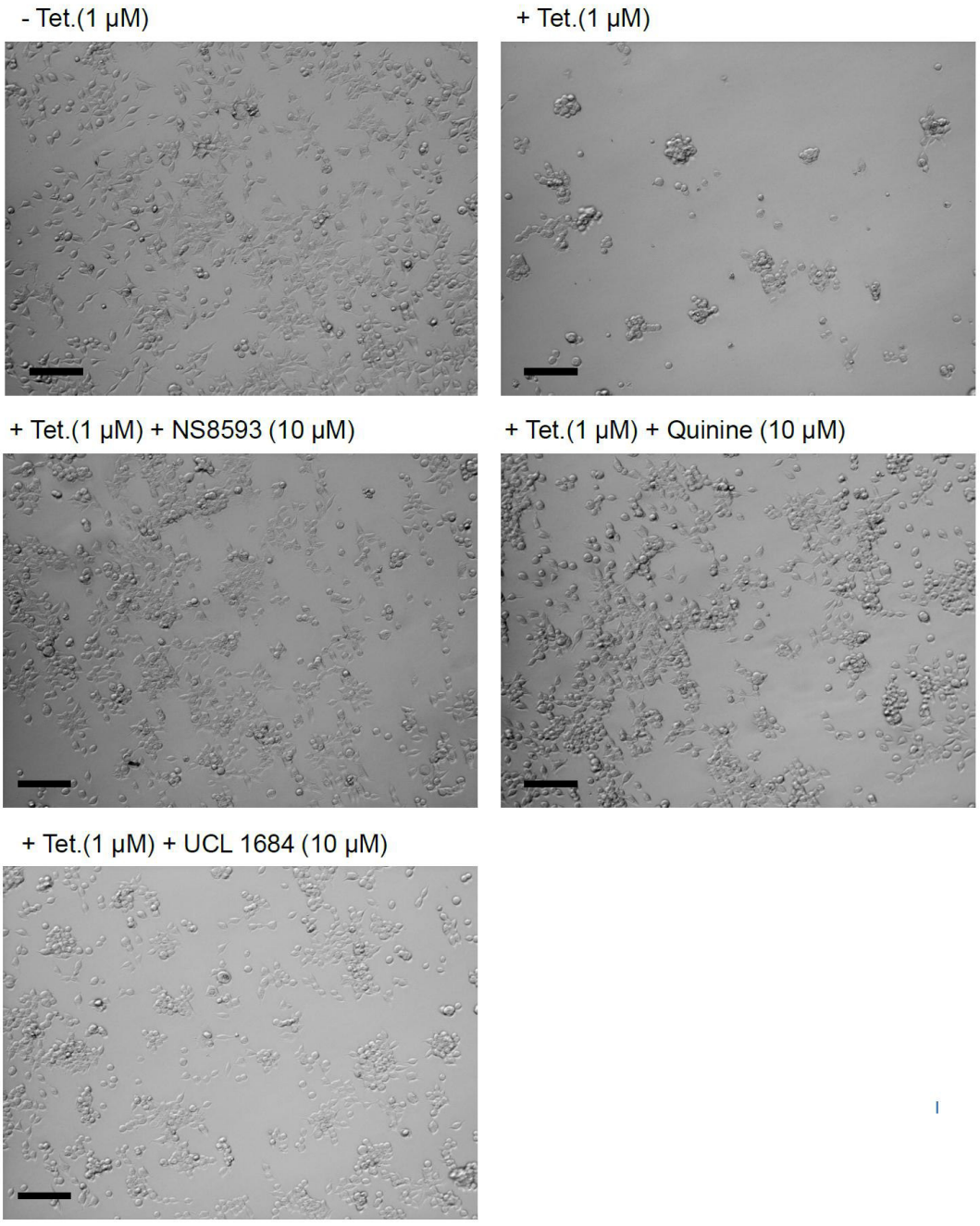

Suppl. Figure 8

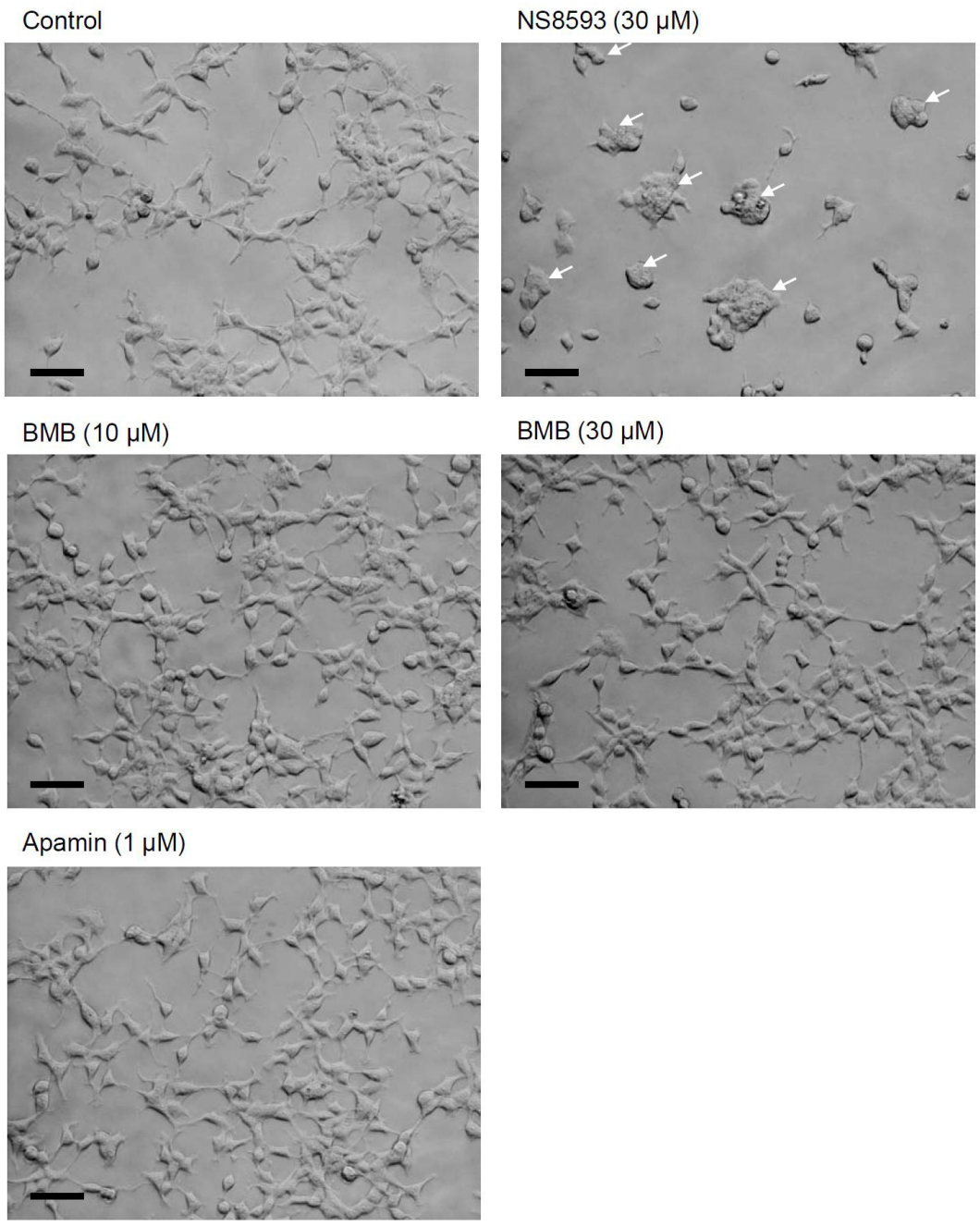

Supplementary material for online publication only

Supplementary methods

Human TRPM2 and human TRPM8 cDNAs in pIRES-eGFP vector (Clontech Laboratories), mouse TRPM5, human TRPC6 in pcDNA3.1-TOPO vector (Invitrogen) were generated as described previously (Chubanov *et al.*, 2004; Mederos y Schnitzler *et al.*, 2008). Human TRPV1 (in pcDNA3.1-TOPO) and human TRPA1 (in pcAGGS-IRES-eGFP vector) were described previously (Hellwig *et al.*, 2004; Story *et al.*, 2003). The pipette solution used to activate TRPM5 contained 120 mM CsCl, 10 mM NaCl, 10 mM HEPES (pH 7.2), 10 mM BAPTA, 0.5 mM $MgCl_2$ 0.937 mM $CaCl_2$ (yielding a final concentration of 3 µM (WebMaxC v2.23)).

Supplementary Figure 1. Voltage dependence of the NS8593 block of TRPM7 and TRPM3 channels. Representative current-voltage (I-V) relationships of whole-cell currents measured in HEK 293 cells transiently transfected with TRPM7 or TRPM3 cDNAs. (**A**) TRPM7 currents acquired before (black) and a few seconds after (blue and red) external application of 5 µM NS8593. Measurements were performed as in Fig. 2B applying voltage ramps from -100 to 200 mV. (**B)** Pregnenolone sulfate (10 µM) induced TRPM3 currents acquired before (black) and a few seconds after (blue, pink and red) external application of 30 µM NS8593. Measurements were performed as in Fig 6B applying voltage ramps from -100 to +200 mV.

Supplementary Figure 2. Run-down of TRPM7 currents in Na^+-based external saline. Whole-cell TRPM7 currents measured in HEK 293 cells transiently transfected with TRPM7 cDNA. Representative currents over time acquired at -100 and 100 mV (*left*) and corresponding I-V relationships (*right*) are shown. (**A**) Effect of a Na^+-based external solution on fully induced TRPM7 currents. Note, that perfusion of cells with a Na^+-based saline results in transient increases of inward and outward currents followed by their fast run-down, which was reversible if cells were perfused again by physiological saline (containing 1 mM Mg^{2+} and 2 mM Ca^{2+}). (**B**) Measurements were performed similar to (A) using a Cs^+-based saline. Monovalent TRPM7 cation currents were fully sustained during recordings in Cs^+-based saline.

Supplementary Figure 3. Effects of SK inhibitors on TRPM7 currents in HEK 293 cells. Representative traces of TRPM7 currents from experiments shown in Fig. 4.A. Inhibitory effects of 30 µM quinine (**A**), dequalinium (**B**), CyPPA (**C**), UCL 1684 (**D**), and 10 nM and 1 µM tamapin (**E, F**) on TRPM7 whole-cell currents are illustrated.

Supplementary Figure 4. Evaluation of NS8593 on Ca^{2+} influx mediated by TRPM3, TRPM8 and TRPM2 channels using fura-2. (**A**) (*Left*) Representative traces obtained with mock- and TRPM3 cDNA-transfected cells stimulated with 10 µM PS; (*right)* mean values of Ca^{2+} transients (Δ ratio F_{340}/F_{380} of fura-2) obtained from 3 independent transfections. (**B**) (*Left*) Representative traces obtained with mock- and TRPM8 cDNA-transfected cells stimulated with 10 µM icillin; (*right)* mean values of Ca^{2+} transients (Δ ratio F_{340}/F_{380} of fura-2) obtained from 3 independent transfections. (**C**) (*Left*) Representative traces (aequorin-based assay) obtained with mock- and TRPM2 cDNA-transfected cells stimulated with 1 mM H_2O_2; (*right)* mean values of Ca^{2+} transients obtained from 3 independent transfections.

Supplementary Figure 5. Evaluation of NS8593 on TRPM5 and TRPC6 currents. HEK 293 cells were transfected with mouse TRPM5 (Hofmann *et al.*, 2003) or a YFP-labeled human TRPC6 (Hofmann *et al.*, 1999; Hofmann *et al.*, 2002), representative recordings are shown. (a) TRPM5 cells were perfused with a pipette solution containing calculated 3 µM Ca^{2+}. In the right panel, cells were superfused with 10 µM NS8593 as indicated by the application bar (n=12), in the left panel without the inhibitor (n=4). (b) TRPC6-expressing cells were stimulated with a moderate concentration of histamine (1 µM) acting at a co-expressed H_1 histamine receptor, and superfused with 10 µM NS8593, as indicated by application bars (n=3).

Supplementary Figure 6. Evaluation of NS8593 on Ca^{2+} influx mediated by TRPA1 and TRPV1 channels in HEK 293 cells using an aequorin-based approach. (**A**) (*Left*) Representative traces obtained with TRPA1 cDNA-transfected cells stimulated with 10 µM AITC; (*right)* mean values of Ca^{2+} rises obtained from 3 independent transfections. (**B**) (*Left*) Representative traces obtained with TRPV1 cDNA-transfected cells stimulated with 1 µM capsaicin; (*right)* mean values of Ca^{2+} rises obtained from 3 independent transfections.

Supplementary Figure 7. Impact of NS8593, Quinine and UCL 1684 on the viability of HEK 293 cells over-expressing recombinant TRPM7. Experiments with tetracycline-induced (1 µM, 40 h) expression of human TRPM7 were performed as described in the Methods section. Scale bars – 60 µm

Supplementary Figure 8. Effects of NS8593, BMB and apamin on the morphology of HEK 293 cells. The images show living HEK 293 cells cultured with or without the compounds indicated for 48 h. Note that in the presence of 30 µM NS8593, HEK 293 cells form tight colonies (indicated by arrows). Scale bars represent 30 µm each.

Supplementary references

Chubanov, V, Waldegger, S, Mederos y Schnitzler, M, Vitzthum, H, Sassen, MC, et al. (2004) Disruption of TRPM6/TRPM7 complex formation by a mutation in the TRPM6 gene causes hypomagnesemia with secondary hypocalcemia. *Proc Natl Acad Sci U S A* **101**(9)**:** 2894-2899.

Hellwig, N, Plant, TD, Janson, W, Schafer, M, Schultz, G, Schaefer, M (2004) TRPV1 acts as proton channel to induce acidification in nociceptive neurons. *J Biol Chem* **279**(33)**:** 34553-34561.

Hofmann, T, Chubanov, V, Gudermann, T, Montell, C (2003) TRPM5 is a voltage-modulated and Ca^{2+}-activated monovalent selective cation channel. *Curr Biol* **13**(13)**:** 1153-1158.

Hofmann, T, Obukhov, AG, Schaefer, M, Harteneck, C, Gudermann, T, Schultz, G (1999) Direct activation of human TRPC6 and TRPC3 channels by diacylglycerol. *Nature* **397**(6716)**:** 259-263.

Hofmann, T, Schaefer, M, Schultz, G, Gudermann, T (2002) Subunit composition of mammalian transient receptor potential channels in living cells. *Proc Natl Acad Sci U S A* **99**(11)**:** 7461-7466.

Mederos y Schnitzler, M, Waring, J, Gudermann, T, Chubanov, V (2008) Evolutionary determinants of divergent calcium selectivity of TRPM channels. *FASEB J* **22**(5)**:** 1540-1551.

Story, GM, Peier, AM, Reeve, AJ, Eid, SR, Mosbacher, J, Hricik, TR, et al. (2003) ANKTM1, a TRP-like channel expressed in nociceptive neurons, is activated by cold temperatures. *Cell* **112**(6)**:** 819-829.

Literaturverzeichnis

Aarts, M., Iihara, K., Wei, W.L., Xiong, Z.G., Arundine, M., Cerwinski, W., MacDonald, J.F., and Tymianski, M. (2003). A key role for TRPM7 channels in anoxic neuronal death. Cell *115*, 863-877.

Bernhardt, M.L., Padilla-Banks, E., Stein, P., Zhang, Y., and Williams, C.J. (2017). Store-operated Ca(2+) entry is not required for fertilization-induced Ca(2+) signaling in mouse eggs. Cell calcium *65*, 63-72.

Bernhardt, M.L., Stein, P., Carvacho, I., Krapp, C., Ardestani, G., Mehregan, A., Umbach, D.M., Bartolomei, M.S., Fissore, R.A., and Williams, C.J. (2018). TRPM7 and CaV3.2 channels mediate Ca(2+) influx required for egg activation at fertilization. Proceedings of the National Academy of Sciences of the United States of America.

Carvacho, I., Ardestani, G., Lee, H.C., McGarvey, K., Fissore, R.A., and Lykke-Hartmann, K. (2016). TRPM7-like channels are functionally expressed in oocytes and modulate post-fertilization embryo development in mouse. Scientific reports *6*, 34236.

Chen, H.C., Xie, J., Zhang, Z., Su, L.T., Yue, L., and Runnels, L.W. (2010a). Blockade of TRPM7 channel activity and cell death by inhibitors of 5-lipoxygenase. PloS one *5*, e11161.

Chen, J.P., Luan, Y., You, C.X., Chen, X.H., Luo, R.C., and Li, R. (2010b). TRPM7 regulates the migration of human nasopharyngeal carcinoma cell by mediating Ca(2+) influx. Cell calcium *47*, 425-432.

Chen, X., Numata, T., Li, M., Mori, Y., Orser, B.A., Jackson, M.F., Xiong, Z.G., and MacDonald, J.F. (2010c). The modulation of TRPM7 currents by nafamostat mesilate depends directly upon extracellular concentrations of divalent cations. Molecular brain *3*, 38.

Chokshi, R., Matsushita, M., and Kozak, J.A. (2012a). Detailed examination of Mg2+ and pH sensitivity of human TRPM7 channels. American journal of physiology Cell physiology *302*, C1004-1011.

Chokshi, R., Matsushita, M., and Kozak, J.A. (2012b). Sensitivity of TRPM7 channels to Mg2+ characterized in cell-free patches of Jurkat T lymphocytes. American journal of physiology Cell physiology *302*, C1642-1651.

Chubanov, V., Mederos y Schnitzler, M., Meissner, M., Schafer, S., Abstiens, K., Hofmann, T., and Gudermann, T. (2012). Natural and synthetic modulators of SK (K(ca)2) potassium channels inhibit magnesium-dependent activity of the kinase-coupled cation channel TRPM7. British journal of pharmacology *166*, 1357-1376.

Chubanov, V., Schafer, S., Ferioli, S., and Gudermann, T. (2014). Natural and Synthetic Modulators of the TRPM7 Channel. Cells *3*, 1089-1101.

Chubanov, V., Schlingmann, K.P., Waring, J., Heinzinger, J., Kaske, S., Waldegger, S., Mederos y Schnitzler, M., and Gudermann, T. (2007). Hypomagnesemia with secondary hypocalcemia

due to a missense mutation in the putative pore-forming region of TRPM6. The Journal of biological chemistry *282*, 7656-7667.

Clark, K., Langeslag, M., van Leeuwen, B., Ran, L., Ryazanov, A.G., Figdor, C.G., Moolenaar, W.H., Jalink, K., and van Leeuwen, F.N. (2006). TRPM7, a novel regulator of actomyosin contractility and cell adhesion. The EMBO journal *25*, 290-301.

Davis, F.M., Azimi, I., Faville, R.A., Peters, A.A., Jalink, K., Putney, J.W., Jr., Goodhill, G.J., Thompson, E.W., Roberts-Thomson, S.J., and Monteith, G.R. (2014). Induction of epithelial-mesenchymal transition (EMT) in breast cancer cells is calcium signal dependent. Oncogene *33*, 2307-2316.

Deason-Towne, F., Perraud, A.L., and Schmitz, C. (2011). The Mg2+ transporter MagT1 partially rescues cell growth and Mg2+ uptake in cells lacking the channel-kinase TRPM7. FEBS letters *585*, 2275-2278.

Demeuse, P., Penner, R., and Fleig, A. (2006). TRPM7 channel is regulated by magnesium nucleotides via its kinase domain. The Journal of general physiology *127*, 421-434.

Du, J., Xie, J., Zhang, Z., Tsujikawa, H., Fusco, D., Silverman, D., Liang, B., and Yue, L. (2010). TRPM7-mediated Ca2+ signals confer fibrogenesis in human atrial fibrillation. Circulation research *106*, 992-1003.

Faouzi, M., Kilch, T., Horgen, F.D., Fleig, A., and Penner, R. (2017). The TRPM7 channel kinase regulates store-operated calcium entry. The Journal of physiology *595*, 3165-3180.

Fleig, A., and Chubanov, V. (2014). Trpm7. Handbook of experimental pharmacology *222*, 521-546.

Fujiwara, Y., and Minor, D.L., Jr. (2008). X-ray crystal structure of a TRPM assembly domain reveals an antiparallel four-stranded coiled-coil. Journal of molecular biology *383*, 854-870.

Gao, H., Chen, X., Du, X., Guan, B., Liu, Y., and Zhang, H. (2011). EGF enhances the migration of cancer cells by up-regulation of TRPM7. Cell calcium *50*, 559-568.

Gwanyanya, A., Amuzescu, B., Zakharov, S.I., Macianskiene, R., Sipido, K.R., Bolotina, V.M., Vereecke, J., and Mubagwa, K. (2004). Magnesium-inhibited, TRPM6/7-like channel in cardiac myocytes: permeation of divalent cations and pH-mediated regulation. The Journal of physiology *559*, 761-776.

Hara, K., Kokubo, Y., Ishiura, H., Fukuda, Y., Miyashita, A., Kuwano, R., Sasaki, R., Goto, J., Nishizawa, M., Kuzuhara, S.*, et al.* (2010). TRPM7 is not associated with amyotrophic lateral sclerosis-parkinsonism dementia complex in the Kii peninsula of Japan. American journal of medical genetics Part B, Neuropsychiatric genetics : the official publication of the International Society of Psychiatric Genetics *153B*, 310-313.

He, Y., Yao, G., Savoia, C., and Touyz, R.M. (2005). Transient receptor potential melastatin 7 ion channels regulate magnesium homeostasis in vascular smooth muscle cells: role of

angiotensin II. Circulation research *96*, 207-215.

Hermosura, M.C., Nayakanti, H., Dorovkov, M.V., Calderon, F.R., Ryazanov, A.G., Haymer, D.S., and Garruto, R.M. (2005). A TRPM7 variant shows altered sensitivity to magnesium that may contribute to the pathogenesis of two Guamanian neurodegenerative disorders. Proceedings of the National Academy of Sciences of the United States of America *102*, 11510-11515.

Hofmann, T., Schafer, S., Linseisen, M., Sytik, L., Gudermann, T., and Chubanov, V. (2014). Activation of TRPM7 channels by small molecules under physiological conditions. Pflugers Archiv : European journal of physiology.

Huguet, F., Calvez, M.L., Benz, N., Le Hir, S., Mignen, O., Buscaglia, P., Horgen, F.D., Ferec, C., Kerbiriou, M., and Trouve, P. (2016). Function and regulation of TRPM7, as well as intracellular magnesium content, are altered in cells expressing DeltaF508-CFTR and G551D-CFTR. Cellular and molecular life sciences : CMLS *73*, 3351-3373.

Jiang, J., Li, M., and Yue, L. (2005). Potentiation of TRPM7 inward currents by protons. The Journal of general physiology *126*, 137-150.

Jiang, J., Li, M.H., Inoue, K., Chu, X.P., Seeds, J., and Xiong, Z.G. (2007). Transient receptor potential melastatin 7-like current in human head and neck carcinoma cells: role in cell proliferation. Cancer research *67*, 10929-10938.

Jiang, Y., Lee, A., Chen, J., Ruta, V., Cadene, M., Chait, B.T., and MacKinnon, R. (2003). X-ray structure of a voltage-dependent K+ channel. Nature *423*, 33-41.

Kerschbaum, H.H., Kozak, J.A., and Cahalan, M.D. (2003). Polyvalent cations as permeant probes of MIC and TRPM7 pores. Biophysical journal *84*, 2293-2305.

Kim, B.J., Lim, H.H., Yang, D.K., Jun, J.Y., Chang, I.Y., Park, C.S., So, I., Stanfield, P.R., and Kim, K.W. (2005). Melastatin-type transient receptor potential channel 7 is required for intestinal pacemaking activity. Gastroenterology *129*, 1504-1517.

Kim, B.J., Nam, J.H., Kwon, Y.K., So, I., and Kim, S.J. (2013). The role of waixenicin A as transient receptor potential melastatin 7 blocker. Basic & clinical pharmacology & toxicology *112*, 83-89.

Kim, B.J., Park, E.J., Lee, J.H., Jeon, J.H., Kim, S.J., and So, I. (2008). Suppression of transient receptor potential melastatin 7 channel induces cell death in gastric cancer. Cancer science *99*, 2502-2509.

Kolisek, M., Launay, P., Beck, A., Sponder, G., Serafini, N., Brenkus, M., Froschauer, E.M., Martens, H., Fleig, A., and Schweigel, M. (2008). SLC41A1 is a novel mammalian Mg2+ carrier. The Journal of biological chemistry *283*, 16235-16247.

Kozak, J.A., Kerschbaum, H.H., and Cahalan, M.D. (2002). Distinct properties of CRAC and MIC channels in RBL cells. The Journal of general physiology *120*, 221-235

Krapivinsky, G., Mochida, S., Krapivinsky, L., Cibulsky, S.M., and Clapham, D.E. (2006). The TRPM7 ion channel functions in cholinergic synaptic vesicles and affects transmitter release. Neuron *52*, 485-496.

Kuhn, F.J., and Luckhoff, A. (2004). Sites of the NUDT9-H domain critical for ADP-ribose activation of the cation channel TRPM2. The Journal of biological chemistry *279*, 46431-46437.

Kuras, Z., Yun, Y.H., Chimote, A.A., Neumeier, L., and Conforti, L. (2012). KCa3.1 and TRPM7 channels at the uropod regulate migration of activated human T cells. PloS one *7*, e43859.

Li, M., Du, J., Jiang, J., Ratzan, W., Su, L.T., Runnels, L.W., and Yue, L. (2007). Molecular determinants of Mg2+ and Ca2+ permeability and pH sensitivity in TRPM6 and TRPM7. The Journal of biological chemistry *282*, 25817-25830.

Li, M., Jiang, J., and Yue, L. (2006). Functional characterization of homo- and heteromeric channel kinases TRPM6 and TRPM7. The Journal of general physiology *127*, 525-537.

Macianskiene, R., Martisiene, I., Zablockaite, D., and Gendviliene, V. (2012). Characterization of Mg(2)(+)-regulated TRPM7-like current in human atrial myocytes. Journal of biomedical science *19*, 75.

Mederos y Schnitzler, M., Waring, J., Gudermann, T., and Chubanov, V. (2008). Evolutionary determinants of divergent calcium selectivity of TRPM channels. FASEB journal : official publication of the Federation of American Societies for Experimental Biology *22*, 1540-1551.

Meng, X., Cai, C., Wu, J., Cai, S., Ye, C., Chen, H., Yang, Z., Zeng, H., Shen, Q., and Zou, F. (2013). TRPM7 mediates breast cancer cell migration and invasion through the MAPK pathway. Cancer letters *333*, 96-102.

Monteilh-Zoller, M.K., Hermosura, M.C., Nadler, M.J., Scharenberg, A.M., Penner, R., and Fleig, A. (2003). TRPM7 provides an ion channel mechanism for cellular entry of trace metal ions. The Journal of general physiology *121*, 49-60.

Nadler, M.J., Hermosura, M.C., Inabe, K., Perraud, A.L., Zhu, Q., Stokes, A.J., Kurosaki, T., Kinet, J.P., Penner, R., Scharenberg, A.M.*, et al.* (2001). LTRPC7 is a Mg.ATP-regulated divalent cation channel required for cell viability. Nature *411*, 590-595.

Norenberg, W., Plotz, T., Sobottka, H., Chubanov, V., Mittermeier, L., Kalwa, H., Aigner, A., and Schaefer, M. (2016). TRPM7 is a molecular substrate of ATP-evoked P2X7-like currents in tumor cells. The Journal of general physiology *147*, 467-483.

Numata, T., and Okada, Y. (2008). Molecular determinants of sensitivity and conductivity of human TRPM7 to Mg2+ and Ca2+. Channels *2*, 283-286.

Paravicini, T.M., Chubanov, V., and Gudermann, T. (2012). TRPM7: a unique channel involved in magnesium homeostasis. The international journal of biochemistry & cell biology *44*, 1381-1384.

Park, H.S., Hong, C., Kim, B.J., and So, I. (2014). The Pathophysiologic Roles of TRPM7 Channel. The Korean journal of physiology & pharmacology : official journal of the Korean Physiological Society and the Korean Society of Pharmacology *18*, 15-23.

Parnas, M., Peters, M., Dadon, D., Lev, S., Vertkin, I., Slutsky, I., and Minke, B. (2009). Carvacrol is a novel inhibitor of Drosophila TRPL and mammalian TRPM7 channels. Cell calcium *45*, 300-309Perraud, A.L., Fleig, A., Dunn, C.A., Bagley, L.A., Launay, P., Schmitz, C.,

Stokes, A.J., Zhu, Q., Bessman, M.J., Penner, R.*, et al.* (2001). ADP-ribose gating of the calcium-permeable LTRPC2 channel revealed by Nudix motif homology. Nature *411*, 595-599.

Prakriya, M., and Lewis, R.S. (2002). Separation and characterization of currents through store-operated CRAC channels and Mg2+-inhibited cation (MIC) channels. The Journal of general physiology *119*, 487-507.

Qin, X., Yue, Z., Sun, B., Yang, W., Xie, J., Ni, E., Feng, Y., Mahmood, R., Zhang, Y., and Yue, L. (2013). Sphingosine and FTY720 are potent inhibitors of the transient receptor potential melastatin 7 (TRPM7) channels. British journal of pharmacology *168*, 1294-1312.

Romero, J.R., Ridker, P.M., and Zee, R.Y. (2009). Gene variation of the transient receptor potential cation channel, subfamily M, member 7 (TRPM7), and risk of incident ischemic stroke: prospective, nested, case-control study. Stroke; a journal of cerebral circulation *40*, 2965-2968.

Rubin, H. (2007). The logic of the Membrane, Magnesium, Mitosis (MMM) model for the regulation of animal cell proliferation. Archives of biochemistry and biophysics *458*, 16-23.

Runnels, L.W., Yue, L., and Clapham, D.E. (2001). TRP-PLIK, a bifunctional protein with kinase and ion channel activities. Science *291*, 1043-1047.

Runnels, L.W., Yue, L., and Clapham, D.E. (2002). The TRPM7 channel is inactivated by PIP(2) hydrolysis. Nature cell biology *4*, 329-336.

Ryazanova, L.V., Rondon, L.J., Zierler, S., Hu, Z., Galli, J., Yamaguchi, T.P., Mazur, A., Fleig, A., and Ryazanov, A.G. (2010). TRPM7 is essential for Mg(2+) homeostasis in mammals. Nature communications *1*, 109.

Rybarczyk, P., Gautier, M., Hague, F., Dhennin-Duthille, I., Chatelain, D., Kerr-Conte, J., Pattou, F., Regimbeau, J.M., Sevestre, H., and Ouadid-Ahidouch, H. (2012). Transient receptor potential melastatin-related 7 channel is overexpressed in human pancreatic ductal adenocarcinomas and regulates human pancreatic cancer cell migration. International journal of cancer Journal international du cancer *131*, E851-861.

Sah, R., Mesirca, P., Van den Boogert, M., Rosen, J., Mably, J., Mangoni, M.E., and Clapham, D.E. (2013). Ion channel-kinase TRPM7 is required for maintaining cardiac automaticity. Proceedings of the National Academy of Sciences of the United States of America *110*, E3037-3046.

Sahni, J., Nelson, B., and Scharenberg, A.M. (2007). SLC41A2 encodes a plasma-membrane Mg2+ transporter. The Biochemical journal *401*, 505-513.

Sahni, J., Tamura, R., Sweet, I.R., and Scharenberg, A.M. (2010). TRPM7 regulates quiescent/proliferative metabolic transitions in lymphocytes. Cell cycle *9*, 3565-3574.

Schäfer, S., Ferioli, S., Hofmann, T., Zierler, S., Gudermann, T., and Chubanov, V. (2015). Mibefradil represents a new class of benzimidazole TRPM7 channel agonists. Pflugers Archiv : European journal of physiology.

Schilling, T., Miralles, F., and Eder, C. (2014). TRPM7 regulates proliferation and polarisation of macrophages. Journal of cell science *127*, 4561-4566.

Schlingmann, K.P., Weber, S., Peters, M., Niemann Nejsum, L., Vitzthum, H., Klingel, K., Kratz, M., Haddad, E., Ristoff, E., Dinour, D.*, et al.* (2002). Hypomagnesemia with secondary hypocalcemia is caused by mutations in TRPM6, a new member of the TRPM gene family. Nature genetics *31*, 166-170.

Schmitz, C., Dorovkov, M.V., Zhao, X., Davenport, B.J., Ryazanov, A.G., and Perraud, A.L. (2005). The channel kinases TRPM6 and TRPM7 are functionally nonredundant. The Journal of biological chemistry *280*, 37763-37771.

Schmitz, C., Perraud, A.L., Johnson, C.O., Inabe, K., Smith, M.K., Penner, R., Kurosaki, T., Fleig, A., and Scharenberg, A.M. (2003). Regulation of vertebrate cellular Mg2+ homeostasis by TRPM7. Cell *114*, 191-200.

Sisquella, X., Nebl, T., Thompson, J.K., Whitehead, L., Malpede, B.M., Salinas, N.D., Rogers, K., Tolia, N.H., Fleig, A., O'Neill, J.*, et al.* (2017). Plasmodium falciparum ligand binding to erythrocytes induce alterations in deformability essential for invasion. eLife *6*.

Stritt, S., Nurden, P., Favier, R., Favier, M., Ferioli, S., Gotru, S.K., van Eeuwijk, J.M., Schulze, H., Nurden, A.T., Lambert, M.P.*, et al.* (2016). Defects in TRPM7 channel function deregulate thrombopoiesis through altered cellular Mg(2+) homeostasis and cytoskeletal architecture. Nature communications *7*, 11097.

Sun, H.S., Jackson, M.F., Martin, L.J., Jansen, K., Teves, L., Cui, H., Kiyonaka, S., Mori, Y., Jones, M., Forder, J.P.*, et al.* (2009). Suppression of hippocampal TRPM7 protein prevents delayed neuronal death in brain ischemia. Nature neuroscience *12*, 1300-1307.

Tashiro, M., Inoue, H., and Konishi, M. (2014). Physiological pathway of magnesium influx in rat ventricular myocytes. Biophysical journal *107*, 2049-2058.

Tian, Y., Yang, T., Yu, S., Liu, C., He, M., and Hu, C. (2018). Prostaglandin E2 increases migration and proliferation of human glioblastoma cells by activating transient receptor potential melastatin 7 channels. Journal of cellular and molecular medicine.

Touyz, R.M., He, Y., Montezano, A.C., Yao, G., Chubanov, V., Gudermann, T., and Callera, G.E. (2006). Differential regulation of transient receptor potential melastatin 6 and 7 cation channels by ANG II in vascular smooth muscle cells from spontaneously hypertensive rats. American journal of physiology Regulatory, integrative and comparative physiology *290*, R73-78.

Tseveleki, V., Rubio, R., Vamvakas, S.S., White, J., Taoufik, E., Petit, E., Quackenbush, J., and Probert, L. (2010). Comparative gene expression analysis in mouse models for multiple sclerosis, Alzheimer's disease and stroke for identifying commonly regulated and disease-specific gene changes. Genomics *96*, 82-91.

Venkatachalam, K., and Montell, C. (2007). TRP channels. Annual review of biochemistry *76*, 387-417.

Visser, D., Langeslag, M., Kedziora, K.M., Klarenbeek, J., Kamermans, A., Horgen, F.D., Fleig, A., van Leeuwen, F.N., and Jalink, K. (2013). TRPM7 triggers Ca2+ sparks and invadosome formation in neuroblastoma cells. Cell calcium *54*, 404-415.

Walder, R.Y., Landau, D., Meyer, P., Shalev, H., Tsolia, M., Borochowitz, Z., Boettger, M.B., Beck, G.E., Englehardt, R.K., Carmi, R.*, et al.* (2002). Mutation of TRPM6 causes familial hypomagnesemia with secondary hypocalcemia. Nature genetics *31*, 171-174.

Wong, R., Turlova, E., Feng, Z.P., Rutka, J.T., and Sun, H.S. (2017). Activation of TRPM7 by naltriben enhances migration and invasion of glioblastoma cells. Oncotarget *8*, 11239-11248.

Yoshimura, M., Oshima, T., Matsuura, H., Ishida, T., Kambe, M., and Kajiyama, G. (1997). Extracellular Mg2+ inhibits capacitative Ca2+ entry in vascular smooth muscle cells. Circulation *95*, 2567-2572.

Zhang, Y.H., Sun, H.Y., Chen, K.H., Du, X.L., Liu, B., Cheng, L.C., Li, X., Jin, M.W., and Li, G.R. (2012). Evidence for functional expression of TRPM7 channels in human atrial myocytes. Basic research in cardiology *107*, 282.

Zierler, S., Yao, G., Zhang, Z., Kuo, W.C., Porzgen, P., Penner, R., Horgen, F.D., and Fleig, A. (2011). Waixenicin A inhibits cell proliferation through magnesium-dependent block of transient receptor potential melastatin 7 (TRPM7) channels. The Journal of biological chemistry *286*, 39328-39335.

Eidesstattliche Versicherung

Ich, Sebastian Schäfer, erkläre hiermit an Eides statt, dass ich die vorliegende Dissertation mit dem Thema „Pharmakologische Beeinflussbarkeit der TRPM7 Kanalkinase“ selbständig verfasst, mich außer der angegebenen keiner weiteren Hilfsmittel bedient und alle Erkenntnisse, die aus dem Schrifttum ganz oder annähernd übernommen sind, als solche kenntlich gemacht und nach ihrer Herkunft unter Bezeichnung der Fundstelle einzeln nachgewiesen habe. Ich erkläre des Weiteren, dass die hier vorgelegte Dissertation nicht in gleicher oder in ähnlicher Form bei einer anderen Stelle zur Erlangung eines akademischen Grades eingereicht wurde.

München, den 24. Februar 2019 Sebastian Schäfer

Danksagung

Ich bedanke mich bei Herrn Prof. Dr. Gudermann, der es mir ermöglichte meine Dissertation am Walther-Straub-Institut zu absolvieren.

Weiterhin bedanke ich mich sehr bei meinem Betreuer Dr. Vladimir Chubanov, der mir ein interessantes Forschungsthema zuwies und sehr viel Zeit in die Betreuung meiner Arbeit investierte. Ohne ihn, wäre diese Arbeit nie in dieser Form zustande gekommen.

Ein großer Dank geht an Ulrike sowie meiner Familie Werner, Berta, Katrin, Andrea und natürlich Hannes, Frieda und Mattis.

Vielen Dank an Maxim, Verena, Jonas, Brüsi, Bodo, Lauti und Thöne für ihr Unterstützung und die gute Zeit.